



universität
wien

DIPLOMARBEIT

Titel der Diplomarbeit

Investigations on Murine Colitis-Associated Bacteria: a quantitative PCR and microscopy approach

verfasst von

Ina Maria Rennisch

angestrebter akademischer Grad

Magistra der Naturwissenschaften (Mag.rer.nat.)

Wien, 2013

Studienkennzahl lt. Studienblatt:

A 444

Studienrichtung lt. Studienblatt:

Diplomstudium Ökologie

Betreut von:

Univ.-Prof. Dipl.-Biol. Dr. Christa Schleper

Eidesstattliche Erklärung

Ich erkläre hiermit an Eides Statt, dass ich die vorliegende Arbeit selbstständig und ohne Benutzung anderer als der angegebenen Hilfsmittel angefertigt habe. Die aus fremden Quellen direkt oder indirekt übernommenen Gedanken sind als solche kenntlich gemacht.

Die Arbeit wurde bisher in gleicher oder ähnlicher Form keiner anderen Prüfungsbehörde vorgelegt und auch nicht veröffentlicht.

Wien, Mai 2013

Ina Maria Rennisch

Acknowledgments

Most of all, I want to thank Univ.-Prof. Dipl.-Biol. Dr. Christa Schleper and Dipl.-Biol. Dr. Tim Urich for accepting me as diploma student at the Department of Genetics in Ecology and for guiding me through my diploma thesis. By this, I got the incredible chance of an insight in scientific research.

Also, I want to thank Clarissa Schwab, my supervisor, who accompanied me all through my work with patience, motivation, encouragement and advice.

I am very grateful for the colleagues of the InflammoBiota project. Especially, I want to thank Eva Hainzl and Isabella Rauch who took care of the mice and Clarissa Schwab, Gabriel Milinovich and David Berry for supplying me with the nucleic acid extractions.

Thanks to the “Mermaids” for their help with immunofluorescence and to Julia for performing FISH.

I had the opportunity to do my thesis at a department where I felt very welcome. Every group member was always willing to help, even if the question did not occur for the first time or was trivial. Also, they were more than colleagues to me. Thanks to Micha, Melina, Romana, Isa, Bella, Lisa, Nika, Amir, Niko, Silvia, Ziga, Ricardo, Julia, Andi, Andrea M., Anja, Pierre, Daniela, Steffi and Andrea S. for making my lab life unforgettable and adding so much fun to it!

My special thanks go to Anna, Chrisi, Jules and Tina who accompanied me all through and were crucial for successfully completing my course of studies. Every one of you pushed me at least through one exam (with physics and chemistry being just the first and probably most difficult ones...)!

Also, I want to thank all my friends, especially Ina, Ulli and Lisi, who were always there for me.

Especially, I want to thank my family, particularly my parents, who supported me the whole time.

Table of Contents

<u>1</u>	<u>ABSTRACT</u>	<u>1</u>
<u>2</u>	<u>INTRODUCTION</u>	<u>3</u>
2.1	HUMAN LIFE INCLUDES MICROORGANISMS	3
2.2	INFLAMMATORY BOWEL DISEASE.....	4
2.2.1	MICROBIOTA IN IBD	4
2.2.2	THE MUCOSA AND ITS IMMUNE SYSTEM.....	6
2.3	THE INFLAMMOBIOTA PROJECT.....	8
2.3.1	CONTROLLED EXPERIMENTAL DESIGN – DSS INDUCED MURINE COLITIS.....	8
2.3.2	THE ROLE OF THE JAK-STAT PATHWAY IN SIGNAL TRANSDUCTION	9
2.4	INCREASE OF LOW ABUNDANT BACTERIAL TAXA IN MURINE COLITIS	10
2.5	SHIFTS IN GUT MICROBIOME FUNCTION DURING ACUTE MURINE COLITIS	12
2.6	THE AIM OF THIS STUDY	14
<u>3</u>	<u>MATERIALS</u>	<u>15</u>
3.1	CHEMICALS.....	15
3.2	KITS	16
3.3	MICE	16
3.4	BUFFERS	16
3.5	MEDIA	17
3.6	ANTIBIOTICS	17
3.7	MICROORGANISMS	18
3.8	VECTORS.....	18
3.9	ENZYMES.....	18
3.10	PRIMERS (5' → 3').....	18
3.10.1	PRIMERS TARGETING 16S rRNA GENES	19
3.10.2	PRIMERS TARGETING PROTEIN GENES	19
3.10.3	PRIMERS FOR SEQUENCING	20
3.11	DNA STANDARDS	20
3.12	MICROSCOPY	21
3.12.1	LIGHT MICROSCOPY	21
3.12.1.1	Preparation of the basic fuchsin stain	21

3.12.2	FLUORESCENT DYES	22
3.12.2.1	Preparation for the NanoOrange® stain.....	22
3.12.2.2	Immunofluorescence antibodies	22
3.12.2.3	FISH probes	23

4 METHODS 24

4.1	ANIMAL TRIALS	24
4.1.1	TRIAL A – ACUTE MURINE COLITIS	24
4.1.2	TRIAL C – DEVELOPMENT OF MURINE COLITIS	25
4.1.3	TRIAL G – RECOVERY OF MURINE COLITIS.....	25
4.1.4	TRIAL I – RECOVERY OF MURINE COLITIS	25
4.2	MOLECULAR ANALYSIS.....	26
4.2.1	SINGLE STRAND CDNA SYNTHESIS	26
4.2.2	AGAROSE GEL ELECTROPHORESIS	27
4.2.3	QUALITATIVE POLYMERASE CHAIN REACTION (PCR).....	27
4.2.3.1	Mastermix for qualitative PCR	27
4.2.3.2	Thermal cycling conditions for qualitative PCR	28
4.2.3.3	Gradient PCR	28
4.2.3.4	Purification of PCR products.....	29
4.2.4	CLONING	29
4.2.4.1	Colony PCR and master plate	29
4.2.4.2	Plasmid isolation	30
4.2.4.3	Restriction digest of recombinant plasmids.....	30
4.2.5	QUANTITATIVE PCR	30
4.2.5.1	Mastermix for quantitative PCR	31
4.2.5.2	Conditions for quantitative PCR.....	31
4.2.5.3	Preparation of the standards for qPCR	32
4.2.5.4	Statistical analysis of the qPCR data	32
4.2.6	SEQUENCING OF THE FLAGELLIN GENE	32
4.2.6.1	Analysis of the sequenced data	33
4.3	MICROSCOPY	33
4.3.1	LIGHT MICROSCOPY	33
4.3.1.1	Basic fuchsin stain.....	33
4.3.2	FLUORESCENCE MICROSCOPY	35
4.3.2.1	NanoOrange®	35
4.3.2.2	Immunofluorescence	35

4.3.2.3	Fluorescence in situ hybridization.....	36
4.4	COMBINATIONS OF MICROSCOPY TECHNIQUES	37
4.4.1	IF-BASIC FUCHSIN	37
4.4.2	FISH-BASIC FUCHSIN	37
4.4.3	DAPI-NANOORANGE®.....	37
4.4.4	DAPI-IF	38
4.4.5	IF-NANOORANGE®.....	38
4.4.6	FISH-NANOORANGE®.....	38
4.4.7	IF-FISH	38
4.4.8	ANALYSIS OF THE MICROSCOPY PICTURES FOR IF-FISH.....	39
5	RESULTS	40

5.1	MOUSE TRIALS	40
5.1.1	WEIGHT CURVES FOR ACUTE COLITIS– TRIAL A.....	40
5.1.2	WEIGHT CURVES FOR COLITIS DEVELOPMENT – TRIAL C.....	41
5.1.3	WEIGHT CURVES FOR RECOVERY OF MURINE COLITIS – TRIAL G & I.....	42
5.2	ESTABLISHMENT OF QUANTITATIVE PCR ASSAYS	44
5.2.1	VALIDATION AND OPTIMIZATION OF THE CONDITIONS FOR QUALITATIVE PCRS.....	44
5.2.1.1	The flagellin primers used for qPCR	46
5.2.1.2	Identification of flagellin genes.....	47
5.2.2	VALIDATION OF REVERSE TRANSCRIPTION AND DNASE DIGEST DURING CDNA SYNTHESIS.....	50
5.2.3	PREPARATION OF THE STANDARDS FOR QPCR	51
5.2.4	ABUNDANCE AND ACTIVITY OF <i>AKKERMANSIA</i> DURING MURINE COLITIS	52
5.2.4.1	<i>Akkermansia</i> in acute murine colitis.....	52
5.2.4.2	<i>Akkermansia</i> during murine colitis development.....	54
5.2.4.3	<i>Akkermansia</i> in the recovery of murine colitis	56
5.2.5	EXAMINING THE CLOSTRIDIAL FLAGELLIN GENE ABUNDANCE	57
5.2.5.1	Flagellin in acute murine colitis.....	57
5.2.5.2	Flagellin during colitis development	58
5.2.5.3	Flagellin in the recovery experiments	60
5.3	MICROSCOPIC APPROACHES TO IDENTIFY FLAGELLATED BACTERIA	63
5.3.1	THE BASIC FUCHSIN STAIN FOR FLAGELLA DETECTION	63
5.3.2	NANOORANGE® – A FLUORESCENT GENERAL FLAGELLA STAIN	65
5.3.3	IMMUNOFLUORESCENCE – DETECTING CLOSTRIDIAL FLAGELLA	67
5.3.4	COMBINATIONS OF DIFFERENT STAINS.....	67

5.3.4.1	Immunofluorescence-basic fuchsin – clostridial flagella compared to total flagella	67
5.3.4.2	FISH-basic fuchsin – assigning flagella to bacteria.....	69
5.3.4.3	Detecting flagella stained with NanoOrange®.....	69
5.3.4.4	DAPI-immunofluorescence – how many bacteria are flagellated?	71
5.3.4.5	IF-FISH – abundance of flagellated <i>Lachnospiraceae</i>	72
5.4	QUANTIFICATION OF FLAGELLATED <i>LACHNOSPIRACEAE</i>.....	75
6	<u>DISCUSSION</u>	77
6.1	WHEN THE INFLAMMATION ARISES.....	77
6.2	<i>AKKERMANSIA</i> AND ITS INCREASE DURING INFLAMMATION.....	79
6.3	THE DECREASE OF FLAGELLIN GENES AND TRANSCRIPTS IN MURINE COLITIS	82
6.3.1	ESTABLISHMENT OF MICROSCOPIC TECHNIQUES TO IDENTIFY FLAGELLATED BACTERIA	85
6.3.1.1	The basic fuchsin approach – a general flagella stain.....	85
6.3.1.2	NanoOrange® - the search for fluorescent flagella	86
6.3.1.3	Assignment of flagella by combining IF and FISH.....	87
6.3.2	QUANTIFICATION OF FLAGELLATED <i>LACHNOSPIRACEAE</i>	87
6.4	THE INFLUENCE OF THE MOUSE GENOTYPE ON GUT MICROBIOTA DIFFERENCES.....	89
7	<u>CONCLUSION</u>	90
8	<u>ZUSAMMENFASSUNG</u>	91
9	<u>REFERENCES</u>	93
10	<u>APPENDIX</u>	102
	LIST OF ABBREVIATIONS.....	102
	LIST OF TABLES	105
	TABLE OF FIGURES	106
	CURRICULUM VITAE	111

1 Abstract

Human health and in particular our digestive system is dependent on the activity of many microorganisms. The continuous presence of high amounts of bacteria in our body demands a delicate homeostasis between the activity of the immune system and the microbiota. In patients suffering from inflammatory bowel disease (IBD) like Crohn's disease (CD) or ulcerative colitis (UC) this homeostasis is disrupted. Until today, the causes of IBD are not known. Therefore, the search for reliable diagnostic markers represents an area of active research. Based on previous results obtained in the frame of a collaborative project (InflammoBiota), it was hypothesized that the bacterium *Akkermansia* and clostridial flagellins are indicators for inflammation.

The aim of this study was to verify whether *Akkermansia* and clostridial flagellins may indeed represent suitable indicators for acute colitis. For this purpose, a mouse model using dextran sodium sulfate (DSS) to induce inflammation was utilized. To examine shifts in the microbiota composition and in the expression of selected genes, quantitative polymerase chain reaction (qPCR) was performed on samples derived from luminal content during acute inflammation, development and recovery. In addition to *Akkermansia* 16S rRNA, three of its functional genes (rubrerythrin, β -N-acetylhexosaminidase and capsular exopolysaccharide synthesis) were investigated. In order to visualize flagella, different microscopy approaches, including immunofluorescence (IF), were used.

It was shown that the 16S rRNA gene abundance of *Akkermansia* increased up to 20,000 fold in acute murine colitis and was negatively correlated to the body weight of the mice. The reason for the increase of *Akkermansia* might have been the mucus detachment from the epithelium which leads to a better accessibility of nutrients for *Akkermansia*, as the organism uses mucin as sole carbon, nitrogen and energy source. Also, the increase of transcripts for rubrerythrin, which is involved in oxidative stress protection, indicated an oxygen directed response of *Akkermansia* to the inflammation during acute colitis.

The abundance of clostridial flagellins decreased during acute inflammation. As the permeability of the epithelium increases during inflammation, this might have led to an increased exposure of the strong flagellin antigen to the immune system which in turn triggered an increased antibacterial activity targeting (flagellated) bacteria. A method combining IF and fluorescence *in situ* hybridization (FISH) was successfully established. This allowed the assignment of flagella to specific bacterial orders. The

Abstract

results obtained by IF-FISH and qPCR were similar. However, for confirmation of the comparability of these two methods, further investigations using more samples will be required.

In conclusion, it was verified that *Akkermansia* and the clostridial flagellins are indicators of acute murine colitis. Future studies will show whether these findings can be validated in human colitis.

2 Introduction

2.1 Human life includes microorganisms

Without microorganisms, human life would be impossible. The interdependent relationship between microbes and humans coevolved (Ley et al., 2006). Each of our body surfaces, both the inner and outer ones, are colonized by microorganisms, including all our skin, the oral cavity, the oesophagus, the gastrointestinal (GI) tract, the respiratory system, etc. Together, the human body cells and the microorganisms form a superorganism (Ley et al., 2006). The amount of microbial cells (from all three domains of life: archaea, bacteria and eucarya) even outnumber the amount of our body cells by an order of magnitude (Peterson et al., 2008). Humans consist of approximately 10^{13} body cells and about 10^{14} microbial cells (Savage, 1977) with over 7,500 different species (Vijay-Kumar and Gewirtz, 2009). It is assumed that the gut microbiome alone contains ≥ 100 times more genes than the human genome (Backhed, 2005, Xu and Gordon, 2003).

The majority of these microorganisms (10^{14} , Luckey, 1972) are located in the GI tract (Peterson et al., 2008, Savage, 1977). Many of them possess physiological features which humans have not evolved, but which are essential for our survival (Gill et al., 2006). These include for example the fermentation of otherwise indigestible food substances, the breakdown of dietary toxins and carcinogens, the absorption of certain electrolytes and trace minerals and the synthesis of micronutrients (DiBaise et al., 2008) and of certain vitamins (Hill, 1997). Additionally, the gut microbiome is important to maintain the intestinal homeostasis, to protect the host from pathogens and it has an immune modulating function (Sheil et al., 2007). Hence, this symbiosis is well adapted and complex. Without disturbances, this system remains stable (Zoetendal et al., 1998). However, antibiotic treatment or inflammation, for example, can cause a disruption of the microbiota homeostasis by killing or inhibiting not just the targeted organisms (Brötz-Oesterhelt and Brunner, 2008) which leads to alterations in the composition of the microbiota (Ubeda and Pamer, 2012).

2.2 Inflammatory bowel disease

Inflammatory bowel disease (IBD) is a condition characterized by the loss of the homeostasis between the intestinal immune system and the microbiome (Carbonnel et al., 2009). However, the precise aetiology has yet to be determined (Reiff and Kelly, 2010; Wong and Ng, 2013). IBD occurs idiopathic and is mainly represented by Crohn's disease (CD) and ulcerative colitis (UC) (Strober et al., 2007). While CD affects the small bowel and colon in a patchy way, UC causes a continuous inflammation of the colon (Strober et al., 2007). Amongst the symptoms reported for IBD are abdominal pain, diarrhea, rectal bleeding, weight loss, fever, fatigue and, for CD patients only, fistulas can occur (Strober et al., 2007).

The most apparent correlation for IBD prevalence seems to be in the western world and in higher socioeconomic groups (Danese et al., 2004), the 'super-civilized' areas. The prevalence in developing countries is lower than in developed countries, but it has to be considered that only very few studies are available for IBD occurrence in developing countries and the available epidemiologic data is impaired by the limited access to health-care (Wong and Ng, 2013). Furthermore, a geographical correlation is observed with a higher occurrence of IBD in urban than in rural areas although this may rather be due to environmental reasons (Baumgart and Carding, 2007). Amongst others, these environmental factors include smoking, diet, drugs (e.g. oral contraceptives and nonsteroidal anti-inflammation drugs), stress, the 'westernization' process and microbial influences (Danese et al., 2004). Also, cumulative incidences of IBD among relatives makes the genetic predisposition a strong influential factor (Baumgart and Carding, 2007).

2.2.1 Microbiota in IBD

In the healthy gut system, ten phyla of bacteria have been detected (Firmicutes, Bacteroidetes, Actinobacteria, Fusobacteria, Proteobacteria, Verrucomicrobia, Cyanobacteria, Spirochaetes, Synergistetes and Lentisphaerae), with Bacteroidetes and Firmicutes being the most dominant ones (Bäckhed et al., 2006). Accordingly, in a gut diversity study > 98 % of 16S rDNA sequences were found to belong to those two phyla (Eckburg et al., 2005).

Alterations in the microbiota composition have been found between healthy and diseased people as well as in the different bowel sections (Figure 2-1; Peterson et al., 2008). During inflammation, huge variabilities in the microbial community composition were observed probably because there are no controlled experimental conditions for humans. Peterson et al. (2008) reported an increased amount of Proteobacteria, *Bacillus* (phylum Firmicutes) and Actinobacteria, whereas the amount of *Clostridiales* (phylum Firmicutes) and Bacteroidetes decreased for IBD suffering patients.

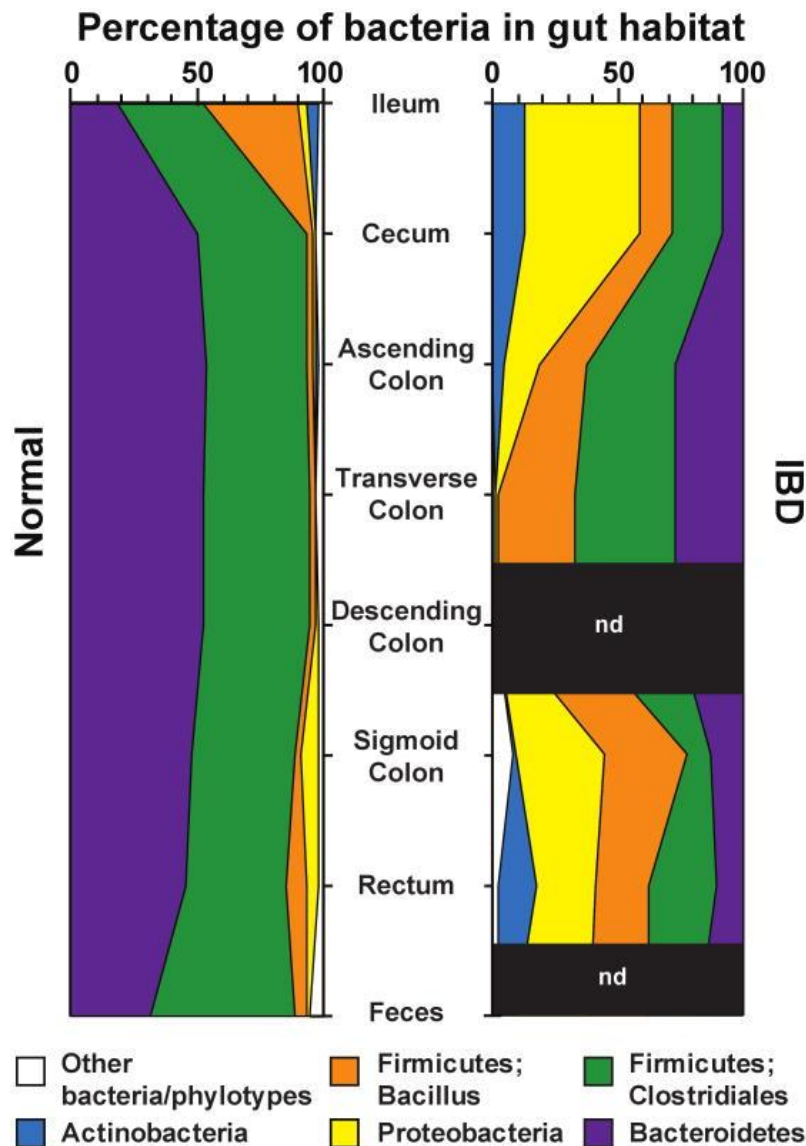


Figure 2-1: Relative abundance of different bacterial phyla along the intestinal tract, comparing healthy and IBD suffering humans (Peterson et al., 2008).

Although Walker et al. (2011) observed huge inter-individual differences in the microbiota composition, the distributions between healthy and IBD patients' biopsy

samples differed significantly with less Firmicutes and a higher abundance of Bacteroidetes and *Enterobacteriaceae* in disease. When looking at lower taxonomic ranks, a shift on species level with an increase of *Ruminococcus gnavus* and *Ruminococcus torques* (Firmicutes) in IBD patients was found by Png et al. (2010). Alterations in the microbiota composition and a decrease in diversity was also reported in other studies (Packey and Sartor, 2009; Reiff and Kelly, 2010; Sokol et al., 2008).

2.2.2 The mucosa and its immune system

One role of the mucosa is to maintain the balance between commensal bacteria and to defend against pathogenic organisms while it is exposed to the largest concentrations of foreign bacterial antigens (Lodes et al., 2004). In order to accomplish this, the mucosa represents a physical barrier and has a fast cell turnover (Niedergang et al., 2004). Also, a biochemical border is built by the epithelial cells by producing antimicrobial agents like defensins (Niedergang et al., 2004). Both, the small and the large intestine are protected by a mucus layer which is permeable for bacteria and, additionally, the large intestine possesses a second, inner mucus layer which is attached to the epithelium and free of bacteria (Johansson et al., 2011). Furthermore, the innate and adaptive immune system help preventing infections (Niedergang et al., 2004). Usually, the epithelium (the innermost layer of the mucosa) together with a mucin layer builds a strict barrier between the lumen and the mucosa of the GI tract (Arseneau et al., 2007). Epithelial cells are the first ones to encounter the bacteria (Ramos et al., 2004). The transit is strictly regulated by tight junctions (Arseneau et al., 2007). The specific antigen recognition and cell-mediated immunity, which are part of the adaptive mucosal immune response, then lead to a phagocytosis of the invading pathogens (Arseneau et al., 2007; Ramos et al., 2004). Also, antigens are sampled by M and dendritic cells and presented to lymphocytes. Additionally, specialized pattern recognition receptors (e.g. toll-like receptors (TLRs)) are expressed in the epithelium by the innate immune system (Figure 2-2) which recognize highly conserved microbe-associated molecular patterns (MAMPs) (Arseneau et al., 2007). MAMPs are important for the survival of the microorganisms so they are hardly altered and represent ideal targets (Arseneau et al., 2007).

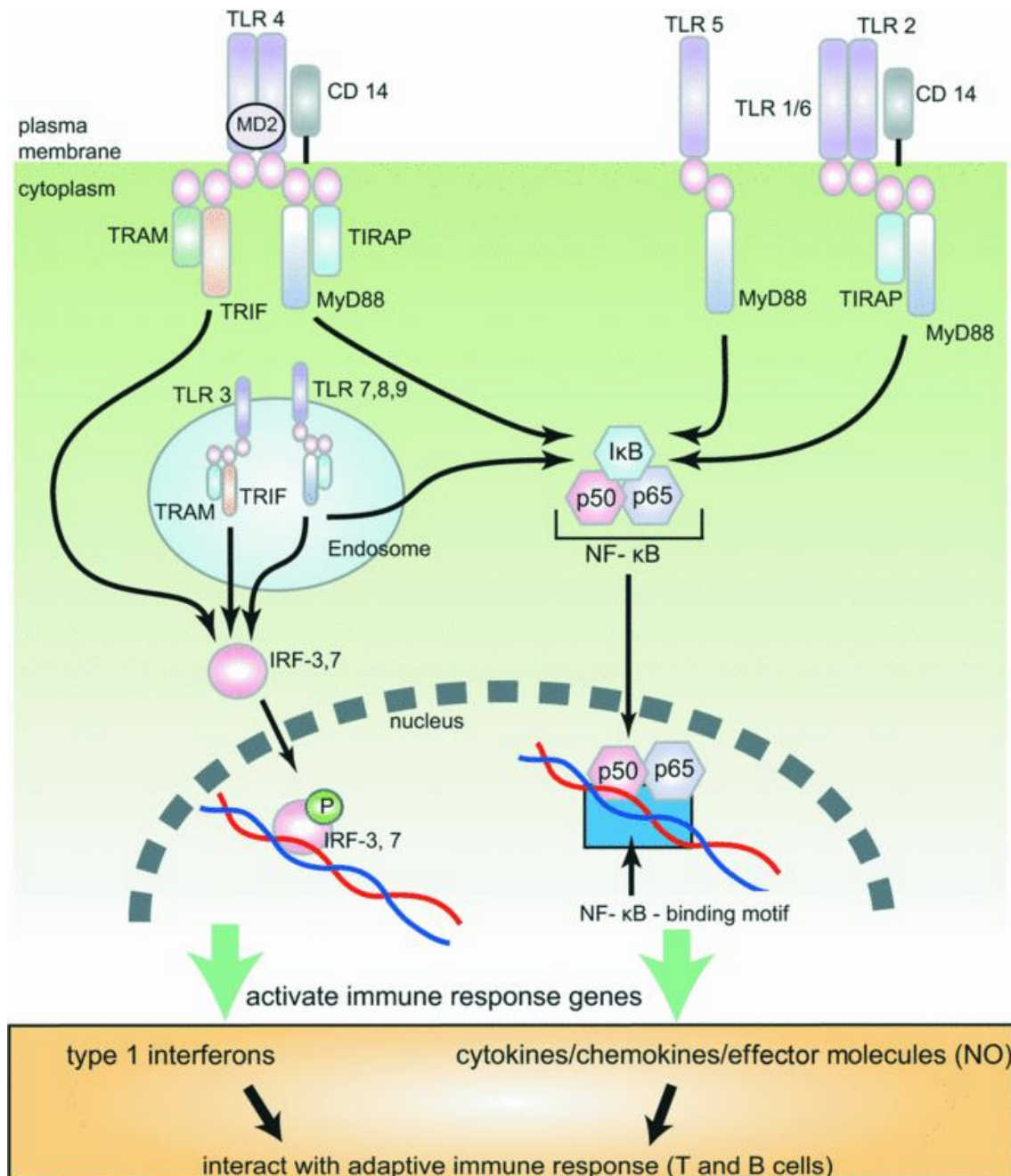


Figure 2-2: The human TLR signalling pathway in an overview (Misch and Hawn, 2008). TLR ligation induces a signalling cascade which leads by translocation of transcription factors to an acute inflammatory response in the nucleus.

An example for MAMPs is the bacterial flagellin, which is widespread within the bacteria (Ramos et al., 2004), as it has highly conserved regions at the N- and C-termini which are involved in the polymerization of the flagellar filament (Vijay-Kumar and Gewirtz, 2009). If these MAMPs bind to the TLRs, inflammatory mediators are produced (Arseneau et al., 2007). When the epithelium becomes more easily accessible for microorganisms, for example by detachment of the mucus layer or by

change of their molecular patterns, inflammation is triggered by the immune system (Johansson et al., 2010). In humans and mice eleven and thirteen different TLRs, respectively, are described, which all target particular MAMPs (Wang et al., 2013). When these MAMPs are recognized by the TLRs this leads to an immediate response of the host against the microorganisms (Garantziotis et al., 2008).

Some TLRs are associated with IBD, for example TLR1, -2 and -6 are believed to have an influence on the extent of IBD (Garantziotis et al., 2008). Additionally, TLR4, which targets lipopolysaccharides (component of the gram-negative wall) is considered to have a role in the pathogenesis of IBD (Garantziotis et al., 2008). Furthermore, TLR5 is linked to IBD because flagellin, which is a dominant antigen in IBD (Lodes et al., 2004), is the only ligand of this receptor (Hayashi et al., 2001). Also, it was shown that Ashkenazi Jewish people carrying a heterozygote TLR5-stop (dominant-negative TLR5 polymorphism) developed significantly less often CD (but no influence on UC), indicating protection of these people against CD (Gewirtz et al., 2006).

2.3 The InflammoBiota project

As the appearance of chronic IBD in the western world is frequent (Wong and Ng, 2013), it is of great interest to investigate its causes and to find diagnostic markers. This study was part of the InflammoBiota project, funded by the GEN-AU programme (Genomforschung in Österreich). Within the InflammoBiota project, a consortium of scientists of different disciplines tried to obtain a better understanding of the causes of IBD (<http://gutmicrobiota.univie.ac.at/inflammobiota>, 22.05.2013). The impact of two factors was investigated: 1) the role of the JAK-STAT pathway during inflammation and 2) the involvement of the microbiota. The experiments were based on mouse models as they, in contrast to humans, can be investigated using controlled conditions.

2.3.1 Controlled experimental design – DSS induced murine colitis

Different mouse trials were set up in order to investigate the development of dextran sodium sulphate (DSS) induced colitis. The model of DSS induced murine colitis using oral administration via the drinking water is the most commonly used (Johansson et al.,

2010). On the one hand, different mouse genotypes (wild-type (wt, C57BL/6N mice), STAT1 and TYK2 knockout (STAT1^{-/-} and TYK2^{-/-}) mice) were used, on the other hand, the experimental setup was varied. Figure 2-3 gives an example of such an experiment (Trial A). After the oral administration of DSS for seven days the mice started losing weight which is an indicator for developing intestinal inflammation.

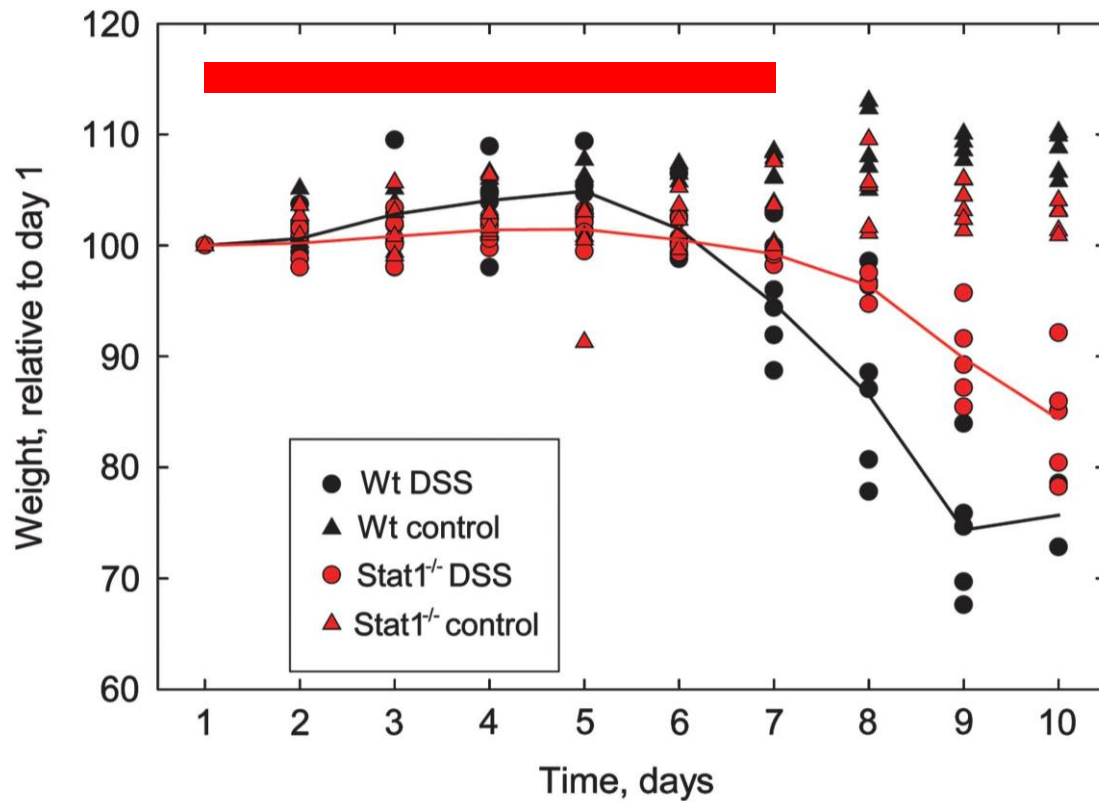


Figure 2-3: The body weight (relative to day 1) for each mouse of the acute murine colitis model (Berry et al., 2012). The red bar indicates DSS treatment, lasting from day 1 to day 7. The sampling took place on day 10.

2.3.2 The role of the JAK-STAT pathway in signal transduction

The immune system has a great influence on IBD (Aaronson and Horvath, 2002). An important signal transduction pathway is the Janus kinase – signal transducer and activator of transcription (JAK-STAT) pathway. There exist four different JAK (including tyrosine kinase 2 (TYK2)) and seven STAT proteins (amongst others STAT1). When the receptor is activated by extracellular signalling polypeptides, the JAKs get activated by auto-phosphorylation. Subsequently, docking sites for STATs are built which then

get activated via phosphorylation, too. The STATs then build dimers and are transported to the nucleus where they induce the transcription of target genes. (Aaronson and Horvath, 2002)

STAT1 knockout (STAT1^{-/-}) mice are reported to have an attenuated course of DSS induced murine colitis due to the alterations in the JAK-STAT signalling pathway (Bandyopadhyay et al., 2008). Due to these findings it was chosen to investigate the effect of DSS on STAT1^{-/-} mice. As TYK2 is also involved in the JAK-STAT pathway, mice lacking this gene were included in order to investigate if differences can be observed.

2.4 Increase of low abundant bacterial taxa in murine colitis

Using this murine model of colitis, Berry et al. (2012) assigned the relative abundance of mRNA and rRNA reads from metatranscriptomic libraries to order level (Figure 2-4). Shifts in the low abundance orders (*Deferribacterales*, *Verrucomicrobiales* and *Enterobacterales*) were observed when the bacterial 16S rRNA transcripts for the control mice were compared to the DSS treated ones.

Especially, the *Verrucomicrobiales* were only present in the DSS treated mice (both wt and STAT1^{-/-}), which are represented by the genus *Akkermansia*. The type strain *Akkermansia muciniphila* (Figure 2-5) is a strictly anaerobic gram-negative bacterium which grows on mucin which is used as sole carbon, nitrogen and energy source (Derrien et al., 2004). It was isolated from the human GI tract (Derrien et al., 2004). The niche specialisation of mucin degradation generates an advantage in nutrient deprivation (Belzer and de Vos, 2012; Costello et al., 2010; Sonoyama et al., 2009). Until now, just one species (*A. muciniphila*) and its genome out of at least eight species of this genus is characterized (van Passel et al., 2011). Other *Verrucomicrobia* were found to colonize the gastrointestinal tract of various animals. They form five distinct clades and share at least 80 % similarity on the 16S rRNA gene level to *A. muciniphila* (Belzer and de Vos, 2012).

A further metatranscriptomic analysis (Berry et al., 2012) showed that *Akkermansia* associated mRNAs of functional genes were also exclusively detected in DSS treated mice. Examples for these are rubrerythrin (*rbr*), which is an indicator for oxidative

stress (Kurtz, 2006; Lehmann et al., 1996), the β -N-acetylhexosaminidase (*bnh*), which is linked to carbohydrate metabolism and may be involved in mucin degradation (Figure 2-6, Turrone et al., 2010), and the capsular exopolysaccharide (*epsc*), as *Akkermansia* is capsule-possessing (Derrien et al., 2004; van Passel et al., 2011).

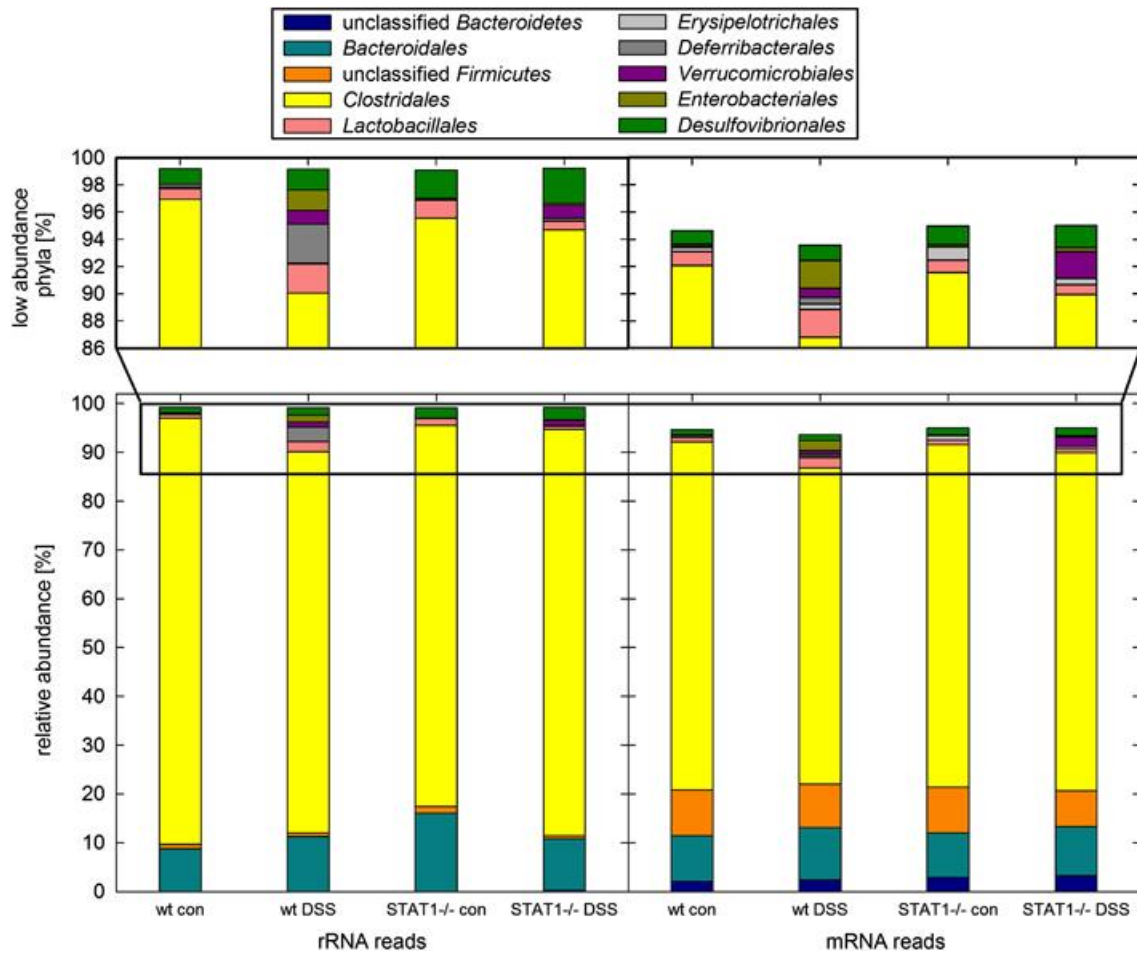


Figure 2-4: Taxonomic composition of rRNA and mRNA reads in acute murine colitis from metatranscriptomic libraries which were assigned to 'order' levels (Berry et al., 2012). The differences in wt compared to STAT1^{-/-} mice and of a control versus a DSS treated group was observed.

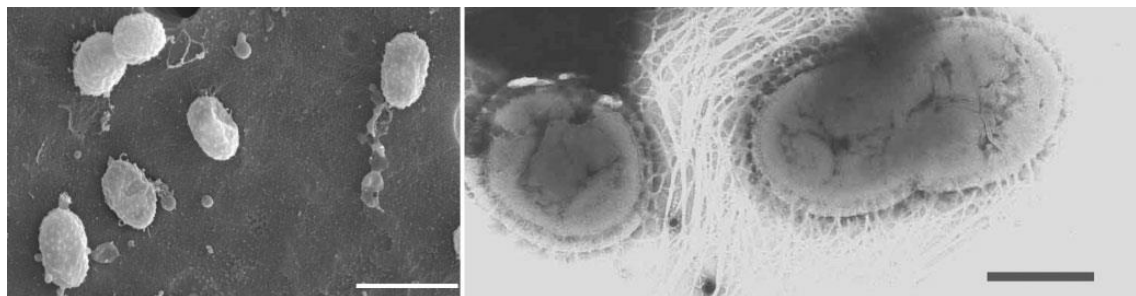


Figure 2-5: Electron microscopic pictures of *Akkermansia muciniphila* (Derrien et al., 2004). A: Transmission electron microscopical picture. B: Scanning electron microscopical picture, showing extensive capsule fibres of the cells. The bar on each picture indicates 0.5 μ m.

Introduction

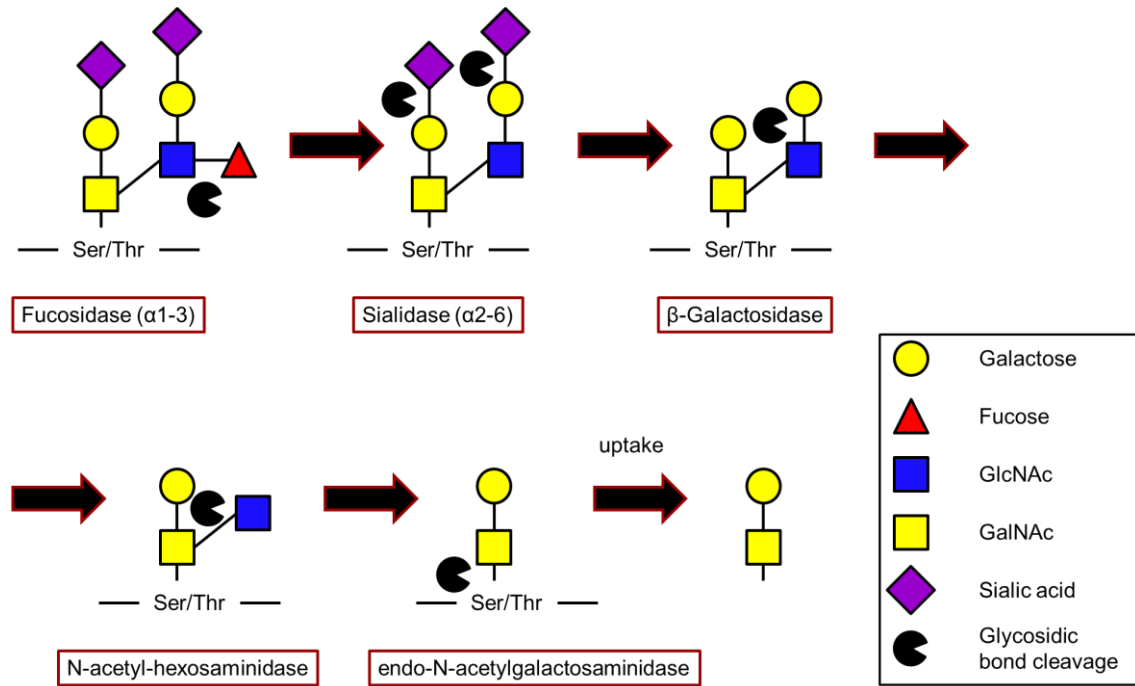


Figure 2-6: Metabolism of mucin degradation of *Bifidobacterium bifidum* and the predicted target sites of involved enzymes (modified from Turroni et al., 2010). Ser: serine; Thr: threonine; GlcNAc: N-acetylglucosamine; GalNAc: N-acetylgalactosamine.

2.5 Shifts in gut microbiome function during acute murine colitis

Berry et al. (2012) showed that the most abundant functional gene categories detected in the transcriptome were carbohydrates, motility and chemotaxis, and protein metabolism (Figure 2-7). The most apparent shift between control and DSS treated mice occurred in the motility and chemotaxis category with a lower transcript appearance in the DSS treated mice for both genotypes (wt and STAT1^{-/-}). This category was mainly represented by clostridal flagellin transcripts.

Introduction

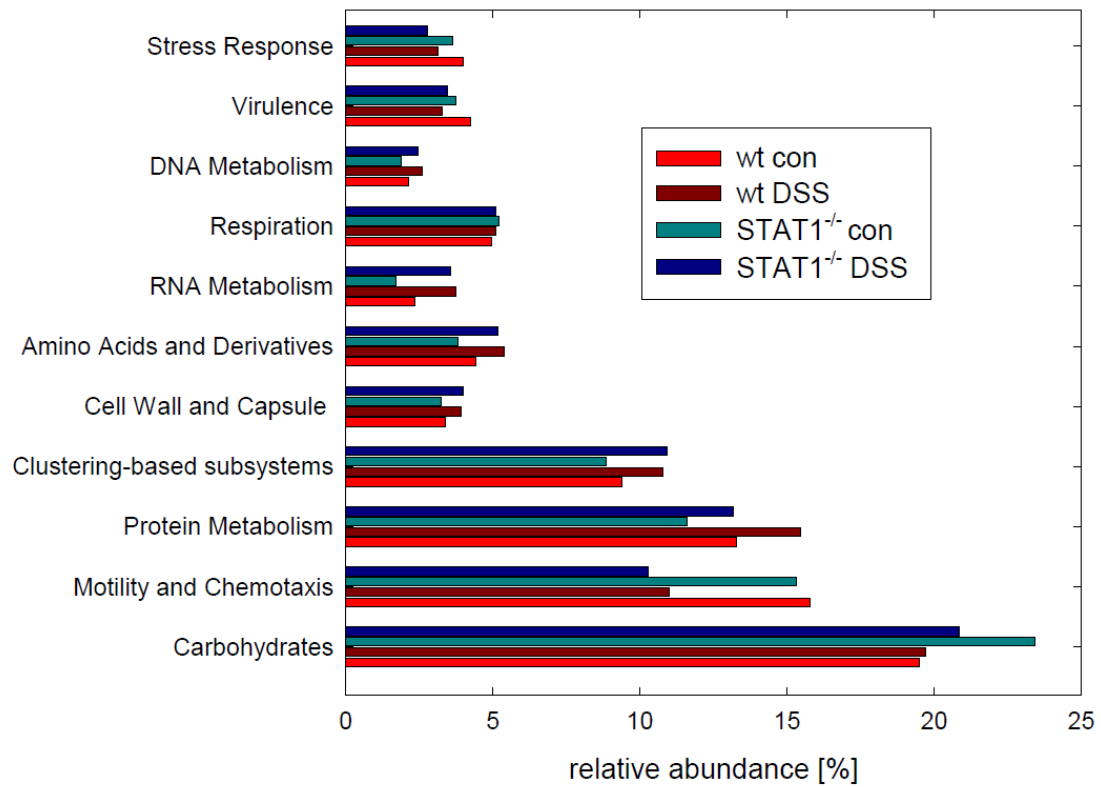


Figure 2-7: Abundance of functional gene categories in acute murine colitis (Berry et al., 2012).

Additionally, the two most abundant phylotypes within the *Lachnospiraceae* order were found to be either drastically decreased (OTU_11021) or increased (OTU_9468) during inflammation (Berry et al., 2012). Combining this observation with the decrease of flagellin abundance during inflammation, they postulated that OTU_11021 was flagellated whereas OTU_9468 did not possess flagella.

2.6 The aim of this study

The overarching goal of the interdisciplinary InflammoBiota project was to identify early microbial markers of IBD for diagnostic purposes and as potential causative agents of the disease. The specific aim of the present study was to investigate and verify earlier identified IBD-specific candidates of bacterial markers which might play a role in disease. *Akkermansia* was analysed as a potential indicator organism and the clostridial flagellin (*fla*) as an indicator protein. Both were chosen based on data obtained by Berry et al. (2012). Also, it was aspired to investigate if different functional genes of *Akkermansia* (*rbr*, *bnh*, *epsc*) can be used as markers for this organism.

To investigate the abundance of *Akkermansia* (16S rRNA and functional genes) and the flagellin gene, quantitative polymerase chain reaction (qPCR) was performed to determine shifts in gene and transcript levels. For this purpose, already published specific primers and newly designed primers were established for qPCR. The specificity of the newly designed primers and the PCR conditions were validated by sequencing of the obtained amplicons and comparing them to published sequences (blastx). Additionally, various microscopy approaches were applied to visualize flagella. Also, immunofluorescence (IF) and fluorescence *in situ* hybridization (FISH) were combined to verify the results obtained by qPCR and to investigate if the decrease in flagellin transcription is linked to the decrease of a specific taxon.

3 Materials

3.1 Chemicals

6 × DNA loading dye	Fermentas
Agarose (LE)	Biozym
Ampicillin	Sigma-Aldrich®
Basic fuchsin	Sigma-Aldrich®
Big dye	Applied Biosystems
Bovine serum albumin (BSA)	Fluka
Citifluor	Citifluor Ltd.
Dextran sodium sulfate (DSS)	Sigma-Aldrich®
4,6-Diamidino-2-phenylindole dihydrochloride (DAPI)	Sigma-Aldrich®
dNTPs	Fermentas
Ethidium bromide (EtBr)	AppliChem
iQ SYBR Green supermix	Bio-Rad
KCl	Merck
LB-Agar	Roth
LB-Medium	Roth
NaCl	AppliChem
Poly-L-lysine	Sigma-Aldrich®
Random hexamer primer	Fermentas
Sequencing buffer	Applied Biosystems
TAE-buffer (Rotiphorese® 50 × TAE buffer)	Roth
Tannic acid	Sigma-Aldrich®
Tween® 20	Roth
Vectashield	Vector laboratories
X-Gal	Fermentas

3.2 Kits

E.Z.N.A.® Plasmid Miniprep Kit II	Omega
NanoOrange® Protein Quantitation Kit	Qiagen
NucleoSpin® Gel and PCR Clean-up kit	Machery-Nagel
QIAprep Spin Miniprep Kit	Qiagen
QIAquick PCR Purification Kit	Qiagen
QuantiTect SYBR Green PCR Kit	Qiagen
SuperScript – Double Stranded cDNA synthesis script kit	Invitrogen
TOPO TA cloning Kit	Invitrogen

All the kits were used with the supplied material.

3.3 Mice

C57BL/6N (wild-type)	Berry et al., 2012
STAT1 ^{-/-}	Meraz et al., 1996
TYK2 ^{-/-}	Hainzl et al. (manuscript in preparation)

3.4 Buffers

Washing buffer (IF)

1 × PBS	50 ml
Tween® 20	50 µl

Blocking buffer (IF)

1 × PBS	50 ml	
Tween® 20	50 µl	
BSA	1 g	
NaAZ	100 µl	(added after sterile filtration)

Hybridization and washing buffers (FISH)

The composition of the hybridization and corresponding washing buffers for FISH are listed in Table 3-1.

Table 3-1: Compositions of hybridization and washing buffers at different FA concentrations.

	Hybridization buffers										
FA concentration	0%	10%	20%	25%	30%	35%	40%	50%	60%	70%	80%
Milli-Q water [μ l]	800	700	600	550	500	450	400	300	200	100	0
FA [μ l]	0	100	200	250	300	350	400	500	600	700	800
1 M NaCl [μ l]	180	180	180	180	180	180	180	180	180	180	180
1 M Tris/HCl [μ l], pH = 8	20	20	20	20	20	20	20	20	20	20	20
SDS (10%) [μ l]	1	1	1	1	1	1	1	1	1	1	1

	Washing buffers										
FA concentration	0%	10%	20%	25%	30%	35%	40%	50%	60%	70%	80%
1 M NaCl [μ l]	9000	4500	2150	1490	1020	700	460	180	40	0	0
1 M Tris/HCl [μ l], pH = 8	1000	1000	1000	1000	1000	1000	1000	1000	1000	1000	1000
0.5 M EDTA [μ l]	0	0	500	500	500	500	500	500	500	500	500
Milli-Q water [ml]	40.0	44.5	46.4	47.0	47.5	47.8	48.0	48.3	48.5	48.5	48.5

3.5 Media

SOB-Medium

2 % Bacto Trypton
0.5 % Yeast extract
10 mM NaCl
2.5 mM KCl

SOC-Medium

SOB-Medium
20 mM Glucose
20 mM Mg²⁺

3.6 Antibiotics

Ampicillin

Sigma-Aldrich®

3.7 Microorganisms

<i>E. coli</i> TOP10 chemically competent cells	Invitrogen
---	------------

3.8 Vectors

pUC19	Invitrogen
pCR [®] 4-TOPO [®] vector	Invitrogen

3.9 Enzymes

Polymerase

GoTaq [®] DNA Polymerase	Promega
-----------------------------------	---------

The reactions were performed with the supplied buffers and solutions.

Restriction endonucleases

<i>Nco</i> I	BioLabs [®] Inc.
<i>Not</i> I	Fermentas
<i>Pst</i> I	Fermentas

The restriction digest was performed with the supplied buffers.

3.10 Primers (5' → 3')

All primers are presented in 5' to 3' direction. They were ordered from Thermo Fisher Scientific.

3.10.1 Primers targeting 16S rRNA genes

Total bacteria (TB, product length: 200 bp)

For: 5'-CGG YCC AGA CTC CTA CGG G-3' (Lee et al., 1996)

Rev: 5'-TTA CCG CGG CTG CTG GCA C-3' (Lee et al., 1996)

Akkermansia spp. (AM, product length: 327 bp)

For: 5'-CAG CAC GTG AAG GTG GGG AC-3' (Collado et al., 2007)

Rev: 5'-CCT TGC GGT TGG CTT CAG AT-3' (Collado et al., 2007)

Clostridial cluster IV: *Ruminococcaceae* (CIIIV, product length: 130 bp)

For: 5'-GCA CAA GCA GTG GAG T-3' (Matsuki et al., 2004)

Rev: 5'-CTT CCT CCG TTT TGT CAA-3' (Matsuki et al., 2004)

Clostridial cluster XIVa: *Lachnospiraceae* (CIXIVa, product length: 438 – 441 bp)

For: 5'-AAA TGA CGG TAC CTG ACT AA-3' (Matsuki et al., 2002)

Rev: 5'-CTT TGA GTT TCA TTC TTG CGA A-3' (Matsuki et al., 2002)

Bacteroides, *Prevotella*, *Porphyromonas* (BPP, product length: 140 bp)

For: 5'-GGT GTC GGC TTA AGT GCC AT-3' (Rinttilä et al., 2004)

Rev: 5'-CGG AYG TAA GGG CCG TGC-3' (Rinttilä et al., 2004)

3.10.2 Primers targeting protein genes

Rubrerhythrin (*rbr*, *Akkermansia*, product length: For1: 194 bp, For2: 146 bp)

For1: 5'-CAA AGC CGC CCA GGA AGG-3' this study

For2: 5'-CAA AGC CGC CCA GGA AGG-3' this study

Rev: 5'-CTA CAT GGA TCT GGA TAT CG-3' this study

Capsular exopolysaccharide (*epsc*, *Akkermansia*, product length: 235 bp)

For: 5'-GAT GAC GGA TGA AAT GGC-3' this study

Rev: 5'-ACG GCA TCC TCC TGT TCC-3' this study

Materials

β -N-Acetyl-hexosaminidase (*bnh*, *Akkermansia*, product length: 156 bp)

For: 5'-GTG GAA CTC CGT TAT ACC ACG-3'	this study
Rev: 5'-GTG GAA CTC CGT TAT ACC ACG-3'	this study

Flagellin (*fla*, *Clostridia*, product length: ~1,500 bp)

For: 5'-GAR AAR ATG MGN AAR CAR AT-3'	(Duck et al., 2007)
Rev: 5'-TTA CTG TAA GAG CTG AAG TAC ACC CTG-3'	(Duck et al., 2007)

primers targeting the conserved region of the flagellin

combined with *fla* For:

NR1Rev: 5'-GCR CCY TCT GCK GTC TG[dl]A-3'	this study
---	------------

combined with *fla* Rev:

CR1For: 5'-CAG AAC MGR YTR GAG CAY ACV AT-3'	this study
CR1Rev: 5'-ATH CGY GAY ACR GAY ATG GC-3'	this study

3.10.3 Primers for sequencing

M13 For (-20): 5'-GTA AAA CGA CGG CCA G-3'	Invitrogen
M13 Rev: 5'-CAG GAA ACA GCT ATG AC-3'	Invitrogen
T3: 5'-ATT AAC CCT CAC TAA AGG GA-3'	Invitrogen
T7: 5'-TAA TAC GAC TCA CTA TAG GG-3'	Invitrogen

3.11 DNA standards

GeneRuler™ 1 kb DNA Ladder, ready-to-use, SM0313	Fermentas
GeneRuler™ 1 kb Plus DNA Ladder, ready-to-use, SM1333	Fermentas
GeneRuler™ 100 bp DNA Ladder, ready-to-use, SM0243	Fermentas
GeneRuler™ 100 bp Plus DNA Ladder, ready-to-use, SM0321	Fermentas
GeneRuler™ 50 bp DNA Ladder, ready-to-use, SM0373	Fermentas

3.12 Microscopy

Confocal laser scanning microscope LSM 510 META

Zeiss

Eclipse 50i Microscope

Nikon

For microscopy, microscope slides from Marienfeld with ten reaction wells (Ø 6 mm) and a black epoxy resin colour mask were used.

3.12.1 Light microscopy

3.12.1.1 Preparation of the basic fuchsin stain

The basic fuchsin stain solution was prepared according to Leifson (1951).

Leifson flagella stain:

Solution A:

NaCl	1.5 g
Milli-Q water	100 ml

Solution B:

Tannic acid	3.0 g
Milli-Q water	100 ml

Solution C:

Basic fuchsin	1.2 g
Ethanol for analysis (97 %)	100 ml

Leave solution C over night on room temperature.

On the next day, the solutions A, B and C were mixed with equal volumes. The pH was adjusted to 5.0 ± 0.2 with 3 % tannic acid or 1 N NaOH.

3.12.2 Fluorescent dyes

3.12.2.1 Preparation for the NanoOrange® stain

The NanoOrange® stain solution was prepared following the protocol of Grossart et al. (2000).

NanoOrange® stain preparation:

10 × protein quantitation diluent	25 µl
Milli-Q water	225 µl
NanoOrange® quantitation reagent	0.5 µl

Before use, the NanoOrange® quantitation reagent was allowed to warm to room temperature, then it was thoroughly mixed and briefly centrifuged. The NanoOrange® stain solution was protected from light.

3.12.2.2 Immunofluorescence antibodies

Primary antibody

Polyclonal antibody to Flagellin Fla1 (Clostridia flagellum) pab0594	Covalab
--	---------

The vial was reconstituted according to the producers information in autoclaved Milli-Q water and, additionally, 0.5 µl NaAZ were added.

Secondary antibodies

Alexa Fluor® 488 Goat Anti-Rabbit IgG (H+L)	life technologies
Alexa Fluor® 555 Goat Anti-Rabbit IgG (H+L)	life technologies
Alexa Fluor® 647 Goat Anti-Rabbit IgG (H+L)	life technologies

3.12.2.3 FISH probes

The EUBmix consisted of the EUB338 (Amann et al., 1990), EUB338-II and EUB338-III (both Daims et al., 1999) probes, all three in equimolar concentrations. For each the *Lachnospiraceae* OTU_11021 and the *Lachnospiraceae* OTU_9468 two probes had to be used that a phylotype specific signal could be obtained (Berry et al., 2012). The Erec482 (Franks et al., 1998) probe was double-labelled to improve the signal quality (Stoecker et al., 2010).

Most bacteria (EUB338, 30 % FA)

5'-GCT GCC TCC CGT AGG AGT-3' Amann et al., 1990

Planctomycetales (EUB338-II, 30 % FA)

5'-GCA GCC ACC CGT AGG TGT-3' Daims et al., 1999

Verrucomicrobiales (EUB338-III, 30 % FA)

5'-GCT GCC ACC CGT AGG TGT-3' Daims et al., 1999

Lachnospiraceae OTU_11021 (Con1127 or LSPotu11021-1127, 30 % FA)

5'-TTC CCA TCT TTC TTG CTG GC-3' Berry et al., 2012

Lachnospiraceae OTU_11021 (Con1448 or LSPotu11021-1448, 30 % FA)

5'-GCA GCT CCC TCC TCT CGG-3' Berry et al., 2012

Lachnospiraceae OTU_9468 (DSS999 or LSPotu9468-999, 10 % FA)

5'-CTT TGC CCA TAC GGC GTC CG-3' Berry et al., 2012

Lachnospiraceae OTU_9468 (DSS1259 or LSPotu9468-1259, 10 % FA)

5'-TGC TCA ACG TCA CCG TCT CG-3' Berry et al., 2012

Most of the *Clostridium coccooides* - *Eubacterium rectale* group (clostridial cluster XIVa and XIVb) (Erec482, 0 % FA)

5'-GCT TCT TAG TCA RGT ACC G-3' Franks et al., 1998

4 Methods

4.1 Animal trials

All experiments with mice were performed and analyzed by collaborators of the InflammoBiota project.

For this study, three different genotypes of mice were investigated. As wild-type (wt), C57BL/6N mice were utilized, the two knockout variants were STAT1^{-/-} (Meraz et al., 1996) and TYK2^{-/-} (Hainzl et al., manuscript in preparation). The mice were each provided with autoclaved drinking water either with or without 2 % DSS *ad libitum*. When the treatment of each mouse reached the scheduled sampling point, they were euthanized and both the luminal content and biopsy samples of the colon were collected (see Berry et al., 2012).

The nucleic acids of these samples were extracted. Afterwards, DNA and RNA were purified (according to Berry et al. (2012) using the AllPrep DNA/RNA Mini kit (Qiagen). In this study, only DNA and RNA recovered from the luminal content samples were used.

Additionally, the body weight was measured daily. For a better comparability, the body weight for each mouse was always calculated compared to day 1.

4.1.1 Trial A – acute murine colitis

For Trial A, 20 mice were used consisting of ten wt (A1 – A10) and ten STAT1^{-/-} (A11 - A20) mice (Table 4-1). For each genotype, five mice were treated with DSS, the other five mice belonged to the control group and were not exposed to DSS at all. For the DSS treated mice the treatment lasted seven days. The samples were taken three days after finishing the DSS treatment (day 10).

Table 4-1: Trial A – labelling of the mice.

	DSS treatment	no DSS treatment
wt	A1 – A5	A6 – A10
STAT1 ^{-/-}	A11 – A15	A16 – A20

4.1.2 Trial C – development of murine colitis

The treatment with DSS for Trial C lasted for maximally seven days with sampling points on days 1, 2, 3, 4 and 7. The measurement of day 1 was right before the DSS treatment, the day 2 sampling was 24 hours after DSS treatment, day 3 sampling 48 hours after DSS treatment, etc. The sampling for each time point was done in triplicates. For Trial C, wt and TYK2^{-/-} mice were used for this study (Table 4-2).

Table 4-2: Trial C – labelling of the mice.

	day 1	day 2	day 3	day 4	day 7
wt	C1 – C3	C4 – C6	C7 – C9	C10 – C12	C13 – C15
TYK2 ^{-/-}	C16 – C18	C19 – C21	C22 – C24	C25 – C27	C28 – C30

4.1.3 Trial G – recovery of murine colitis

In the first recovery model of murine colitis, wt and TYK2^{-/-} mice were used. The DSS treatment lasted for five consecutive days. Afterwards, no DSS was given in the drinking water any more. Sampling points for Trial G were days 1 and 14 with day 1 being sampled right before the DSS treatment. The sampling was done in triplicate (Table 4-3).

Table 4-3: Trial G – labelling of the mice.

	day 1	day 14
wt	G1 – G3	G10 – G12
TYK2 ^{-/-}	G7 – G9	G16 – G18

4.1.4 Trial I – recovery of murine colitis

For Trial I, only wt mice were investigated. The DSS treatment lasted for five consecutive days before the drinking water was DSS free. Sampling points were the days 1, 5, 8, 14 and 25, with day 1 being sampled right before the DSS treatment started. For each time point, four samples were taken (Table 4-4). Until day 16, the weight of every mouse was measured daily, afterwards the weight measurement took place on days 19, 22 and 25.

Table 4-4: Trial I – labelling of the mice.

	day 1	day 5	day 8	day 14	day 25
wt	I1 – I4	I9 – I12	I17 – I20	I25 – I28	I33 – I36

4.2 Molecular analysis

In order to analyze the composition and changes of the bacteria and functional genes in the control mice compared to the ones with DSS induced murine colitis, various molecular methods like qPCR and sequencing were used.

4.2.1 Single strand cDNA synthesis

The reaction was performed according to the Invitrogen SuperScript™ Double-Stranded cDNA Synthesis Kit Manual.

Briefly, 2 µl random hexamers (100 µM), 1 µl dNTPs (10 mM), 9 µl DEPC H₂O and 2 µl template RNA were combined on ice in PCR stripes. Then, they were put in a thermocycler at 70 °C for 10 min and afterwards immediately put on ice again. Next, 4 µl of 5 × Buffer, 1 µl DTT (100 mM) and 1 µl reverse transcriptase (200 u/µl) were added. This mixture was subsequently put into the thermocycler again for 5 min at 25 °C, 1 h at 42 °C, 15 min at 70 °C followed by 4 °C. Further storage was at -20 °C.

Control for chromosomal DNA contamination in the RNA preparation

A polymerase chain reaction (PCR) using the TB primers was performed with RNA as a template following the conditions described above. The RNA was diluted 1:10 times to resemble the concentration in the cDNA synthesis reaction.

4.2.2 Agarose gel electrophoresis

To analyze the length of the DNA fragments, agarose gel electrophoresis with 2 % agarose gels was used. 120 ml 1 × TAE Buffer and 3 g agarose LE were mixed and subsequently heated in a microwave until the agarose was completely solubilized. After cooling down to about 40 °C, approximately two drops of a 1:40 dilution of EtBr (stock solution: 1 %) were added. As running buffer, 0.5 × TAE was used. After the agarose gels were loaded with the samples, 120 V were applied for approximately 30 min to separate the DNA fragments.

4.2.3 Qualitative polymerase chain reaction (PCR)

To amplify specific DNA sequences, a PCR (Mullis et al., 1986) was performed. With exception of the *fla* primers, the suggested conditions were used. Every run contained a negative control without template.

4.2.3.1 Mastermix for qualitative PCR

Mastermix for PCR (50 µl)

buffer	10 µl
MgCl ₂	3 µl
dNTP	1 µl
forward primer (25 pmol/µl)	1 µl
reverse primer (25 pmol/µl)	1 µl
GoTaq®-Polymerase	0.25 µl
DEPC H ₂ O	32.75 µl
template	1 µl

4.2.3.2 Thermal cycling conditions for qualitative PCR

Basic PCR program (30 amplification cycles)

preheat		99 °C
initialization	05:00	95 °C
denaturation	00:30	95 °C
annealing	00:30	60 °C
elongation	00:30	72 °C
final elongation	05:00	72 °C
	hold	4 °C

The PCR program was used for all primer combinations, except for the *epsc* primers (56 °C annealing temperature).

PCR program for the *f/a* primers (36 amplification cycles)

preheat		99 °C
initialization	05:00	95 °C
denaturation	00:30	95 °C
annealing	01:00	44 °C
elongation	01:00	72 °C
final elongation	05:00	72 °C
	hold	4 °C

4.2.3.3 Gradient PCR

Under the conditions suggested for the *f/a* primers (Duck et al., 2007) only a low amplicon yield was obtained. Therefore, a gradient PCR was performed to investigate if the quality of the received amplicons can be improved.

Gradient PCR program for the *fla* primers (36 amplification cycles)

preheat		99 °C
initialization	03:00	95 °C
denaturation	00:30	95 °C
annealing	01:00	44 °C to 52.2 °C
elongation	01:00	72 °C
final elongation	10:00	72 °C
	hold	4 °C

4.2.3.4 Purification of PCR products

The PCR products were purified before cloning, either by the QIAquick PCR Purification Kit or the NucleoSpin® Gel and PCR Clean-up kit, according to the manuals.

4.2.4 Cloning

The protocol of the TOPO TA Cloning Kit for Sequencing (Invitrogen) was followed, with the exception of the duration of the first two incubations (10 min room temperature, 10 min on ice). TA cloning was performed with the previously purified PCR products. Two times 100 µl of the *E. coli* cells were spread on separate LB plates (ampicillin: 100 mg/l). After incubation, a colony PCR was done and the colonies were additionally conserved on a separate agar plate ('master' plate).

4.2.4.1 Colony PCR and master plate

Clones from the original plates were picked with a sterile tip, dipped into PCR-strips containing mastermix (T3 and T7 primers) and then streaked out on new LB plates (ampicillin: 100 mg/l).

4.2.4.2 Plasmid isolation

Colonies grown on the master plate were used for inoculation of 50 ml LB medium (supplemented with 50 µg/ml ampicillin). Cultures were incubated at 37 °C at 200 rpm for about 20 hours. Cells were harvested by centrifugation for 10 min at 5,000 rpm. They were resuspended in 500 µl TE buffer and centrifuged again for 7 min at 4,500 rpm. The supernatant was discarded and plasmid isolation from the cells was performed following the Plasmid Mini Kit II Spin Protocol (starting with step 3).

4.2.4.3 Restriction digest of recombinant plasmids

For the restriction digests, the restriction endonucleases *NotI*, *PstI* and/or *NcoI* were chosen after testing the sequences (<http://tools.neb.com/NEBcutter2/index.php>, 22.05.2013) for cutting sites. Every plasmid was cut with two of the restriction endonucleases. For the reaction, the following components were combined:

plasmid	5 µl
buffer	5 µl
restriction endonuclease	2.5 µl
DEPC H ₂ O	37.5 µl

The mixture was then incubated at 37 °C for 75 min. When *NcoI* was used, an incubation for 20 min at 65 °C followed to inactivate the enzyme. Afterwards, an agarose gel electrophoresis was performed.

4.2.5 Quantitative PCR

In order to quantify bacteria and the transcription of selected genes in the lumen, quantitative PCR (qPCR) was used with either DNA or cDNA as template.

4.2.5.1 Mastermix for quantitative PCR

Even very small amounts of DNA or cDNA can be detected and quantified via qPCR, so this approach was used to be able to compare the abundance of different 16S rRNA and functional genes. For a better comparability, the DNA samples were diluted so that their concentrations (ng/μl) were approximately the same.

Mastermix for qPCR (20 μl)

iQ SYBR Green Supermix	10 μl
forward primer (10 pmol/μl)	1 μl
reverse primer (10 pmol/μl)	1 μl
DEPC H ₂ O	7 μl
template	1 μl

4.2.5.2 Conditions for quantitative PCR

Basic qPCR program (40 amplification cycles)

initialization	02:00	95 °C
denaturation	00:15	95 °C
annealing	00:20	60 °C
elongation	00:30	72 °C
	00:15	95 °C

Afterwards, the melting curves were analyzed and an agarose gel electrophoresis was performed to verify the amplicon identity and length, respectively.

qPCR program for the flagellin primers (40 amplification cycles)

initialization	02:00	95 °C
denaturation	00:15	95 °C
annealing	00:30	50 °C
elongation	00:30	72 °C
	00:15	95 °C

Afterwards, the melting curves were analyzed and an agarose gel electrophoresis was performed to verify the amplicon identity and length, respectively.

4.2.5.3 Preparation of the standards for qPCR

As standards, linearized plasmids were used with exception of the standards for the TB primer where purified PCR products were used. Each standard was diluted six times, each tenfold in DEPC H₂O (ranging from 1:10 to 1:1,000,000). For every qPCR run, the standards were freshly prepared. The range of the R² and efficiency for each primer pair is listed in Table 4-5.

Table 4-5: Efficiency and R² of the primers used for qPCR.

targeting	primer	efficiency	R ²
16S rRNA	TB ^a	0.87 – 1.02	0.981 – 0.986
	AM ^b	0.80 – 0.87	0.983 – 0.999
	CIIV ^c	0.82 – 0.95	0.996 – 0.999
	CIXIVa ^d	0.82 – 0.95	0.996 – 0.999
protein gene	<i>rbr</i> ^e	0.80 – 0.92	0.995 – 0.999
	<i>epsc</i> ^f	0.81 – 0.92	0.996 – 0.999
	<i>bnh</i> ^g	0.86 – 0.9	0.992 – 1
	<i>fla</i> ^h	0.75 – 0.86	0.997 – 1

^a total bacteria; ^b *Akkermansia*; ^c clostridial cluster IV; ^d clostridial cluster XIVa; ^e rubrerythrin; ^f capsular exopolysaccharide; ^g β -N-acetylhexosaminidase; ^h clostridial flagellin

4.2.5.4 Statistical analysis of the qPCR data

With the obtained qPCR data, the log gene (transcript) copies/ μ g DNA (RNA), their average and standard deviation were calculated in Microsoft Excel 2010. The further statistical analysis and graph design was done with SigmaPlot 11.0. As statistical tests, either the Student's t-test or, if the normality test failed, the Mann-Whitney Rank Sum test was performed for the Trials A and G. For the Trials C and I, a One-Way ANOVA with the Holm-Sidak test or Dunn's test as post-hoc test were performed to identify which groups were significantly different. $p \leq 0.05$ was considered significant. If not described differently, the outcomes were not significant.

4.2.6 Sequencing of the flagellin gene

The sequencing reaction was performed in house by Sanger sequencing using the conditions suggested by the BigDye[®] Terminator v3.1 Cycle Sequencing Kit Protocol

(Applied Biosystems). First, 2 µl PCR product, 2 µl BigDye, 1 µl sequencing buffer, 1 µl primer (either T3 or T7 primer) and 4 µl DEPC H₂O were mixed together. The sequencing program comprised 5 min at 95 °C, followed by 30 cycles of 30 sec at 95 °C, 10 sec at 55 °C and 4 min at 60 °C.

4.2.6.1 Analysis of the sequenced data

The received sequences were compared against the NCBI non-redundant database using blastx

(http://blast.ncbi.nlm.nih.gov/Blast.cgi?PROGRAM=blastx&BLAST_PROGRAMS=blastx&PAGE_TYPE=BlastSearch&SHOW_DEFAULTS=on&BLAST_SPEC=&LINK_LOC=blasttab&LAST_PAGE=blastx, 22.05.2013).

4.3 Microscopy

For microscopy, cells were fixed with 4 % PFA. All samples were analysed by phase contrast microscopy (basic fuchsin stain), fluorescence microscopy (NanoOrange®, IF and FISH) and combinations of the stains.

4.3.1 Light microscopy

4.3.1.1 Basic fuchsin stain

Protocol for the basic fuchsin stain

For preparation of the slides, 5 µl of a 1:100 dilution of the samples in Milli-Q water were spread on a well of the microscope slide. Then, the samples were left to air dry at room temperature. It was not possible to heat fix the samples because this procedure would destroy the proteinaceous flagella structure (Mellies, 2008).

To stain the samples, three big drops of the Leifson dye solution were put on the wells. The samples were carefully observed to avoid that the wells dry out during the staining

time. The slides were incubated at room temperature for 7 to 15 min. The development of a golden film on the dye surface served as an indicator for the end of the staining procedure. The optimal incubation time had to be determined for each stock of dye by a time series (performed in 2 min steps between 7 and 15 min). Then, the stain was removed by floating off the film by gently flowing tap water. After that, the slides were left to air dry. As original mounting medium, tap water was used.

Optimization of the basic fuchsin stain

With regard to combine the basic fuchsin stain with other microscope methods, experiments with various conditions were performed.

Rinse with tap water/Milli-Q water

After the incubation with the basic fuchsin solution on the slide, the slides are originally rinsed with tap water. The same procedure was tested using Milli-Q water instead of the tap water.

Mounting medium – Vectashield/Citifluor

Originally, tap water was used as mounting medium. As Vectashield or Citifluor are usually used for fluorescent dyes, these two were tested as mounting medium. Therefore, after removing the basic fuchsin solution from the slides, they were left to air dry. Then, either Vectashield or Citifluor was applied on the slides.

EtOH-series

As the EtOH-series is important for FISH to dehydrate the samples, it was tested if there was any impact on the basic fuchsin stain. Therefore, after letting the samples air dry, the slide was put for 3 min each in 50 %, 80 % and 97 % EtOH.

Flame treatment of the slides

As it is suggested to wipe the slides clean with 95 % ethanol using a lint-free tissue and then flame the slide to dry (Mellies, 2008), it was investigated if the stain can be used without that treatment, too.

Dilution of the sample in Milli-Q water or 1 × PBS

To determine if the dilution of the samples with different solutions has an impact on the basic fuchsin stain, the dilution with Milli-Q water or 1 × PBS was investigated.

Sterile filtered

Since there was some grainy background using the basic fuchsin stain it was tested if sterile filtration (\varnothing 0.45 μ m) caused an improvement.

Poly-L-lysine

To investigate if the attachment of the bacteria on the slides could be improved, 0.1 % poly-L-lysine was put on the wells. Everything of the poly-L-lysine but a thin layer was pipetted off again and the slides were then left to air dry before the samples were applied.

4.3.2 Fluorescence microscopy

4.3.2.1 NanoOrange®

Stain protocol

10 μ l of a 1:100 dilution in 1 \times PBS were spread on the wells of the slide and left to air dry. Then, 10 μ l 1 \times PBS were applied on each well for a better distribution of the 0.5 μ l NanoOrange® solution which were added right afterwards. After a light protected incubation of 10 to 15 min, the liquid was pipetted off. As mounting medium, Vectashield was used.

4.3.2.2 Immunofluorescence

Protocol for immunofluorescence

This method was used according to Bulgheresi et al. (2006). For immunofluorescence, 5 μ l sample were spread on a well with the desired dilution in 1 \times PBS. The slide was left to air dry. Then, the slide was washed three times for 5 min with each 30 μ l washing buffer. In between, the liquid was pipetted off. Afterwards, 30 μ l of blocking solution were applied on each well. When the incubation of 1 h was finished, the liquid was pipetted off and 30 μ l of a 1:500 dilution of primary antibodies was applied. The slide was then put on 4 °C over night in a Greiner tube with a tissue soaked in Milli-Q

water. On the next day, the liquid was pipetted off and a three times 5 min washing step with each 30 µl washing buffer followed. The liquid was pipetted off in between. Then, an incubation for 1 h with 30 µl secondary antibodies (1:250 dilution in blocking buffer of a glycerol stock) followed. After pipetting the liquid off, the last washing step with three times 5 min was performed where, again, the liquid was pipetted off in between. Finally, Vectashield was applied.

Negative control

For the negative control, blocking solution was applied instead of the primary antibody to observe if the secondary antibody also binds unspecifically.

4.3.2.3 Fluorescence in situ hybridization

On the slides, 5 µl of the sample was applied and afterwards dried. Then, the samples were dehydrated by the EtOH series (50 %, 80 %, 97 % EtOH for each 3 min). For each slide, a hybridization buffer was prepared using the Formamide concentration which was attuned to the FISH probes. Each well was applied with 10 µl hybridization buffer and 1 µl of probe mix per probe. Then, the slides were put in a hybridization chamber. 50 ml Greiner tubes containing a piece of tissue soaked with the residual hybridization buffer served as hybridization chambers. After at least two hours of hybridization at 46 °C, the samples were dipped into a preheated washing buffer solution, placed in a 48 °C water bath. After ten minutes, the slides were shortly dipped into ice-cold Milli-Q water and immediately dried using an air-jet. Finally, the slides were analyzed by confocal laser scanning microscopy. This method was performed as described by Daims et al. (2005).

All the FISH was done by Julia Ramesmayer (Department of Microbial Ecology, Vienna).

4.4 Combinations of microscopy techniques

4.4.1 IF-basic fuchsin

Both orders of the stains were tested (IF → basic fuchsin and basic fuchsin → IF). The techniques were always performed as reported before. On each well, 5 µl of the sample (1:100 dilution in Milli-Q water) were spread. For a better distribution of the sample, the slide was flamed prior to use. To rinse off the basic fuchsin stain, Milli-Q water was used. The basic fuchsin solution which was applied was either sterile filtered or not. Either Milli-Q water or Citifluor were used as mounting medium.

4.4.2 FISH-basic fuchsin

When combining FISH with the basic fuchsin stain, independent of the order of the used techniques, the EtOH-series had to be done prior to starting either of the stains. Then, the two techniques were performed one after another as reported before with as well starting with FISH as the basic fuchsin stain.

4.4.3 DAPI-NanoOrange®

10 µl of sample (1:100 dilution in Milli-Q water) were applied on a slide and left to air dry. DAPI was used in a 1:1,000 dilution in 1 × PBS. The procedure was performed as follows:

1 × PBS	10 µl	5 min	
DAPI	10 µl	10 min	(from this point on in the dark)
1 × PBS	30 µl	5 min	
NanoOrange®	2 µl	15 min	

It was not possible to pipet off the remaining liquid after any step because it was already dried. Finally, Vectashield was applied.

4.4.4 DAPI-IF

For this combination of stains, the immunofluorescence protocol was followed as written above. After the last washing step, 30 µl of a 1:1,000 dilution of DAPI in 1 × PBS were applied and incubated for 10 min in the dark. Then, the slide was washed once more with 30 µl 1 × PBS (with Tween® 20 DAPI fades faster). Finally, Vectashield was applied.

4.4.5 IF-NanoOrange®

The immunofluorescence protocol was followed as reported above. After the last washing step, 10 µl 1 × PBS and 0.5 µl NanoOrange® were applied on the wells. The incubation lasted for 15 min in the dark. Vectashield was used as mounting medium.

4.4.6 FISH-NanoOrange®

The FISH protocol was performed as reported above. Then, 10 µl 1 × PBS and 0.5 µl, 1 µl or 1.5 µl NanoOrange® solution, respectively, were applied on the wells. After 10 min of incubation the liquid was pipetted off. Vectashield was used as mounting medium.

4.4.7 IF-FISH

Before either of the stains was executed, the EtOH-series took place. Then, the protocols which are written above were followed, for both FISH and immunofluorescence being the first stain. This method was performed with and without poly-L-lysine. As mounting medium, either Vectashield or Citifluor was used.

4.4.8 Analysis of the microscopy pictures for IF-FISH

For quantification of the bacteria, the *daime* image analysis software (Daims et al., 2006) was used. Correlation with the qPCR data for the flagellin gene was tested with the Pearson Product Moment Correlation using SigmaPlot 11.0.

5 Results

The experiments were based on previous studies where shifts of *Akkermansia* and flagellin abundance had been reported during inflammation. These two potential markers for colitis were investigated during acute inflammation, development and recovery. For this purpose, mouse models using DSS were utilized. After establishing qPCR, this method was used to analyze *Akkermansia* 16S rRNA genes and the flagellin gene as taxonomic and functional markers, respectively. Additionally, to assign the flagella to specific bacterial orders or species, immunofluorescence and FISH were combined.

5.1 Mouse trials

All the mouse trial experiments were performed by collaborators of the InflammoBiota project.

5.1.1 Weight curves for acute colitis– Trial A

During the experiment, the body weight of each mouse was measured every day (Figure 5-1). Three of the DSS treated wt mice had to be euthanized before the experiment ended due to their weight loss of more than 30 % of their initial weight (Berry et al., 2012). Over the whole time, the weight of the control mice (both the wt and STAT1^{-/-} without treatment), stayed about the same or even gained some weight. The weight of the DSS treated mice also did not change over the first five days. However, starting on day 6, the mice began to lose weight until the end of the trial. The weight loss for the DSS treated mice was more pronounced in the wt compared to the STAT1^{-/-} mice with significant differences on days 5 and 9 (day 5: $t = 2.453$, $p = 0.040$; day 9: $t = 4.604$, $p = 0.002$).

Results

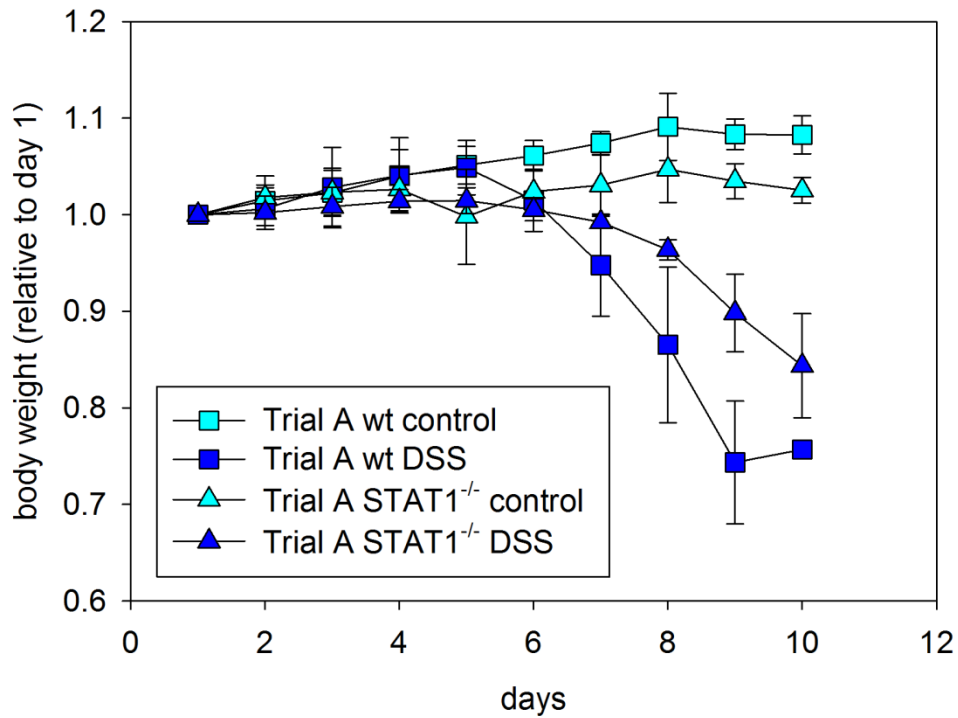


Figure 5-1: Weight curve during DSS induced acute murine colitis for Trial A. DSS treatment started on day 1 and lasted until day 7. The samples for the metatranscriptome analysis were taken on day 10. Three of the five DSS treated wt mice succumbed before day 10.

5.1.2 Weight curves for colitis development – Trial C

During the colitis development experiment, the mice started to lose weight beginning on day 6 (Figure 5-2). As the mice were only investigated until day 7, the weight loss was just at the beginning. No difference occurred comparing wt and TYK2^{-/-} mice.

Results

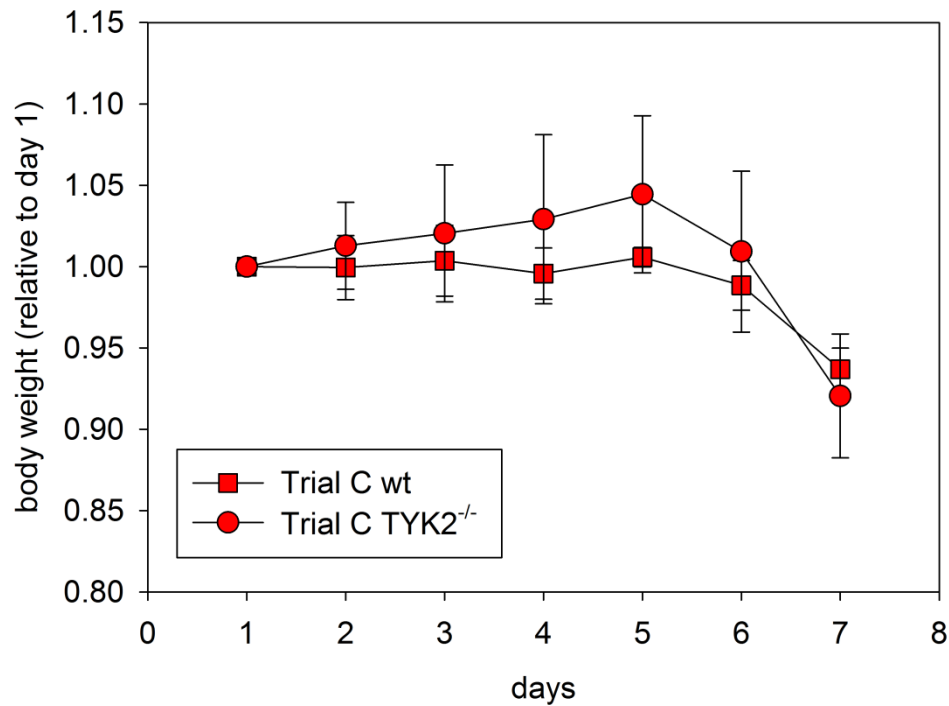


Figure 5-2: Weight curve during DSS induced murine colitis development for Trial C. DSS treatment started on day 1 and lasted until day 7. Samples for the metatranscriptome analysis were taken on the days 1, 2, 3, 4 and 7.

5.1.3 Weight curves for recovery of murine colitis – Trial G & I

In the recovery models, the weight loss began on day 6 with the lowest relative body weight on days 10 (Trial G: Figure 5-3) and 9 (Trial I: Figure 5-4), respectively. Afterwards, the mice started to gain weight again until they were even heavier than their initial weight. In both trials, the mice regained their initial weight again at about day 14. No differences in the weight curves were observed between the mouse genotypes in Trial G (wt and TYK2^{+/-}).

Results

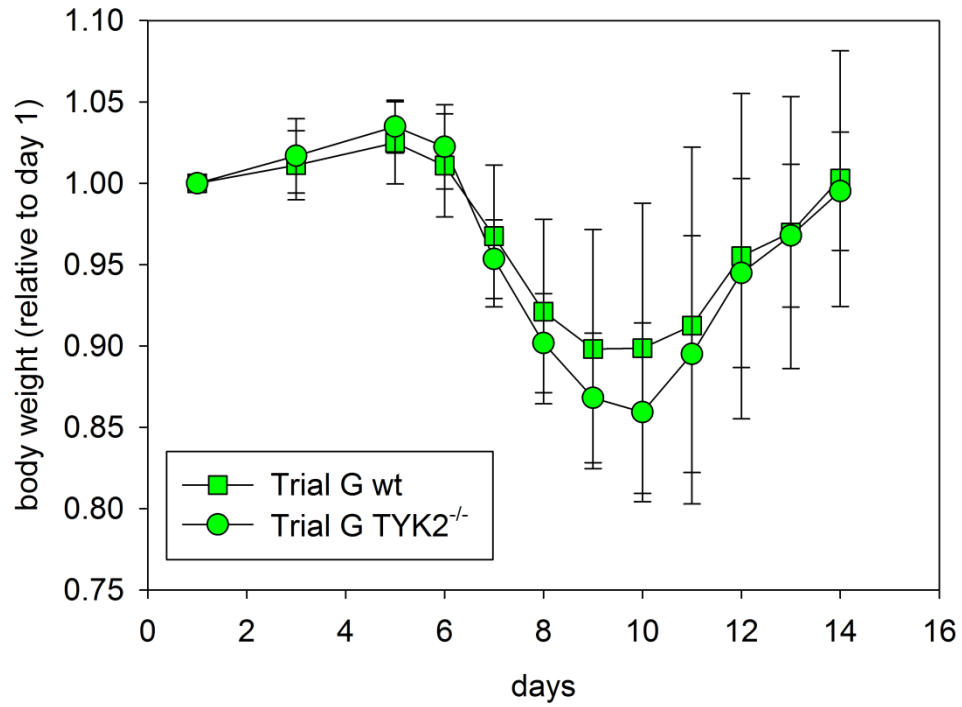


Figure 5-3: Weight curve for DSS induced murine colitis recovery for Trial G. DSS treatment started on day 1 and lasted until day 5. Samples for the metatranscriptome analysis were taken on the days 1 and 14.

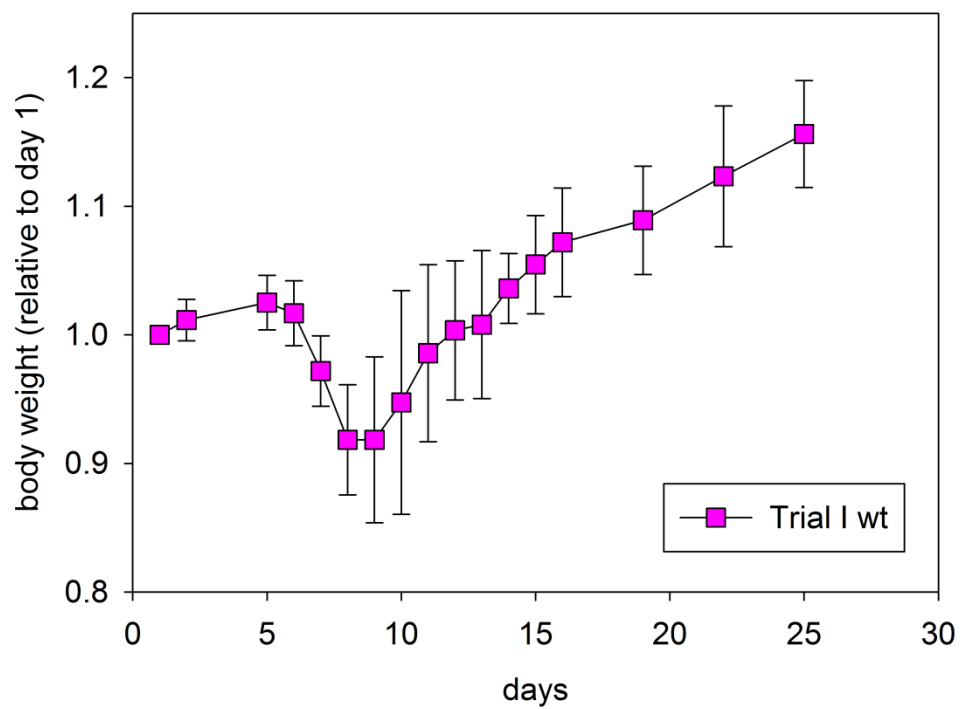


Figure 5-4: Weight curve during the DSS induced murine colitis recovery for Trial I. DSS treatment started on day 1 and lasted until day 5. Samples for the metatranscriptome analysis were taken on the days 1, 5, 8, 14 and 25.

5.2 Establishment of quantitative PCR assays

5.2.1 Validation and optimization of the conditions for qualitative PCRs

All primers targeting either the 16S rRNA (Table 5-1) or functional genes (Table 5-2) were tested with the Trial A DNA samples. For all the primers, amplicons with the correct length were obtained using the basic conditions with exception of the *fla* primers. As a better performance of the *fla* primers than that obtained with the suggested parameters (Duck et al., 2007) was attempted, a gradient PCR was executed to determine the best temperature settings (Figure 5-5). All the amplicons had the correct length of about 1,500 bp with most of the product obtained with the lower annealing temperatures. Henceforth, 44 °C was subsequently used as annealing temperature for qualitative PCR.

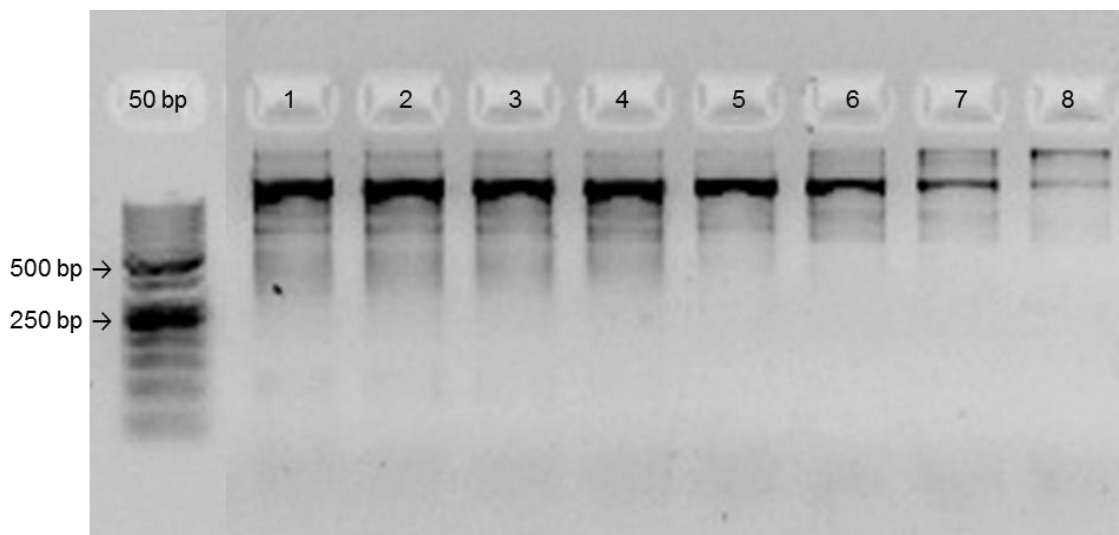


Figure 5-5: Agarose gel electrophoresis picture for the gradient PCR of the *fla* primers using sample A8. The temperatures for the lanes are as follows: 1: 44 °C, 2: 44.3 °C, 3: 45.2 °C, 4: 46.4 °C, 5: 47.8 °C, 6: 49.2 °C, 7: 50.8 °C, 8: 52.2 °C.

For the primers targeting the 16S rRNA genes (Table 5-1) of the total bacteria, the *Bacteroides-Prevotella-Porphyromonas* group, clostridial cluster IV and CIXIVa, an amplicon was obtained for every sample of Trial A. *Akkermansia* 16S rRNA genes mainly appeared in the samples of the DSS treated mice. This outcome resembled the one of Berry et al. (2012) where Bacteroidetes and Firmicutes (especially *Lachnospiraceae* and *Ruminococcaceae*) also occurred in all samples whereas the

Results

Verrucomicrobia (represented by *Akkermansia*) were just detected in the samples of the DSS treated mice of both genotypes.

Table 5-1: 16S rRNA primers tested with qualitative PCR using Trial A DNA as template.

		presence of bacterial groups				
		primer	TB ^d	BPP ^e	AM ^f	CIIV ^g CIXIVa ^h
wt DSS	A3	+	+	+	+	+
	A5	+	+	+	+	+
wt cont. ^a	A6	+	+	+	+	+
	A7	+	+	+	+	+
	A8	+	+	— ^c	+	+
	A9	+	+	—	+	+
	A10	+	+	—	+	+
STAT1 ^{-/-} DSS	A11	+	+	+	+	+
	A12	+	+	+	+	+
	A13	+	+	+	+	+
	A14	+	+	+	+	+
	A15	+	+	+	+	+
STAT1 ^{-/-} cont.	A16	+	+	—	+	+
	A17	+	+	—	+	+
	A18	+	+	—	+	+
	A19	+	+	—	+	+
	A20	+	+	—	+	+

^a control; ^b amplicon obtained; ^c no amplicon obtained; ^d total bacteria; ^e *Bacteroides-Prevotella*-*Porphyromonas*; ^f *Akkermansia*; ^g clostridial cluster IV; ^h clostridial cluster XIVa

When targeting the protein genes (

Table 5-2) with primers covering rubrerythrin, capsular exopolysaccharide and β -N-acetylhexosaminidase (all functional genes of *Akkermansia*), the results mainly followed the trend of the 16S rRNA gene abundance as products were only present in the samples of the DSS treated STAT1^{-/-} samples. With the flagellin-specific-primers, just the Trial A wt samples were tested where an amplicon was received for the control samples.

Results

Table 5-2: Testing protein gene targeting primers with qualitative PCR using Trial A DNA as template.

		presence of selected genes			
<div>primer sample</div>		<i>rbr</i> ^e	<i>epsc</i> ^f	<i>bnh</i> ^g	<i>fla</i> ^h
wt DSS	A3	— ^c	—	—	—
	A5	—	—	—	—
wt cont. ^a	A6	—	—	—	+
	A7	—	—	—	+
	A8	—	—	—	+
	A9	—	—	—	+
	A10	—	—	—	+
STAT1 ^{-/-} DSS	A11	—	+	+	n.d. ^d
	A12	+ ^b	+	+	n.d.
	A13	+	+	+	n.d.
	A14	—	+	+	n.d.
	A15	—	+	+	n.d.
STAT1 ^{-/-} cont.	A16	—	—	—	n.d.
	A17	—	—	—	n.d.
	A18	—	—	—	n.d.
	A19	—	—	—	n.d.
	A20	—	—	—	n.d.

^a control; ^b amplicon obtained; ^c no amplicon obtained; ^d not determined; ^e rubrerythrin; ^f capsular exopolysaccharide; ^g β-N-acetylhexosaminidase; ^h clostridial flagellin

5.2.1.1 The flagellin primers used for qPCR

As the product which can be amplified by the published *fla* primers (Duck et al., 2007) was too long for qPCR, new primers were designed. The N- and the C-termini of the flagellin gene are highly conserved whereas the region in between is highly variable (Duck et al., 2007, Lodes et al., 2004). Therefore, the new primers were designed targeting shorter sequences in the outer regions (Figure 5-6). An amplification using the two newly designed primers (each one in combination with the *fla* Rev primer) targeting the C-terminus was possible. For further experiments, the CR1For in combination with the *fla* Rev primer was chosen. The primers targeting the N-terminus had a very low efficiency in qualitative PCR, so they were not further used (data not shown).

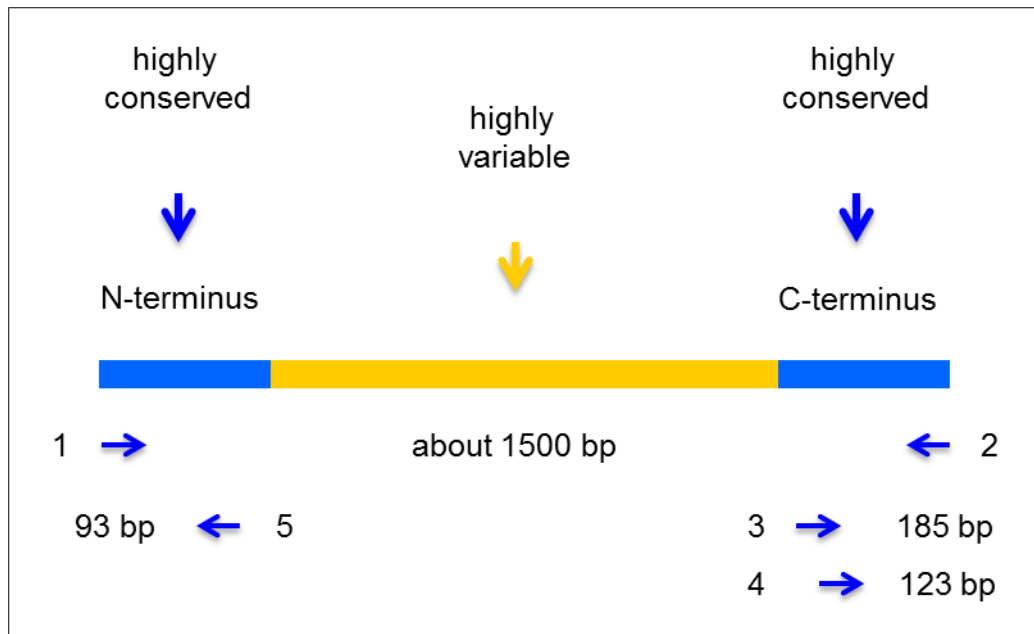


Figure 5-6: Schematic overview of the flagellin gene. The highly conserved N- and C-termini are targeted by the *fla* primers (1 & 2) with a sequence length of about 1,500 bp (Duck et al., 2007). In order to target a shorter sequence, new primers were designed. Covering the C-terminus, *fla* Rev was used with CR1For (3, product length: 185 bp) or CR1Rev (4, product length: 123 bp), combining *fla* For with Nr1Rev (5, product length: 93 bp) targeted the N-terminus.

5.2.1.2 Identification of flagellin genes

After cloning of purified products obtained by PCR with the *fla* primers (targeting the whole flagellin protein gene), a colony PCR was done to examine the products in the plasmids. The length of the products was analyzed via agarose gel electrophoresis (Figure 5-7). The expected length was approximately 1,500 bp which was obtained for most of the clones. A6/9 and A8/8 were selected due to their length which differed from the expected one, in order to investigate if those products also stemmed from flagellin genes.

Results

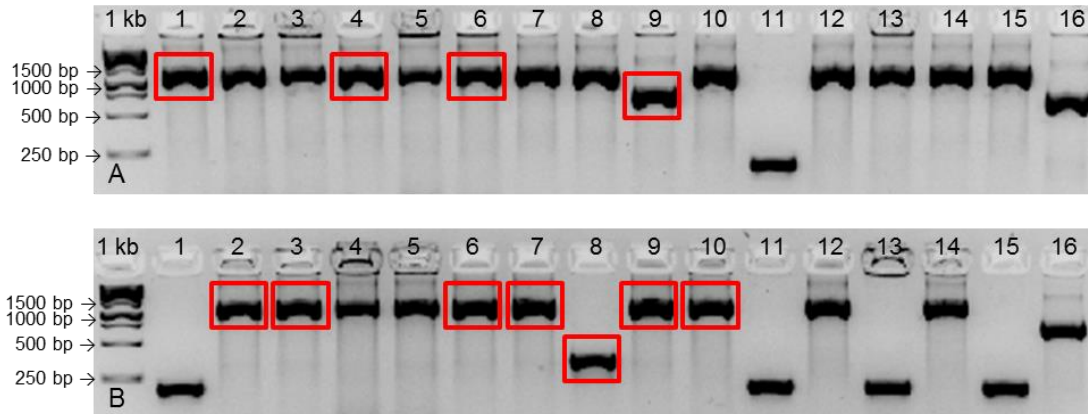


Figure 5-7: Agarose gel electrophoresis for the colony PCR for the clones containing sequences obtained by a PCR with the *fla* primers. The red squares indicate the products used for sequencing. A: sample A6; B: sample A8.

For sequencing, which was done in house via the Sanger sequencing method, the T3 and T7 primers were used. From each sequencing reaction (either the N- or C-terminus) approximately 500 nt were received. Hence, there was no overlap of the sequences due to the length of about 1,500 bp of the flagellin gene (Duck et al., 2007). The gained sequences were then analyzed by comparing them against the NCBI non-redundant database using blastx. The identified genes are listed in Table 5-3 which shows that the primers were specific for flagellin genes. Comparing the blastx output with the corresponding agarose gel electrophoresis pictures, all the amplicons with the same length (~1,300 bp) were assigned to flagellin genes. These genes had the highest similarity to the flagellin gene of the *Lachnospiraceae* bacterium A4 (Duck et al., 2007) which belongs to the clostridial cluster XIVa. A6/9 consisted of a shorter sequence (~700 bp) but nevertheless belonged to a flagellin domain-containing protein and also to the Clostridia. The only sequence which was not a flagellin was A8/8 (~350 bp), representing a SH3 domain protein which belonged to the Eurotiomycetes which are fungi. Apparently, this last sequence would be too short for a flagellin, so it was possibly a contamination.

Results

Table 5-3: Best hits for the blastx search for the sequences derived for the clones containing sequences of the samples A6 and A8 using the *fla* primers.

sample/ lane	terminus	description	order (organism)	class	max. ident. in xx AA
A6/1	N	Fla2 flagellin (ACC ¹ : ABI48299)	<i>Lachnospiraceae</i> (bacterium A4) (ACC: ABI48288)	Clostridia	98/124 (79%)
	C	Fla3 flagellin (ACC: ABI48284)			88/125 (70%)
A6/4	N	Fla3 flagellin	<i>Lachnospiraceae</i> (bacterium A4)	Clostridia	152/257 (59%)
	C	Fla3 flagellin			58/83 (70%)
A6/6	N	Fla2 flagellin	<i>Lachnospiraceae</i> (bacterium A4)	Clostridia	119/143 (83%)
	C	Fla2 flagellin			99/149 (66%)
A6/9	N	flagellin domain- containing protein (ACC: YP_003992178)	<i>Thermoanaero- bacterales</i>	Clostridia	125/232 (54%)
	C				124/235 (53%)
A8/2	N	Fla2 flagellin	<i>Lachnospiraceae</i> (bacterium A4)	Clostridia	70/99 (71%)
	C	Fla3 flagellin			116/187 (62%)
A8/3	N	Fla3 flagellin	<i>Lachnospiraceae</i> (bacterium A4)	Clostridia	152/240 (63%)
	C	did not work			
A8/6	N	Fla3 flagellin	<i>Lachnospiraceae</i> (bacterium A4)	Clostridia	113/143 (79%)
	C	Fla2 flagellin			99/157 (63%)
A8/7	N	Fla3 flagellin	<i>Lachnospiraceae</i> (bacterium A4)	Clostridia	127/171 (74%)
	C	did not work			
A8/8	N	SH3 domain protein (ACC: XP_002379761)	<i>Aspergillus</i>	Eurotio- mycetes	21/63 (33%)
	C				21/63 (33%)
A8/9	N	Fla3 flagellin	<i>Lachnospiraceae</i> (bacterium A4)	Clostridia	225/387 (58%)
	C	Fla3 flagellin			228/409 (56%)
A8/10	N	Fla3 flagellin	<i>Lachnospiraceae</i> (bacterium A4)	Clostridia	223/389 (57%)
	C	Fla3 flagellin			207/386 (54%)

¹ NCBI GenBank accession number

Results

In addition to those obtained by the the original *fla* primers, amplicons obtained by the newly designed primers (*fla* Rev with CR1For) were sequenced (Table 5-4). Using blastx, these sequences showed the highest similarity to the Fla2 flagellin which is highly similar to FlaX and one out of at least six flagellin genes detected for *Lachnospiraceae* bacterium A4 by Duck et al. (2007).

Table 5-4: Results for the blastx search for the sequences using the *fla* Rev and CR1For primers.

description	order	class	max. ident. in xx AA
Fla2 flagellin	<i>Lachnospiraceae</i> (bacterium A4)	Clostridia	27/36 (75%)
Fla2 flagellin	<i>Lachnospiraceae</i> (bacterium A4)	Clostridia	53/66 (80%)
Fla2 flagellin	<i>Lachnospiraceae</i> (bacterium A4)	Clostridia	36/53 (68%)
flagellin	uncultured bacterium		18/28 (64%)

5.2.2 Validation of reverse transcription and DNase digest during cDNA synthesis

In order to investigate changes at the transcription level, cDNA was synthesized. This was performed for all the samples of the Trials A, C, G and I where the RNA yield was higher than 10 ng/μl. The samples which had a lower RNA yield and therefore no cDNA was synthesized were C18, C19, C20, C21, C22, C23, C24, C25, C26, I4, I12 and I35. To verify the success of the cDNA synthesis, a PCR with the TB primers targeting the 16S rRNA gene was performed. First, to validate the reaction, the synthesized cDNA was used (represented by Trial A STAT1^{-/-} in Figure 5-8). The PCR products were specific and had the correct size of 200 bp. Second, DNase treated RNA (1:10 dilution with DEPC H₂O) was used to examine if the RNA still contained chromosomal DNA. As there were no products obtained with the 16S rRNA primers, the RNA was free of contaminating DNA (picture not shown).

Results

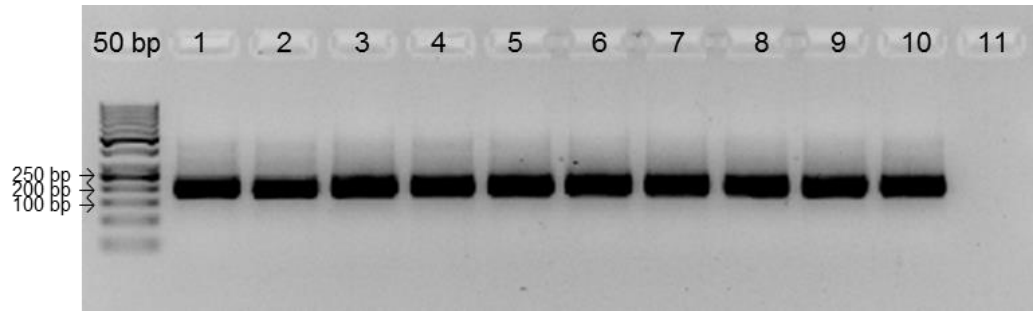


Figure 5-8: Agarose gel electrophoresis picture for the PCR products obtained with the TB primers targeting the 16S rRNA to validate the cDNA synthesis using Trial A (STAT1^{-/-}) samples as an example. The expected length is 200 bp. 1: A11, 2: A12, 3: A13, 4: A14, 5: A15, 6: A16, 7: A17, 8: A18, 9: A19, 10: A20, 11: neg. contr.

5.2.3 Preparation of the standards for qPCR

In order to have templates for qPCR standards, DNA was amplified via PCR. After purification, the PCR products were cloned. The obtained plasmids were then isolated and purified. These plasmids were linearized using the restriction enzymes *NcoI*, *NotI* or *PstI*. Afterwards, linearized plasmids were analyzed via agarose gel electrophoresis in comparison with the uncut plasmid, to examine the restriction digest and verify that there was just one cutting site. The result can be seen in Figure 5-9 which shows the outcome representative for *Akkermansia* 16S rRNA (AM), β -N-acetylhexosaminidase (*bnh*) and rubrerythrin (*rbr*). The observed length corresponded to the expected size taking into account the length of the plasmid (3,900 bp) and the length of the sequences obtained by the specific primers (resulting in 4,227 bp for AM, 4,056 bp for *bnh* and 4,049 bp for *rbr*).

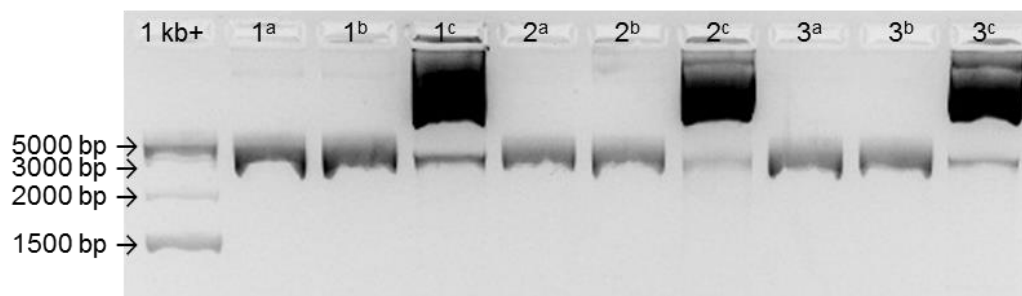


Figure 5-9: Agarose gel electrophoresis picture for the restriction digest (AM, *bnh*, *rbr*) in comparison to the uncut plasmid. The obtained length was as expected. The samples are as follows: 1: AM, 2: *bnh*, 3: *rbr*, ^a NotI, ^b PstI, ^c uncut plasmid.

5.2.4 Abundance and activity of *Akkermansia* during murine colitis

In order to investigate whether *Akkermansia*, which is a mucin degrader, increased during inflammation, qPCR on samples of the different trials was performed. Additionally, selected functional genes of *Akkermansia* (*rbr*, *bnh* and *epsc*) were analyzed to examine if their abundance correlates with the *Akkermansia* abundance. To determine the amount of gene (transcript) copies per μg DNA (RNA), qPCR with DNA (cDNA) as template was used.

5.2.4.1 *Akkermansia* in acute murine colitis

With the qPCR data, the gene copies for *Akkermansia* 16S rRNA and functional genes (*rbr*, *bnh*, *epsc*) were calculated. When DNA was used as template, the gene copies referred to μg DNA (Figure 5-10 A), when cDNA was used as template, the transcript copies were calculated per μg RNA (Figure 5-10 B). Regarding the gene copies for the total bacterial 16S rRNAs (both amplified from DNA and cDNA), there was no significant difference between the control and DSS treated groups for each mouse genotype.

For the *Akkermansia* 16S rRNA genes, the copy numbers were always significantly higher for the mice which were treated with DSS (wt: $t = 4.931$, $p = 0.004$; $\text{STAT1}^{-/-}$: $t = 14.874$, $p \leq 0.001$). The increase of *Akkermansia* 16S rRNA gene copies for the wt mice was about 100 fold and for the $\text{STAT1}^{-/-}$ mice approximately 20,000 fold. Comparing the DNA results of the control mice of the two genotypes, *Akkermansia* 16S rRNA is significantly more abundant in the wt compared to the $\text{STAT1}^{-/-}$ mice ($t = 6.081$, $p \leq 0.001$). For the *Akkermansia* associated protein genes, the same tendency was observed (wt *rbr*: $t = 3.69$, $p = 0.014$; $\text{STAT1}^{-/-}$ *bnh*: $t = 15.349$, $p \leq 0.001$; $\text{STAT1}^{-/-}$ *rbr*: $t = 10.05$, $p \leq 0.001$). *Rbr* genes increased 30 fold in the wt and 50 fold in the $\text{STAT1}^{-/-}$ mice. The *bnh* genes increased 1,000 (8,000) fold in the wt ($\text{STAT1}^{-/-}$) mice. There was no significant difference observed for the *epsc* gene.

Results

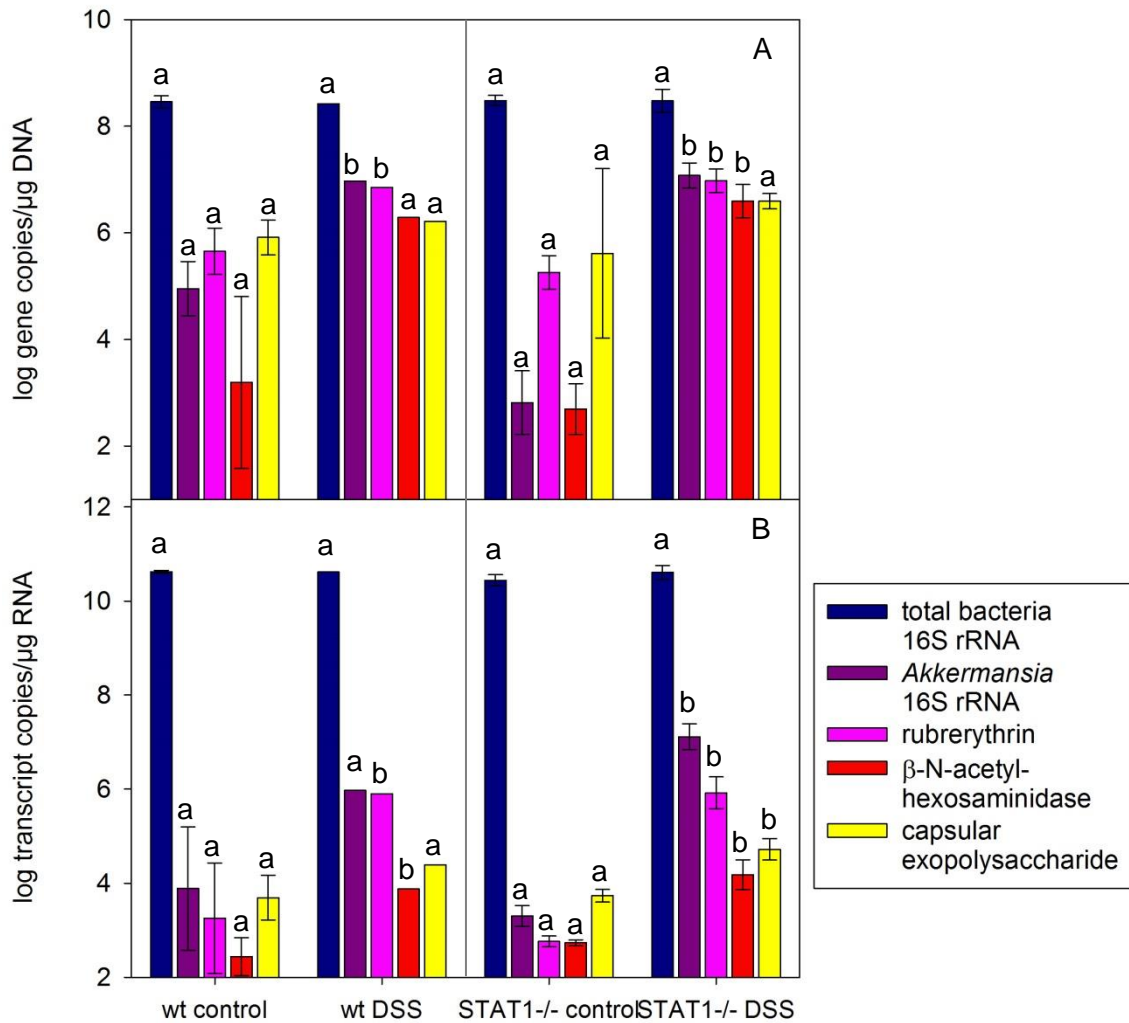


Figure 5-10: Trial A wt and STAT1^{-/-} – quantification for total bacteria 16S rRNA, *Akkermansia* 16S rRNA, the rubrerythrin, β-N-acetylhexosaminidase and capsular exopolysaccharide protein genes. The DSS treatment lasted for seven consecutive days and sampling took place on day 10. The different letters indicate a significant difference of gene or transcript abundance between treatments (p ≤ 0.05). A: using DNA as template; B: using cDNA as template.

The *Akkermansia* 16S rRNA transcripts differed by about two orders of magnitude (7.7×10^3 for the control mice compared to 9.4×10^5 for the DSS treated mice; $t = 2,123$, $p = 0.087$) for the wt and by about four orders of magnitude (2.0×10^3 for the control mice compared to 7.1×10^7 for the DSS treated mice; $t = 24.206$, $p \leq 0.001$) for the STAT1^{-/-} mice. The protein transcripts followed this trend with *rbr* and *bnh* of the wt mice having significant differences (*rbr*: $t = 2.948$, $p = 0.032$; *bnh*: $t = 4.407$, $p = 0.007$). For the STAT1^{-/-} mice, all three *Akkermansia* functional gene transcripts were significantly higher in the DSS treated compared to the wt mice (*rbr*: $t = 19.756$, $p \leq 0.001$; *bnh*: $t = 9.971$, $p \leq 0.001$; *epsc*: $t = 8.377$, $p \leq 0.001$). The increase of the *rbr*

Results

transcripts was 400 fold for the wt and 1,000 fold for the STAT1^{-/-} mice, the *bnh* transcript copy numbers in both mice types increased 30 fold in the DSS treated mice. The *epsc* transcripts mainly stayed the same with just the transcript numbers of the STAT1^{-/-} mice elevating tenfold.

Summarizing, the *Akkermansia* 16S rRNA gene and transcript numbers were always elevated during inflammation. Accordingly, two out of the three candidate protein genes (*rbr* and *bnh*) were also elevated after DSS treatment of the mice.

5.2.4.2 *Akkermansia* during murine colitis development

The quantification for the Trial C wt mice for both *Akkermansia* 16S rRNA and its associated functional genes showed no significant difference when the different days were compared to each other (Figure 5-11 A). However, the *Akkermansia* 16S rRNA genes increased until day 3 where the *rbr* genes were also more abundant.

In the TYK2^{-/-} mice (Figure 5-11 B), *Akkermansia* 16S rRNA and its functional protein genes all became more abundant after day 1 with a significant increase between day 1 and day 7 for *rbr*, *bnh* and *epsc*. The amount of gene copies per µg DNA for the *Akkermansia* 16S rRNA showed no difference. However, the *rbr* gene was significantly increased between days 3, 4 and 7 compared to day 1 (One-Way ANOVA with Holm-Sidak post-hoc test: day 3: $t = 4.557$; day 4: $t = 4.879$; day 7: $t = 5.826$; p always ≤ 0.05) and day 7 compared to day 2 (One-Way ANOVA with Holm-Sidak post-hoc test: $t = 4.557$, $p \leq 0.05$). The *bnh* gene was significantly increased on day 7 compared to day 1 (One-Way ANOVA with Holm-Sidak post-hoc test: $t = 4.167$, $p \leq 0.05$). Regarding *epsc*, the amount of gene copies increased on days 3, 4 and 7 compared to day 1 (One-Way ANOVA with Holm-Sidak post-hoc test: day 3: $t = 3.887$; day 4: $t = 3.633$; day 7: $t = 4.278$, p always ≤ 0.05).

Results

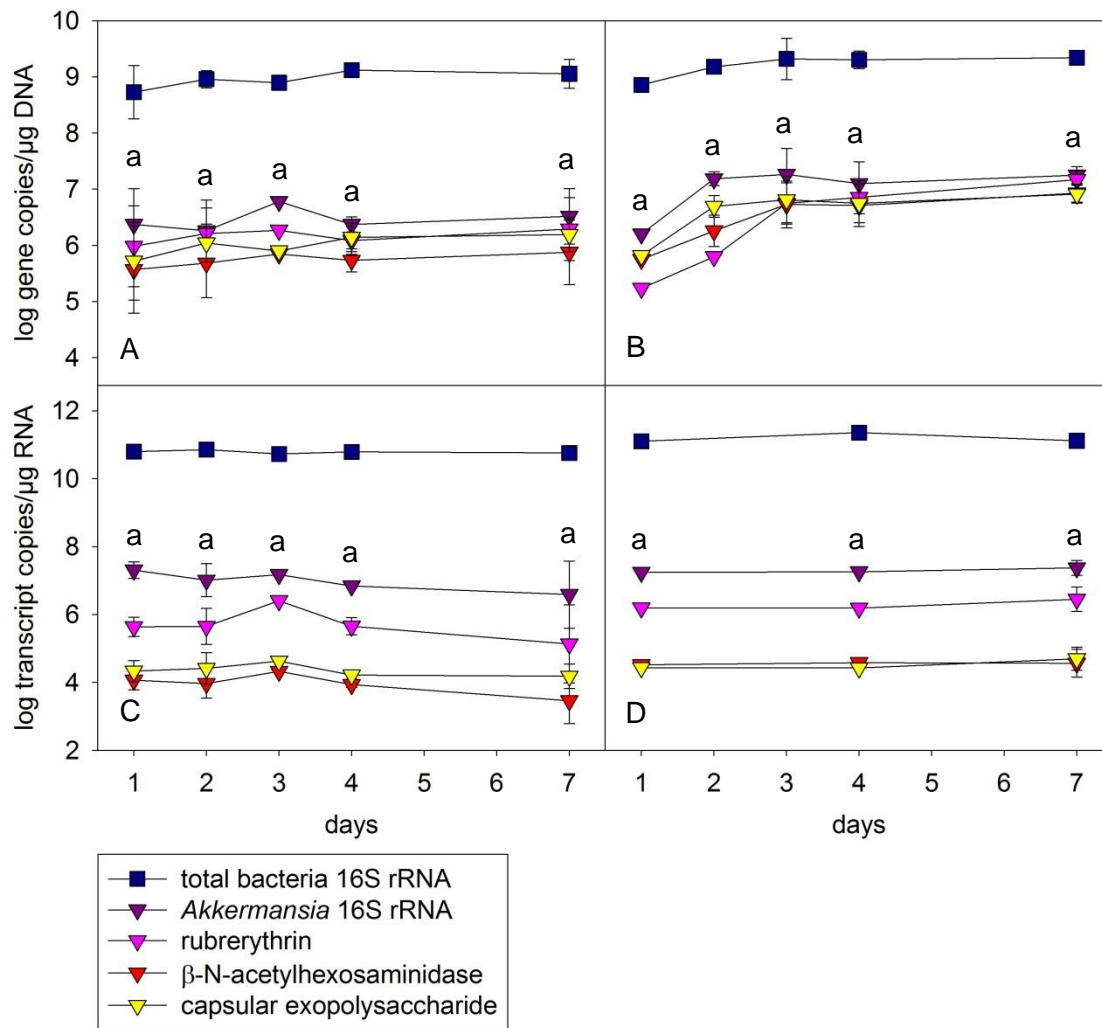


Figure 5-11: Trial C – time series for the quantification of total bacteria 16S rRNA, *Akkermansia* 16S rRNA, the rubrerythrin, β -N-acetylhexosaminidase and capsular exopolysaccharide protein genes. The DSS treatment lasted for seven consecutive days. Samples were taken on the days 1, 2, 3, 4 and 7. The different letters indicate a significant difference of gene or transcript abundance between treatments for *Akkermansia* ($p \leq 0.05$). A: wt, using DNA as template; B: TYK2^{-/-}, using DNA as template; C: wt, using cDNA as template; D: TYK2^{-/-}, using cDNA as template.

The *Akkermansia* 16S rRNA, *rbr*, *bnh* and *epsc* transcripts for the Trial C wt (Figure 5-11 C) and TYK2^{-/-} (Figure 5-11 D) mice did not change. Due to a low RNA yield in most of the samples for the TYK2^{-/-} mice, cDNA was just synthesized for six of them.

Summarizing, no increase of *Akkermansia* 16S rRNA genes and transcripts in early disease development occurred. The only exception was an increase of the three protein gene copies for the TYK2^{-/-} mice starting after day 1. However, this increase may be due to individuality (for example caging conditions) or other causes, as the

Results

gene copies on day 1 were lower than for all the other trials. Also, the gene copies stayed about the same after day 2.

5.2.4.3 *Akkermansia* in the recovery of murine colitis

The qPCR revealed that the copy numbers of *Akkermansia* 16S rRNA and the protein genes (Figure 5-12 A) were not significantly different between the different time points.

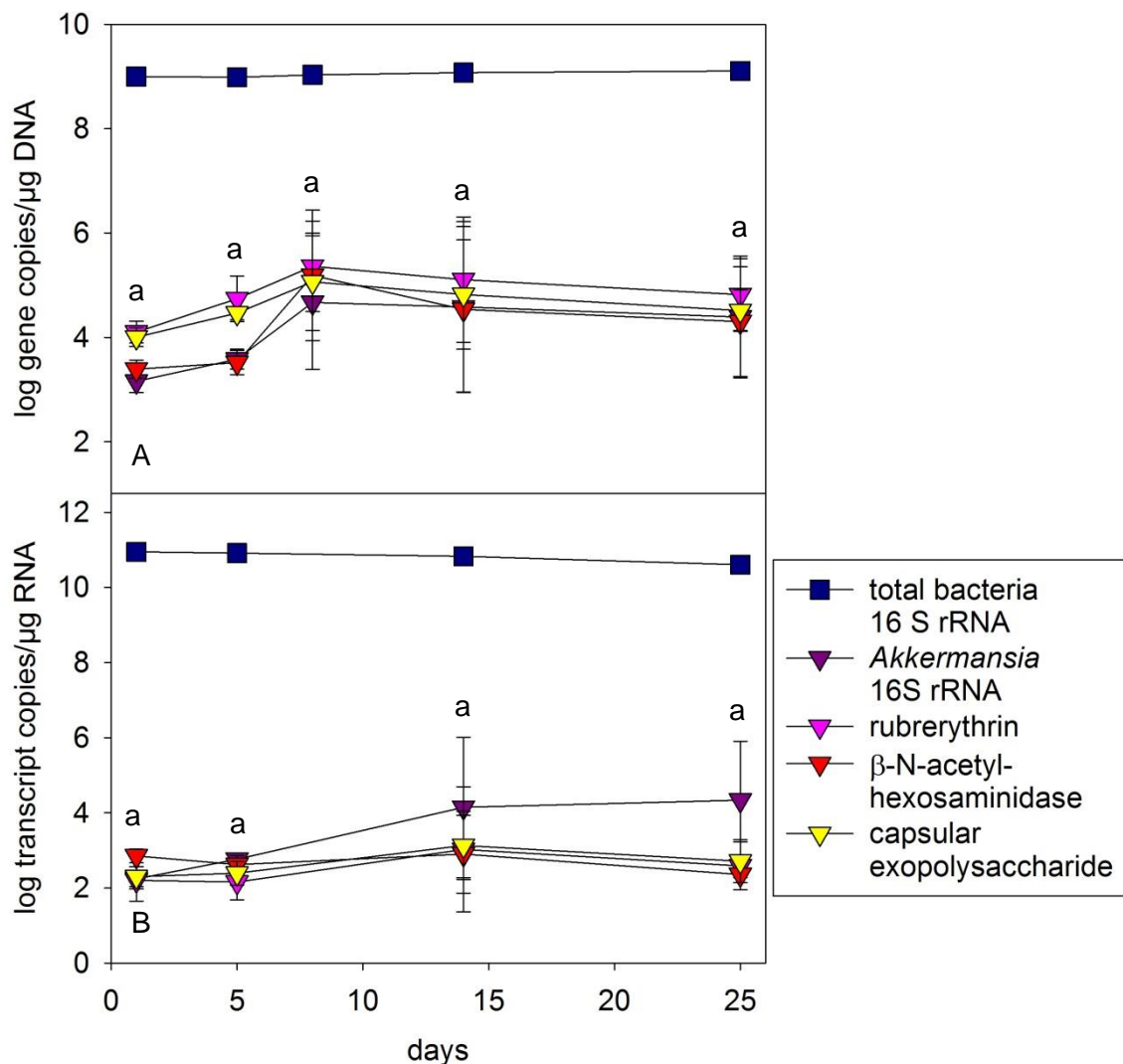


Figure 5-12: Trial I wt – time series for the quantification of total bacteria 16S rRNA, *Akkermansia* 16S rRNA, the rubrerythrin, β-N-acetylhexosaminidase and capsular exopolysaccharide protein genes. DSS treatment lasted for five consecutive days. Samples were taken on the days 1, 5, 8, 14 and 25. For day 8, only one cDNA sample was available, therefore it was omitted. The different letters indicate a significant difference of gene or transcript abundance between treatments for *Akkermansia* ($p \leq 0.05$). A: using DNA as template; B: using cDNA as template.

Also for the transcripts in Trial I no significant difference was observed (Figure 5-12 B). For day 8 only one cDNA sample was available, so this data point was excluded from further analyses. However, comparing the transcript copy numbers of the total bacterial rRNA, both the days 1 and 5 were significantly higher in relation to day 25 (One-Way ANOVA with Holm-Sidak post-hoc test: day 1: $t = 4.521$; day 5: $t = 4.049$; p always ≤ 0.05).

5.2.5 Examining the clostridial flagellin gene abundance

The flagellin protein was reported to be a dominant antigen in murine colitis (Lodes et al., 2004). It was desired to investigate whether shifts occurred during inflammation for the different mouse experiments. This was combined with the 16S rRNA of clostridial clusters IV and XIVa since the investigated flagellins belonged to the Clostridia.

5.2.5.1 Flagellin in acute murine colitis

By means of the qPCR data, the gene/transcript copies per μg DNA/RNA for the clostridial clusters IV and XIVa 16S rRNA and for the flagellin gene were calculated (Figure 5-13 A). In the $\text{STAT1}^{-/-}$ mice a significant increase in clostridial cluster IV rRNA and a decrease in flagellin genes for the DSS treated mouse samples was observed (CIIV: $t = 12.632$, $p \leq 0.001$; *fla*: $t = 3.841$, $p = 0.005$). Likewise, the same trend was seen in the wt mice, although the outcome was not significant due to too few samples. Additionally, clostridial cluster XIVa 16S rRNA was always up to tenfold more abundant than cluster IV 16S rRNA.

The expression of flagellin transcripts in Trial A was significantly higher in the control $\text{STAT1}^{-/-}$ mice compared to the DSS treated ones (Figure 5-13 B; $t = 8.377$, $p \leq 0.001$). However, in the wt mice, no difference was observed presumably as only two wt control mice survived the DSS treatment.

Results

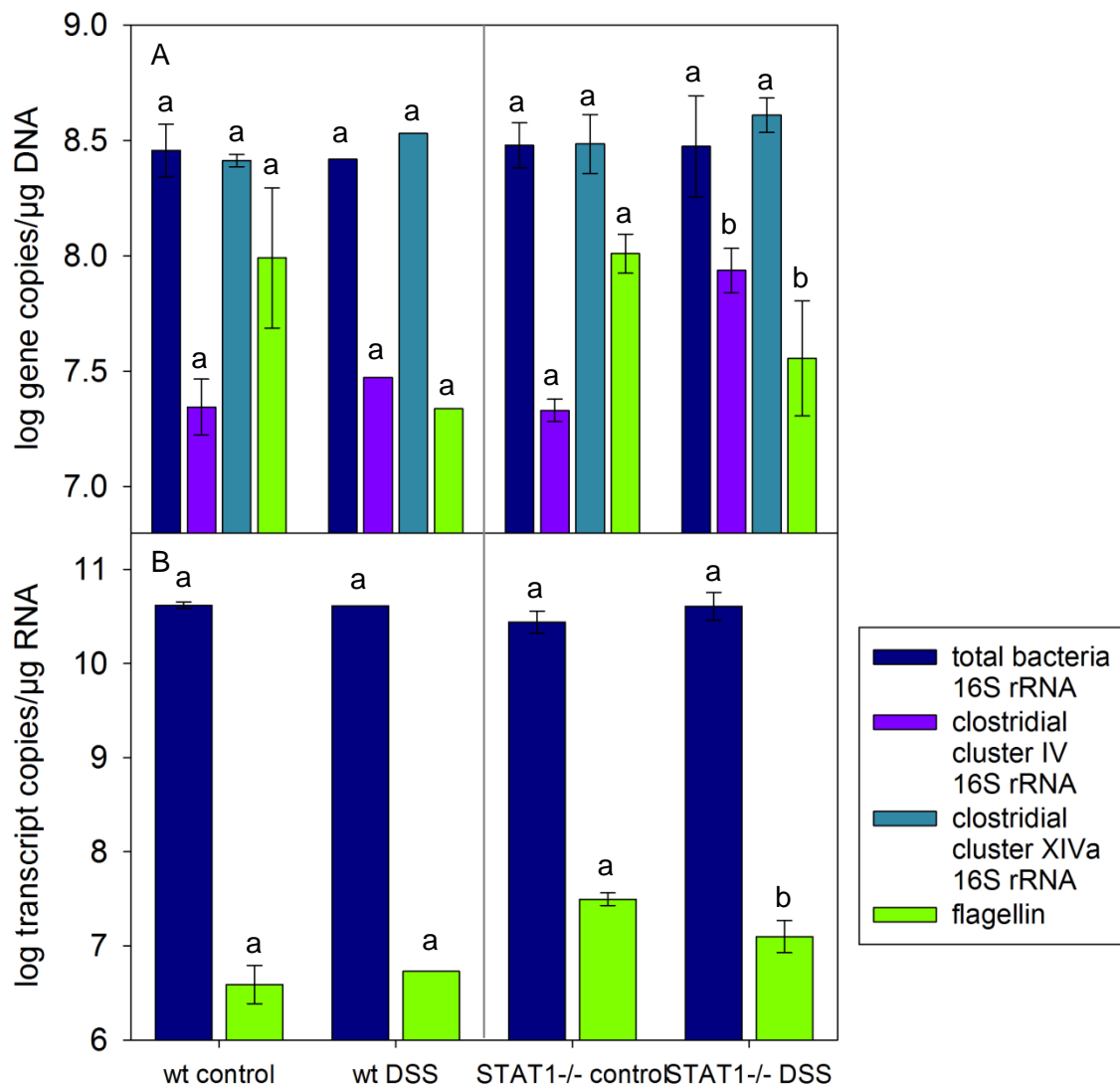


Figure 5-13: Trial A wt and STAT1^{-/-} – quantification for total bacteria 16S rRNA, clostridial cluster IV and XIVa 16S rRNA and the flagellin protein gene. DSS treatment lasted for seven consecutive days and the sampling took place on day 10. The different letters indicate a significant difference of gene or transcript abundance between treatments ($p \leq 0.05$). A: using DNA as template; B: using cDNA as template.

5.2.5.2 Flagellin during colitis development

In the Trial C wt mice (Figure 5-14 A) the abundance of the flagellin gene was significantly increased for the days 4 and 7 compared to day 1 (One-Way ANOVA with Holm-Sidak post-hoc test: day 4: $t = 3.761$; day 7: $t = 3.828$; p always ≤ 0.05).

Results

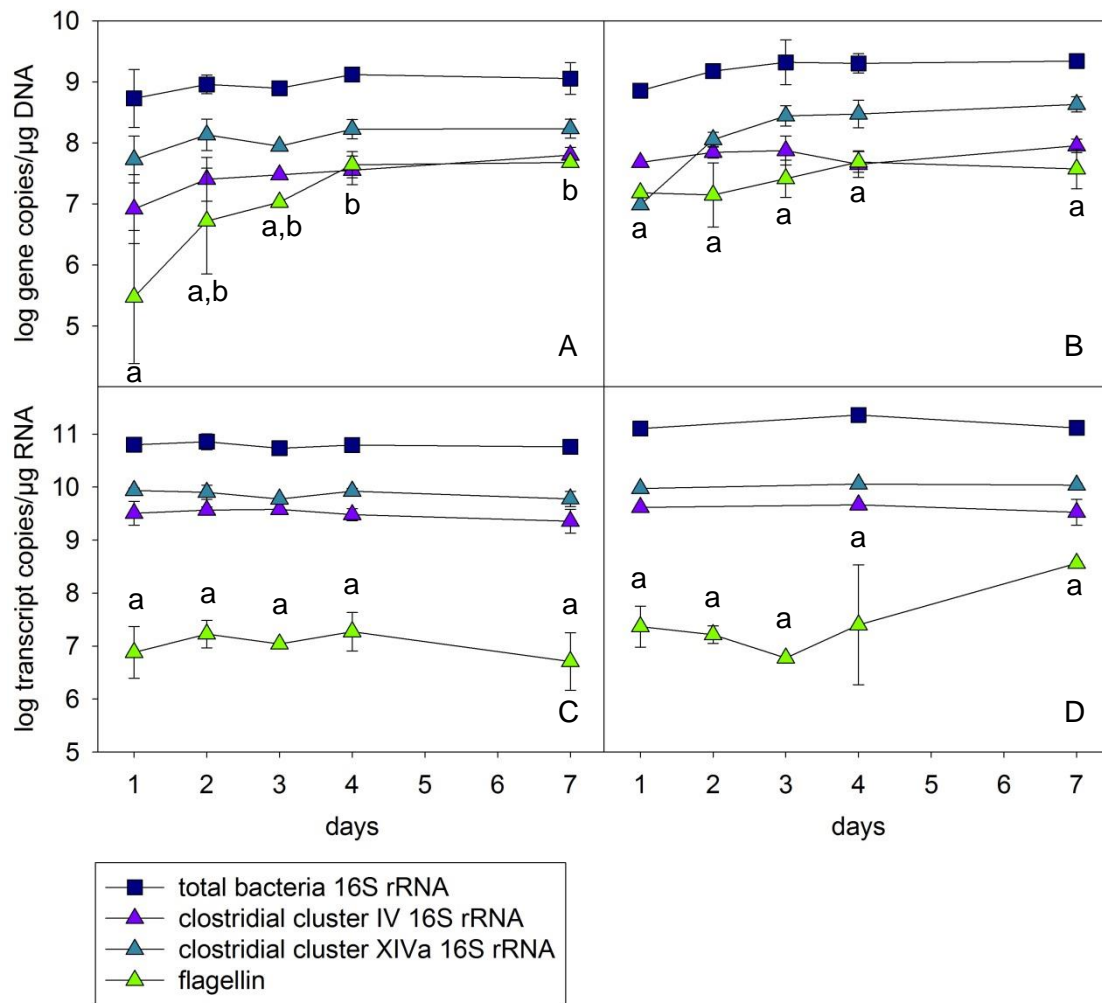


Figure 5-14: Trial C – time series for the quantification of total bacteria 16S rRNA, clostridial cluster IV and XIVa 16S rRNA and the flagellin protein gene. The DSS treatment lasted for seven consecutive days. Samples were taken on the days 1, 2, 3, 4 and 7. The different letters indicate a significant difference of gene or transcript abundance between treatments for the flagellin ($p \leq 0.05$). A: wt, using DNA as template; B: TYK2^{-/-}, using DNA as template; C: wt, using cDNA as template; D: TYK2^{-/-}, using cDNA as template.

The analysis of the TYK2^{-/-} mice (Figure 5-14 B) showed that the numbers of 16S rRNA genes of the clostridial cluster XIVa were significantly higher at all days compared to day 1 (One-Way ANOVA with Holm-Sidak post-hoc test: day 2: $t = 5.336$; day 3: $t = 7.579$; day 4: $t = 7.742$; day 7: $t = 8.651$; p always ≤ 0.05) and also at day 7 compared to day 2 ($t = 3.705$). Clostridial cluster XIVa 16S rRNA genes were always approximately one order of magnitude more abundant than cluster IV.

There was no significant difference in transcription of all genes for either the Trial C wt (Figure 5-14 C) and TYK2^{-/-} (Figure 5-14 D) mice. For the transcripts, too, the abundance of clostridial cluster XIVa was higher than of cluster IV.

Results

A significant increase of flagellin genes in the wt and of clostridial cluster XIVa 16S rRNA genes in the TYK2^{-/-} mice were observed in the early disease development. However, these differences may be caused by individuality or a technical error like due to different caging conditions, problems during the nucleic acid extraction or qPCR. Additionally, the gene copy numbers at the starting point for the other trials were always higher. For the transcript copy numbers no changes were observed.

5.2.5.3 *Flagellin in the recovery experiments*

In Trial G, the flagellin gene copies (Figure 5-15 A) in the gut content of the TYK2^{-/-} mice were significantly higher at day 1 compared to day 14 ($t = 3.504$, $p = 0.025$). As for the other genes, both in wt and TYK2^{-/-} mice, no difference in copy numbers was observed. However, comparison of the copy numbers of the two clostridial clusters revealed again an approximately ten-fold higher abundance of cluster XIVa compared to cluster IV.

For the transcripts (Figure 5-15 B), no significant difference could be identified at all. Here, too, more transcripts for clostridial cluster XIVa than for cluster IV were observed.

Results

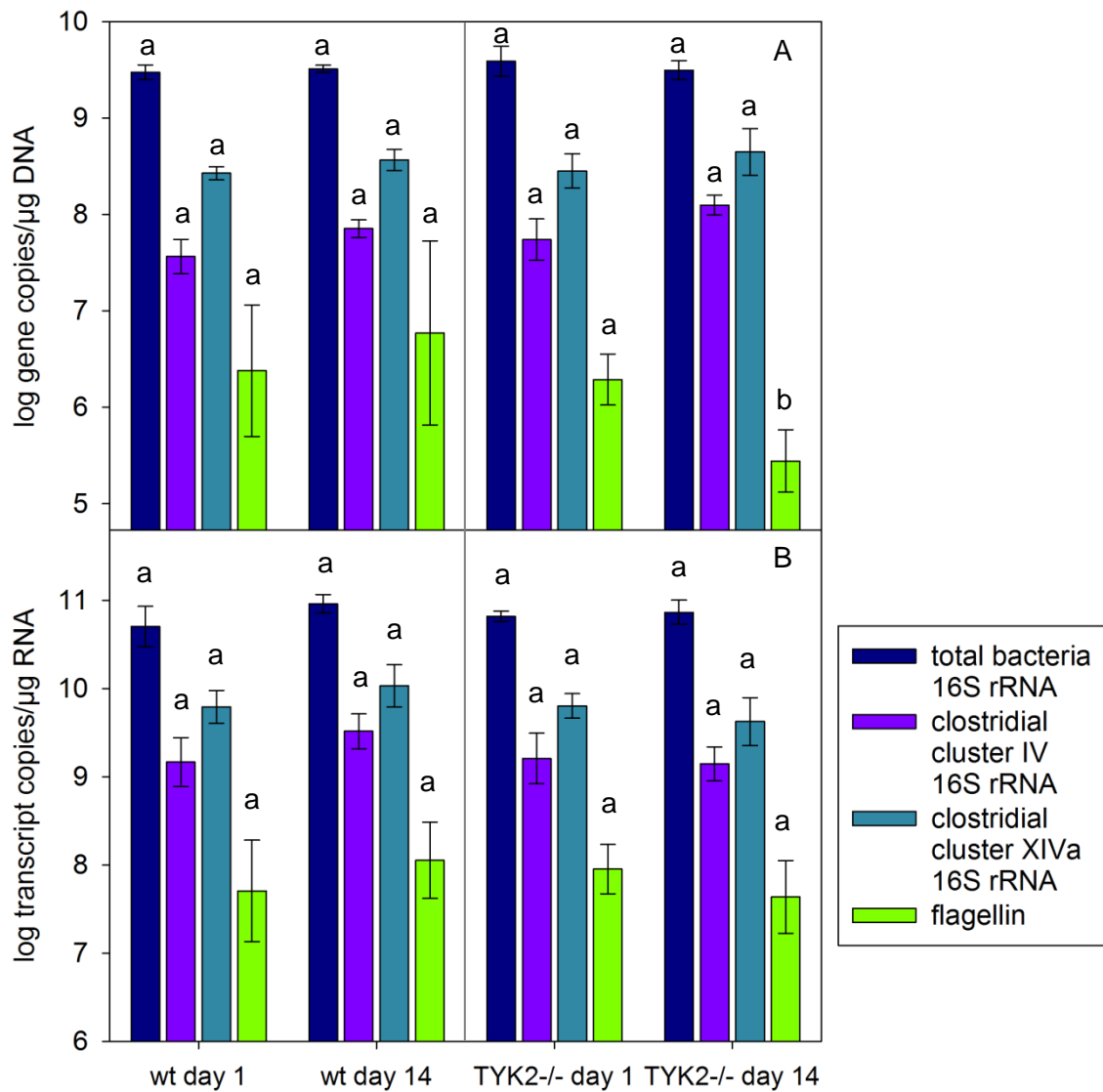


Figure 5-15: Trial G wt and TYK2^{-/-} - quantification for the days 1 and 14 of total bacteria 16S rRNA, clostridial cluster IV and XIVa 16S rRNA and the flagellin protein gene. The DSS treatment lasted for five consecutive days. Samples were taken on the days 1 and 14. The different letters indicate a significant difference of gene or transcript abundance between treatments ($p \leq 0.05$). A: using DNA as template; B: using cDNA as template.

In the recovery model of Trial I, the clostridial cluster XIVa showed a significant increase over time (Figure 5-16 A) compared to day 1 (One-Way ANOVA with Holm-Sidak post-hoc test: day 5: $t = 3.747$; day 8: $t = 3.596$; day 14: $t = 4.691$; day 25: $t = 4.740$; p always ≤ 0.05). Other than that, no significant differences in gene abundance were observed. However, there seemed to be a decrease of flagellin genes on day 8. Again, clostridial cluster XIVa was more abundant than cluster IV by about an order of magnitude.

Results

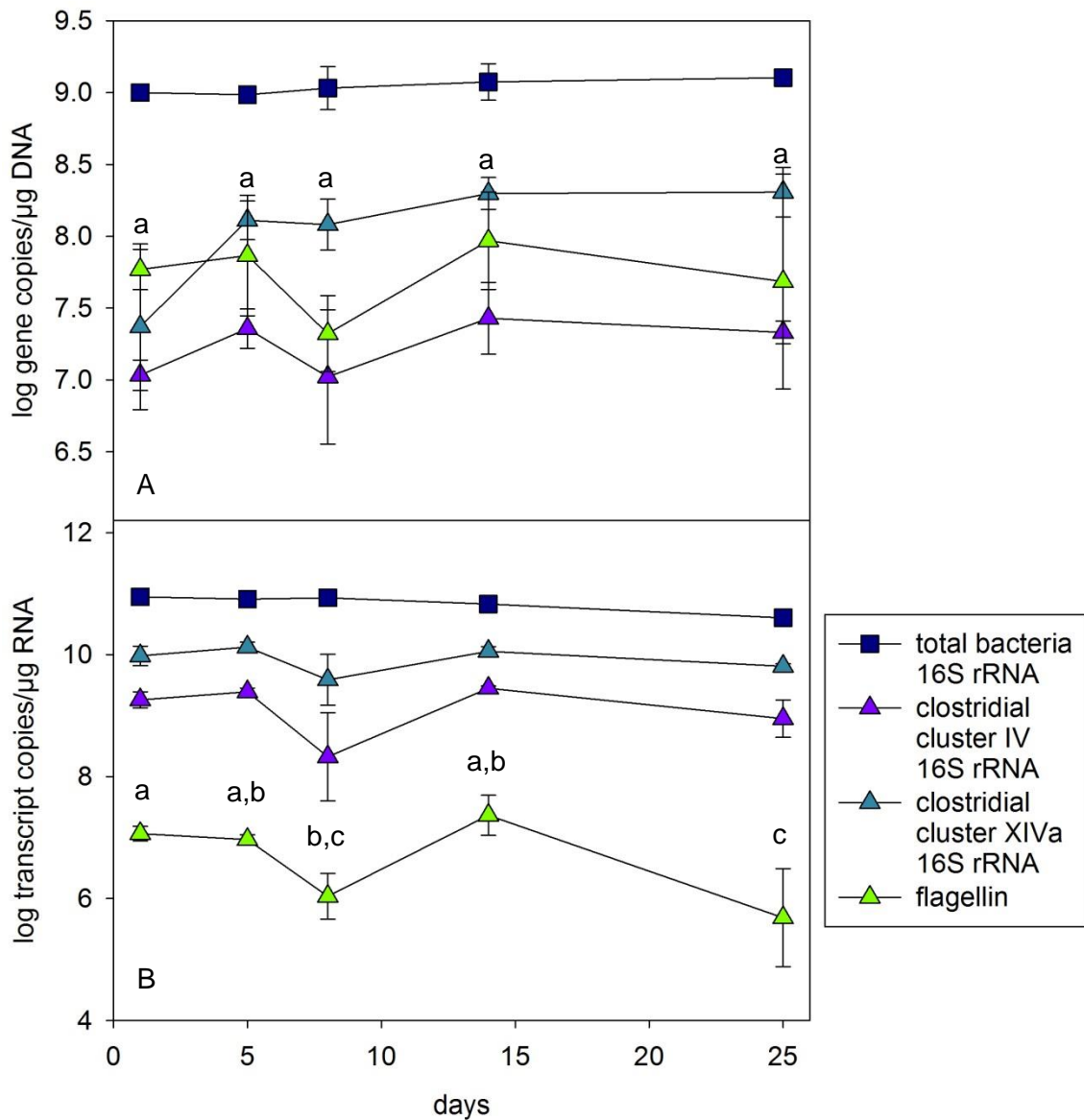


Figure 5-16: Trial I wt – time series for the quantification of total bacteria 16S rRNA, clostridial cluster IV and XIVa 16S rRNA and the flagellin protein gene. The DSS treatment lasted for five consecutive days. Samples were taken on the days 1, 5, 8, 14 and 25. The different letters indicate a significant difference of gene or transcript abundance between treatments for the flagellin ($p \leq 0.05$). A: using DNA as template; B: using cDNA as template.

The number of flagellin transcripts in Trial I decreased (Figure 5-16 B) when the days 8 and 25 were compared to day 1 (One-Way ANOVA with Holm-Sidak post-hoc test: day 8: $t = 3.227$; day 25: $t = 4.056$; p always ≤ 0.05), decreased when day 8 and 25 were compared to day 14 (day 8: $t = 4.507$; day 25: $t = 5.281$) and also decreased when comparing day 25 to day 5 ($t = 3.771$). The number of 16S rRNA transcripts of clostridial cluster IV, increased between day 8 and 14 (One-Way ANOVA with Dunn's

post-hoc test: $q = 3.291$, $p \leq 0.05$). Also, the amount of transcripts for clostridial cluster XIVa 16S rRNA was higher than the one of cluster IV 16S rRNA.

In summary, a decrease in flagellin genes occurred on day 8, although the difference was not significant. For the flagellin transcripts, a significant decrease was observed on day 8 compared to day 1. Also, compared to the days 5 and 14 the flagellin transcripts were slightly decreased on day 8 where the inflammation was the most severe. Correspondingly, the clostridial cluster IV and XIVa 16S rRNA transcripts were slightly decreased on day 8.

5.3 Microscopic approaches to identify flagellated bacteria

A major part of this study was the investigation of the clostridial flagellin genes and their shifts during murine colitis. Through polymerization, the flagellin protein forms the flagellar filament (Vijay-Kumar and Gewirtz, 2009). Therefore, it was aspired to visualize and enumerate flagella using different microscopy approaches. Also, the phylogenetic identification of the flagellated bacteria was desired.

5.3.1 The basic fuchsin stain for flagella detection

As a general flagella stain, the basic fuchsin stain was used to visualize all flagella present in a sample. The ingredients of the basic fuchsin stain solution induce an enlargement of the flagella (Leifson, 1951) such that they can be identified more easily under the light microscope. In Figure 5-17, one example for this stain is given. The different colouring of the bacterium and the flagella in Figure 5-17 A & B is due to the different focal planes observed with the microscope. Since this stain visualizes all flagella, these cannot be assigned to specific bacteria, like for example Clostridia.

Results

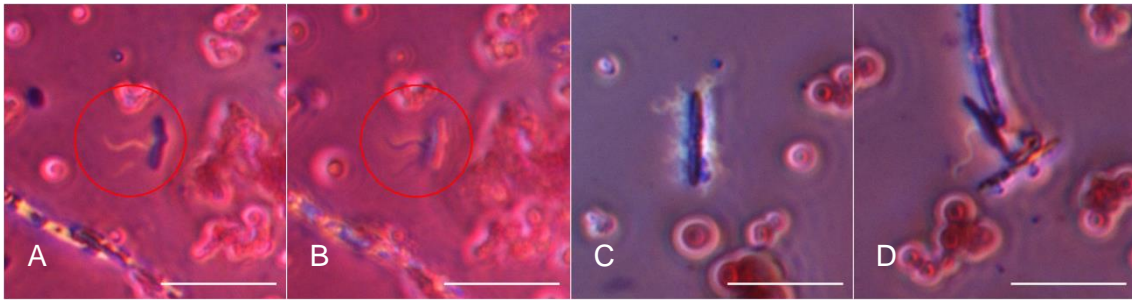


Figure 5-17: The basic fuchsin stain using sample A9 (A – D). A & B show the same bacterium at different focal planes, so the bacteria and flagella have a different colouring. The white bar on each image indicates 10 μm .

It was desired to combine the basic fuchsin stain with fluorescent techniques. As this technique stains all bacterial flagella, the combination with immunofluorescence was hoped to deliver an estimation of the proportion of the flagellated Clostridia within all flagellated bacteria. The second attempt was the combination with FISH. There, the aim was to determine the identity of flagellated bacteria through the application of group-specific FISH probes.

As the procedure for the basic fuchsin stain differs from the ones for the fluorescent stains, a series of tests was performed to identify conditions under which a combination of the techniques was possible.

- The flaming of the slides prior to applying the samples on the slide as proposed by Clark (1976) turned out to be unnecessary as no difference was observed. Additionally, the sample distribution was better on the wells of slides that were not flamed.
- The use of 1 \times PBS to dilute the samples did not have an influence on the stain per se but resulted in much more background due to the formation of salt crystals.
- The application of the EtOH-series (which is necessary for FISH) had no negative influence on the basic fuchsin stain.
- When poly-L-lysine was used to improve attachment of bacteria to the slide, the bacteria were stained well. However, some cracks occurred in the poly-L-lysine layer (Figure 5-18) which sometimes looked very similar to flagella. These even showed the same behaviour when observed at different focal planes under the microscope. Also, the background was enhanced.

Results

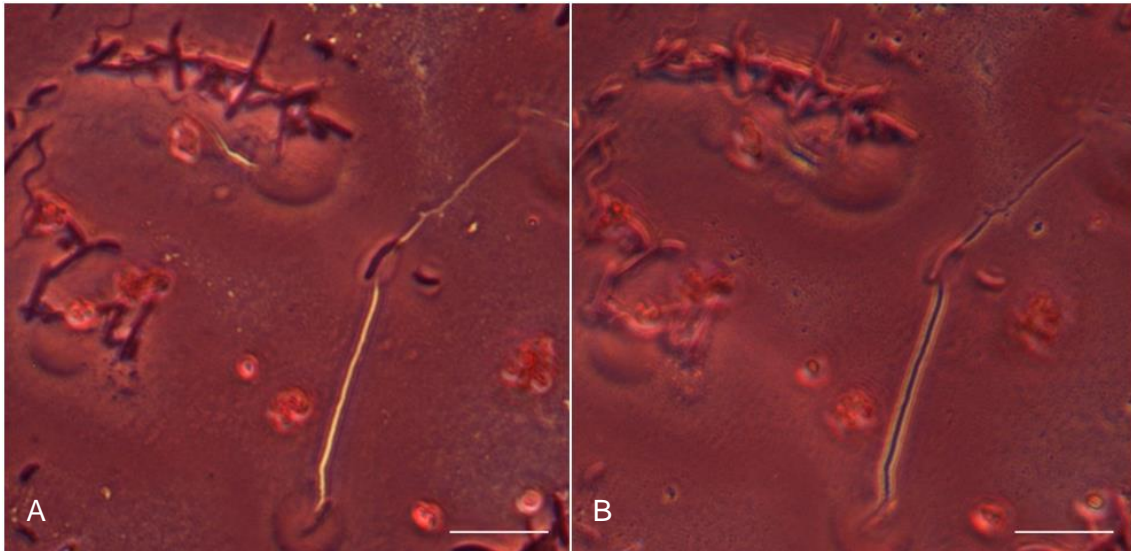


Figure 5-18: Basic fuchsin stain for sample A12. The slide was treated with poly-L-lysine before applying the sample. At the poles of the bacterium, cracks in the poly-L-lysine layer occurred which could be mistaken for flagella, especially when they were less pronounced. A & B display the same detail at different focal planes. The white bar on each image indicates 10 μ m.

- The sterile filtration seemed to have no effect on the stain quality, with the only difference being less background staining.
- The use of Citifluor had no influence on the basic fuchsin stain, although the slides had to be immediately processed under the microscope. Otherwise “halos” surrounded the bacteria that negatively influenced the visibility of the flagella. Vectashield could not be used as mounting medium since immediately after its application, the basic fuchsin stain of the sample disappeared.

Taken together, the sample processing conditions needed for the application of the fluorescence techniques were applicable with the basic fuchsin stain procedure. The only exception was the use of Vectashield since the basic fuchsin stain bleached immediately. Using Citifluor as mounting medium was suitable when the microscopic slides were examined immediately afterwards.

5.3.2 NanoOrange® – a fluorescent general flagella stain

One fluorescence technique that stains all flagella is using NanoOrange®. It stains all proteins by binding to their hydrophobic regions (Hesse and Kim, 2009) and enables also the visualization of flagella. The excitation peak of NanoOrange® is centred at

Results

about 470 nm, the emission peak at about 570 nm (source: NanoOrange® Protein Quantitation Kit). Therefore, the fluorescence signal can be detected with two different microscope filters (TRITC (excitation: 557 nm, emission: 576 nm) and FITC (excitation: 490 nm, emission: 525 nm)). Figure 5-19 shows the same bacterium observed with the FITC and TRITC filters (A & B) and with the light microscope (C). The NanoOrange® stain enables the visualization of proteinaceous structures in the vicinity of the bacteria.

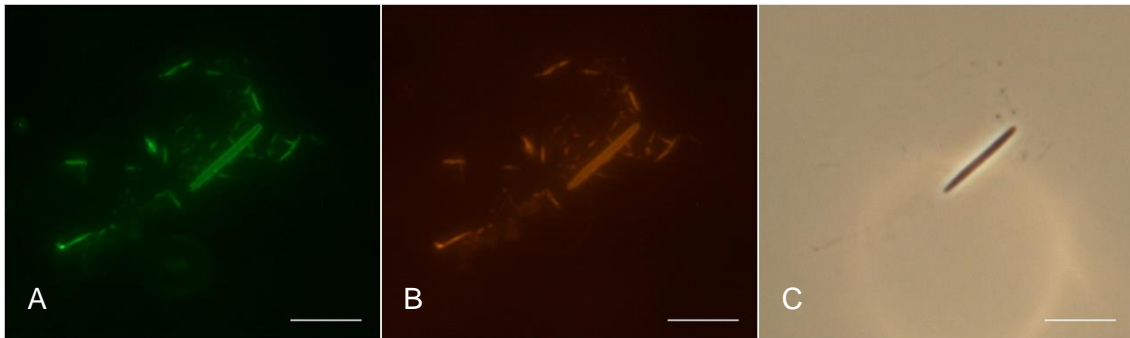


Figure 5-19: NanoOrange® stain using sample A6. All three pictures show the same bacterium. A: FITC channel; B: TRITC channel; C: light microscope. The white bar on each image indicates 10 μm .

An image of possible flagella using the NanoOrange® stain can be seen in Figure 5-20 where the bacterium observed with the fluorescent filter (A) shows flagella-like structures in the vicinity of the cell which cannot be seen in the light microscope (B). However, this was one of the very few bacteria where these extracellular proteinaceous structures resembled flagella. As flagella are very thin (\varnothing ca. 20 nm (Macnab, 1999)), it is difficult to identify them.

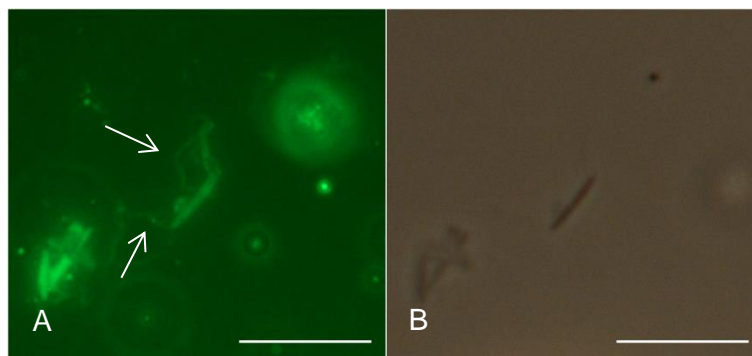


Figure 5-20: NanoOrange® stain for sample A6. The structures arising from the bacterium (A, indicated by the arrows) could be flagella. A: FITC channel; B: light microscope. The white bar on each image indicates 10 μm .

5.3.3 Immunofluorescence – detecting clostridial flagella

To detect clostridial flagella, a specific antibody against the flagellin Fla1 of *Roseburia hominis* (Clostridia) was used. As the flagellin contains conserved N- and C-terminal regions (Duck et al., 2007; Lodes et al., 2004), it is assumed that they also target other clostridial flagellins, although the specificity of these primary antibodies was never tested. This flagella detection method was very sensitive and even small flagella could be visualized. An example for a flagellated bacterium can be seen in Figure 5-21. The negative control without primary antibody showed no fluorescence signal (picture not shown), which shows that the primary antibody does not bind to other cellular structures.

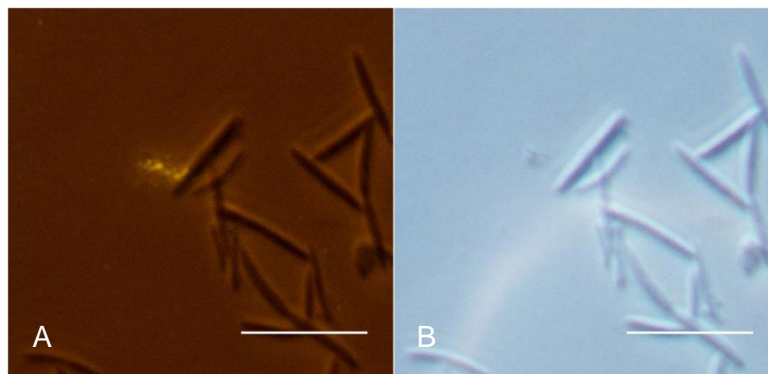


Figure 5-21: A flagellated bacterium of sample A6. The flagella was visualized by immunofluorescence (Cy3). A: TRITC channel, B: light microscope. The white bar on each image indicates 10 μm .

5.3.4 Combinations of different stains

5.3.4.1 Immunofluorescence-basic fuchsin – clostridial flagella compared to total flagella

The combination of these techniques was chosen to enumerate the contribution of clostridial flagella to all bacterial flagella. This would be achieved determining by the difference between the numbers of flagella observed with the clostridia-specific fluorescent stain and all flagella stained with basic fuchsin. The techniques were performed in both combinations, with the immunofluorescence technique being applied

Results

as well the and second. In addition, all bacteria were stained with DAPI to enable their visualization with the fluorescent microscope channels.

Unfortunately, these two techniques could not be applied together. When Milli-Q water was used as mounting medium (because this was more suitable for the basic fuchsin stain), the fluorescence signals bleached out immediately (within seconds). Consequently, it was not possible to observe the clostridial flagella reliably. Using Citifluor as mounting medium resulted in a lowered quality of the fuchsin stain. Thus, the detection of fuchsin stained flagella was unreliable as they could easily be missed. Example pictures of the combination can be seen in Figure 5-22.

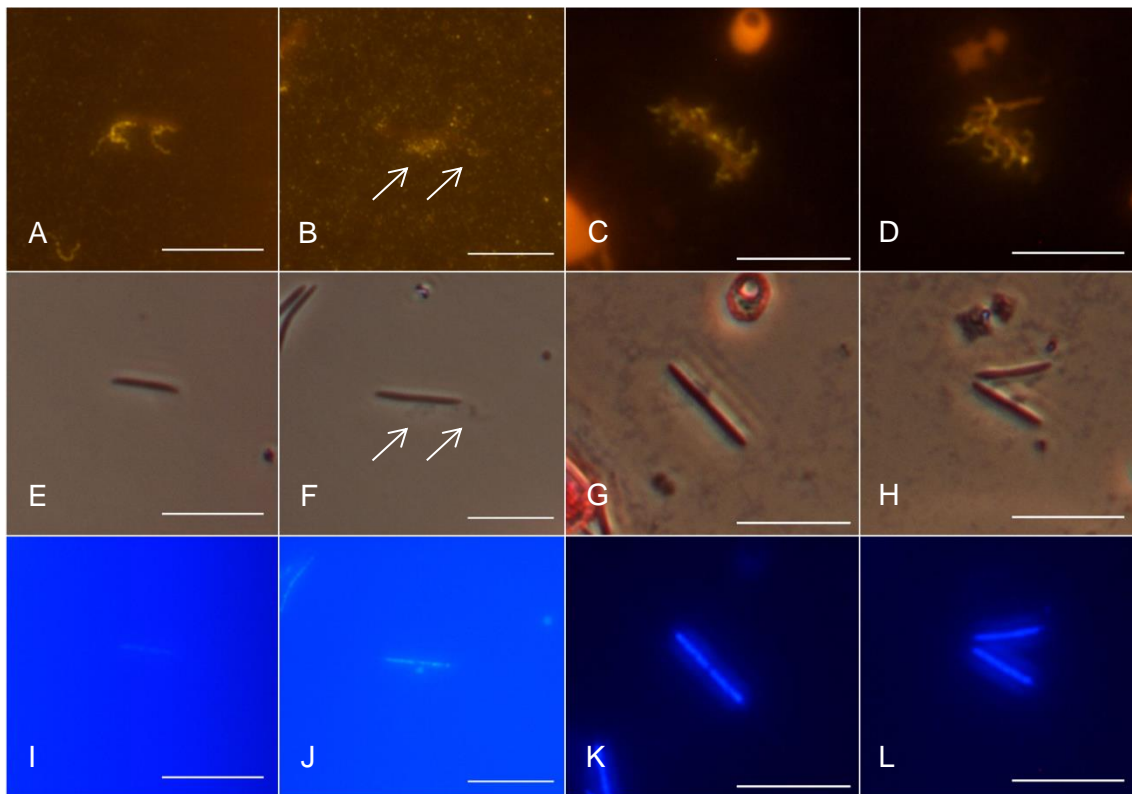


Figure 5-22: A combination of immunofluorescence, basic fuchsin stain and DAPI. Each column shows the same bacterium with the different stains. A, E, I and B, F, J represent sample A9; C, G, K and D, H, L show sample A12. The pictures in the upper row display immunofluorescence, the middle row illustrates the basic fuchsin stain and the lower row the DAPI stain. The arrows in the pictures B and F indicate flagella. For the basic fuchsin stain, they are just visible for the bacterium in image F where the signal for immunofluorescence was very faint. The white bar on each image indicates 10 μm .

When analyzing the immunofluorescence or DAPI stained samples with the fluorescent channels, at first the visual fields were very foggy and besides this fog nothing else was visible. After staying some time at the same position, the fog became clearer and the bacteria and flagella became visible. However, when switching back to the light microscopy channel, the basic fuchsin stain was gone. Also, when observing the basic

Results

fuchsin stain first, the flagella were indeed visible but not as good as when only applying the basic fuchsin stain. Hence, this method was discarded because it was not reliable enough.

5.3.4.2 FISH-basic fuchsin – assigning flagella to bacteria

As the basic fuchsin stain covers all bacterial flagella and FISH probes can be specific on different phylogenetic levels, the aim of this combination was to identify which bacteria were flagellated.

The result for this combination can be seen in Figure 5-23. The combination of the two techniques was possible, but not without problems. For instance, there were flagella identifiable with the basic fuchsin stain but these bacteria were surrounded by a “halo” which made it difficult to identify the flagella. In addition, the fluorescent signal was not very good.

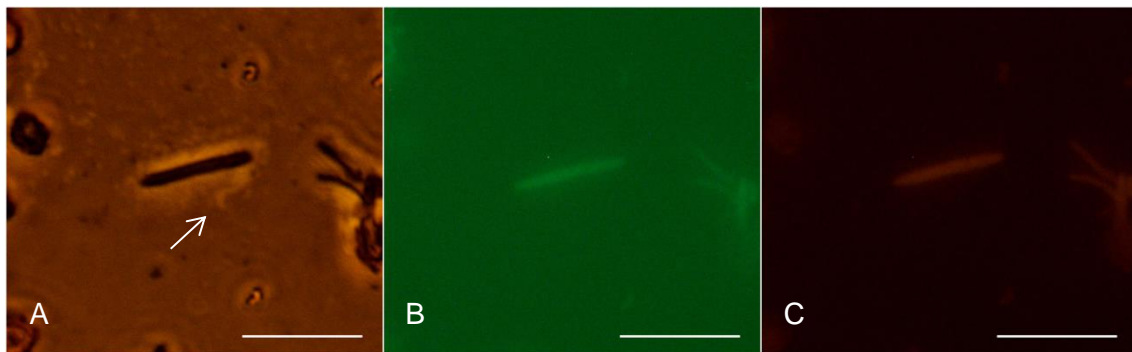


Figure 5-23: A combination of the basic fuchsin stain (A) and FISH (B & C, using two probes for *Lachnospiraceae* OTU_11021 in Fluos and Cy3). The flagellum visible using the basic fuchsin stain is indicated with an arrow. Unfortunately, a “halo” surrounded the bacterium which made the identification of flagella more difficult, especially if they would be broken off because then they could hardly be distinguished from the bacteria. A: light microscope, B: FITC channel, C: TRITC channel. The white bar on each image indicates 10 µm.

5.3.4.3 Detecting flagella stained with NanoOrange®

As NanoOrange® stains all proteins, both the bacteria and all the extracellular proteinaceous structures are stained. An approach to improve the differentiation of flagella and bacteria with the NanoOrange® stain was the combination with either DAPI, immunofluorescence or FISH.

Results

To investigate if extracellular structures can reliably be distinguished from the bacterial cells, the DNA stain DAPI was used. Hence, everything which was just stained with NanoOrange® could be considered extracellular structures like flagella. However, because flagella are very thin, they could not really be distinguished from other proteinaceous extracellular structures. Additionally, it was observed that not all bacteria were stained with DAPI (Figure 5-24).

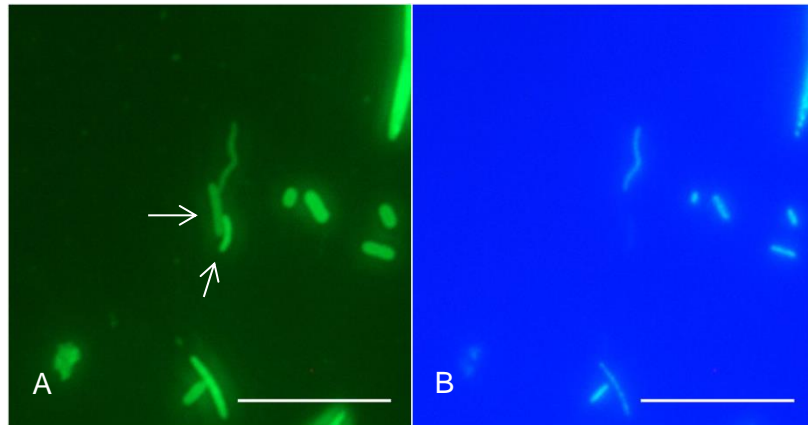


Figure 5-24: A combination of the NanoOrange® stain (A, FITC channel) and DAPI (B) using sample A6. The bacteria indicated with the arrows were visible with the NanoOrange® stain but not with DAPI. The white bar on each image indicates 10 μm .

The second approach was the combination of NanoOrange® with immunofluorescence, using a clostridial flagella specific primary antibody. The combination of these two techniques could also give a hint of the proportion of flagellated Clostridia within all flagellated bacteria. Fluorescent signals were obtained for both of the stains but still it was not easy to distinguish the flagella stained with NanoOrange® (data not shown).

A further approach was to combine NanoOrange® with FISH. Like the FISH-basic fuchsin combination, this method was chosen in order to investigate which bacteria are flagellated as the NanoOrange® stain is not specific for any kind of flagella. All in all, fluorescent signals were obtained for both of the stains (Figure 5-25) but nonetheless, the flagella were not easy to identify due to their small diameter. Another problem was that the NanoOrange® stain gives a fluorescent signal in two channels (FITC and TRITC). Therefore, just one FISH probe (in Cy5) could be combined with it. However, some FISH probes could just be used in a set of two because their signals were not specific otherwise.

Results

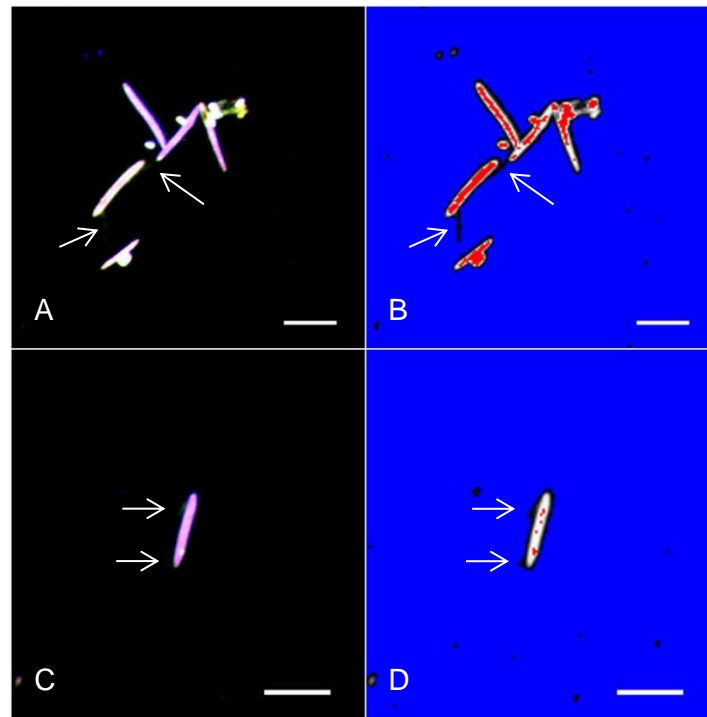


Figure 5-25: A combination of NanoOrange® and FISH for sample A6. A & C show the merged pictures for the stains (NanoOrange® for the FITC and TRITC channel; EUBmix in Cy5 for FISH). B & D illustrate the range indicator picture for the same bacteria. The arrows indicate the flagella which were hardly visible on the image for the fluorescent dyes. On the range indicator pictures, the flagella were better detectable. The white bar on each image indicates 10 µm.

5.3.4.4 DAPI-immunofluorescence – how many bacteria are flagellated?

To investigate how many bacteria were flagellated, immunofluorescence was used together with DAPI. Via immunofluorescence, all clostridial flagella are stained, and via DAPI, all bacteria are visualized. For both of the stains fluorescence signals were obtained as shown in Figure 5-26. Although no problems occurred with this combination, it was decided to proceed with IF-FISH as FISH probes can be chosen specific on different phylogenetic levels.

Results

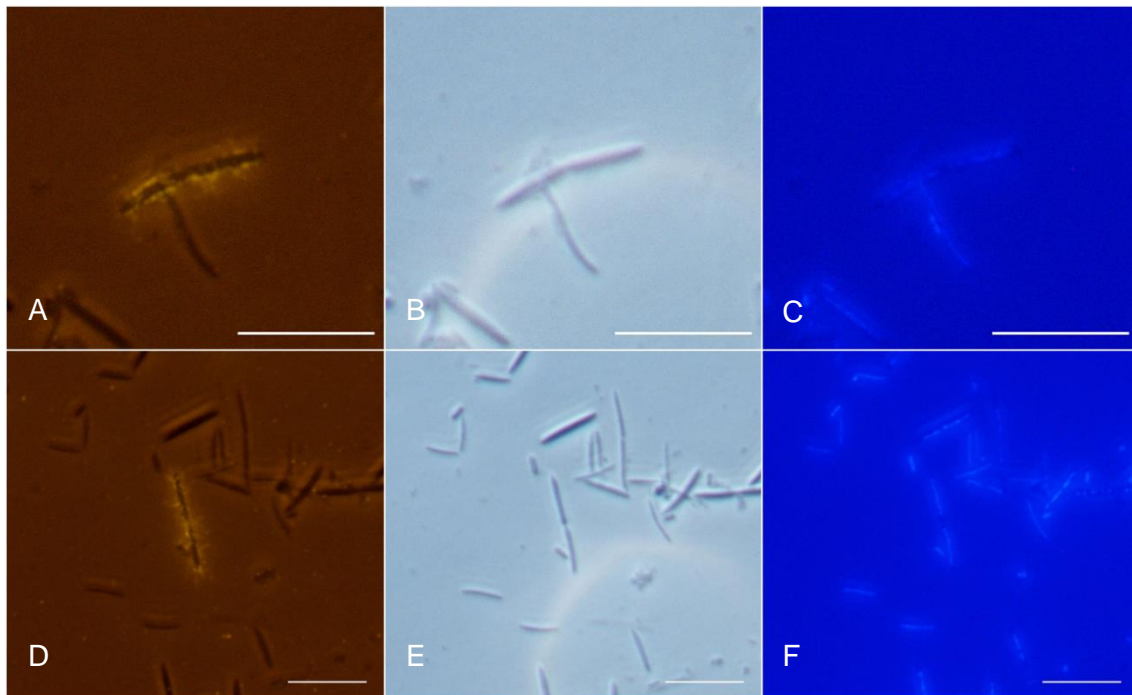


Figure 5-26: Immunofluorescence in combination with the light microscope and DAPI. Each row shows the same bacteria, both from sample A9. The left column (A & D) represents immunofluorescence, the middle row (B & E) shows light microscope pictures and the right row (C & F) illustrates the DAPI stain. The white bar on each image indicates 10 μm .

5.3.4.5 IF-FISH – abundance of flagellated Lachnospiraceae

The majority of the flagellin in the murine gut was assigned to Clostridia (according to the analysis of the metatranscriptome by Berry et al. (2012)). These clostridial flagellins should be covered by the primary antibody used in this study. By combining immunofluorescence with FISH, the aim was to identify which clostridial OTU's were flagellated and if their abundance was decreased in acute murine colitis.

Establishment of IF-FISH

The method combination was tested in both orders, with immunofluorescence or FISH being applied first, respectively. It turned out that the FISH signal was weaker when it was performed first, so it was decided to always start with the immunofluorescence stain. The same observation was made by Gmür and Lüthi-Schaller (2007).

Results

Identification of flagellated *Lachnospiraceae*

To identify which *Lachnospiraceae* carried flagella, immunofluorescence was combined with different FISH probes specific for OTU's within this family. Figure 5-27 (*Lachnospiraceae* OTU_9468) and Figure 5-28 (*Lachnospiraceae* OTU_11021) show that both observed OTU's were flagellated. For both of these OTU's FISH probes two have to be used for a specific signal. Thus, to be able to additionally use FISH probes on, for example, other phylogenetic levels, the Erec482 probe was chosen as a general probe for the *Eubacterium rectale* group (Figure 5-29) within the *Lachnospiraceae*.

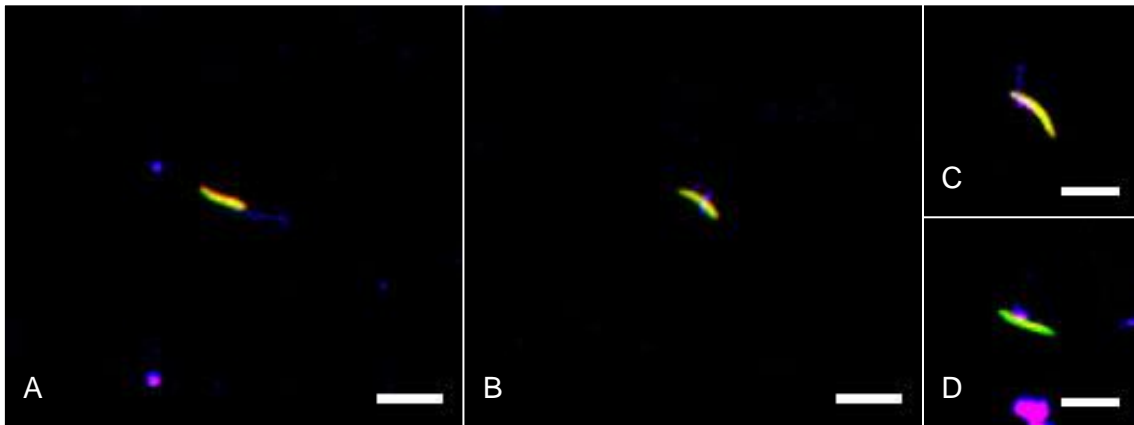


Figure 5-27: A combination of immunofluorescence (Cy5) and FISH (*Lachnospiraceae* OTU_9468 in Cy3 and Fluos, resulting in yellow when specific). A & B: sample A12; C & D: sample A13. The white bar on each image indicates 5 μ m.

Results

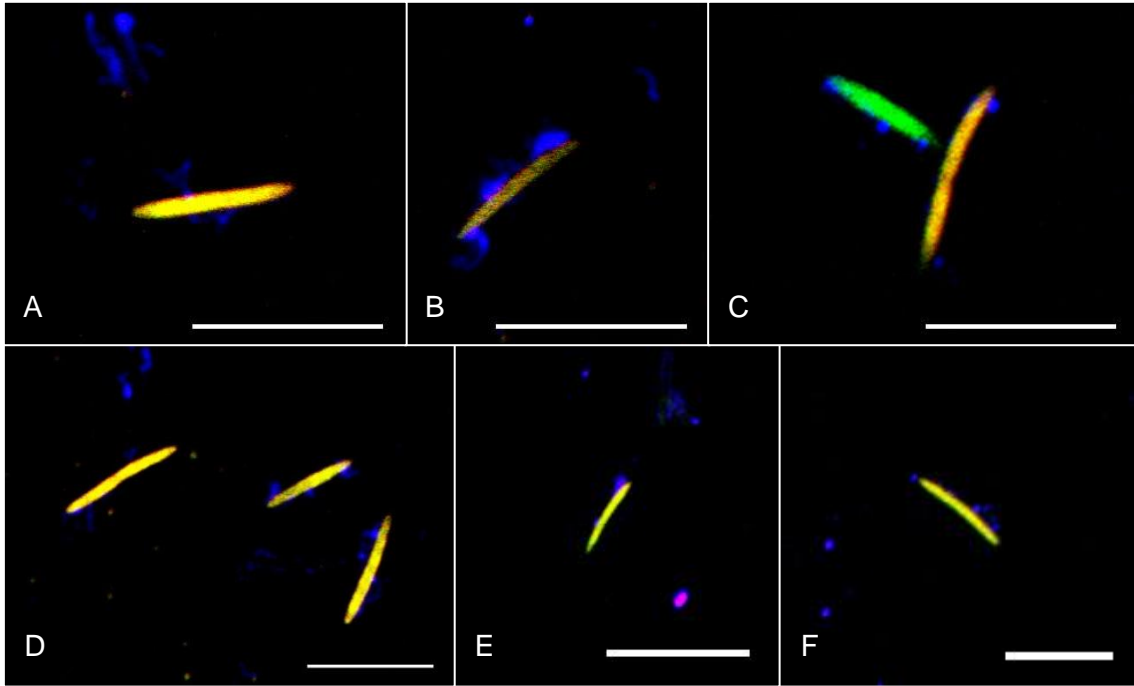


Figure 5-28: A combination of immunofluorescence (Cy5) and FISH (*Lachnospiraceae* OTU_11021 in Cy3 and Fluos, resulting in yellow when specific). A, B, C, E & F: sample A6; D: sample A9. In picture C, presumably broken off flagella are visible. The white bar on each image indicates 10 µm.

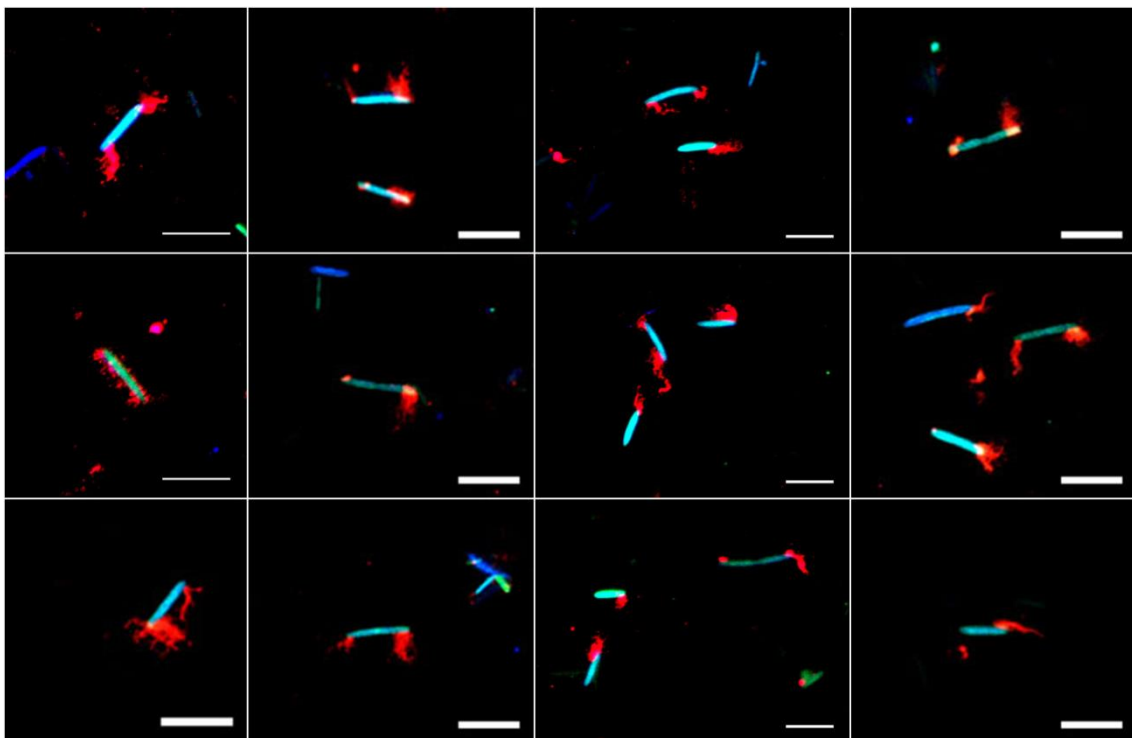


Figure 5-29: A selection of pictures combining immunofluorescence (Cy3) and FISH (Erec482 in Cy5 and EUBmix in Fluos) representing sample A17. The white bar on each image indicates 10 µm.

Results

Summarizing, Table 5-5 shows which stains could be combined. The best results were obtained when immunofluorescence was combined with FISH or DAPI and when NanoOrange® was combined with DAPI.

Table 5-5: Combination of stains – which could be used together and which not.

	BF ^a	NO ^b	IF ^c	FISH ^d	DAPI ^e
BF	 	n.d. ^f	~ ^g	~	n.d.
NO	n.d.	 	~	~	+ ^h
IF	~	~	 	+	+
FISH	~	~	+	 	n.d.
DAPI	n.d.	+	+	n.d.	

^a basic fuchsin stain; ^b NanoOrange®; ^c immunofluorescence; ^d fluorescence *in situ* hybridization; ^e 4,6-Diamidino-2-phenylindole dihydrochloride; ^f not determined; ^g unreliable when combined; ^h successful combination of stains

5.4 Quantification of flagellated *Lachnospiraceae*

To investigate if the quantification of the flagellated bacteria using data obtained by microscopy is comparable to the results of the qPCR, the microscopy pictures were analyzed using the *daime* image analysis software (Daims et al., 2006).

The FISH probes were the EUBmix and Erec482. This combination enabled the detection of the proportion of flagellated *Lachnospiraceae* within the total bacteria. For this experiment, samples from the Trial A STAT1^{-/-} mice were used. Samples A12 and A14 were represented luminal content from the control mice, whereas A17 and A19 were from DSS treated mice, respectively. For each sample, pictures of at least ten visual fields were taken and then analyzed. For statistics, a One-Way ANOVA with Holm-Sidak post-hoc test was used (Figure 5-30). It turned out that there was a high variability within the control mice. For sample A12, significantly more flagellated bacteria were observed compared to the other samples (A12 vs. A14: $t = 4.863$, $p \leq 0.001$; A12 vs. A17: $t = 3.100$, $p = 0.004$; A12 vs. A19: $t = 3.006$, $p = 0.005$).

Results

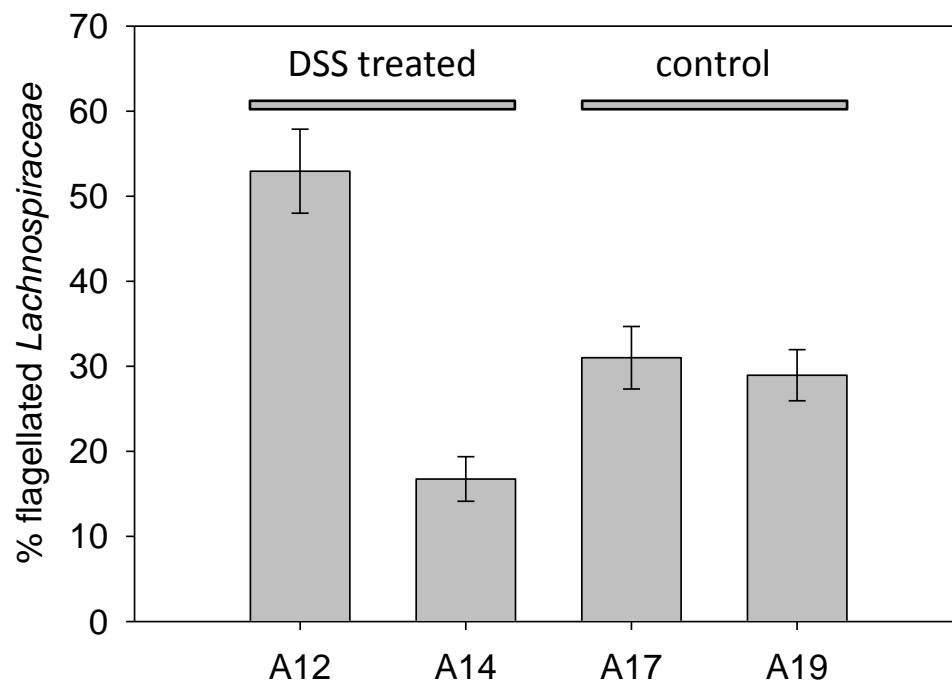


Figure 5-30: Percent of flagellated *Lachnospiraceae* for the samples A12 and A14 (DSS treated mice) and A17 and A19 (control mice). A One-Way ANOVA was performed to compare the percentage of flagellation ($p < 0.05$).

6 Discussion

A previous study by Frank et al. (2007) for human gut wall tissue samples showed by comparing samples of IBD patients with a control group changes in the microbiota composition. However, until now no IBD specific bacteria or genes could be identified. In this study, a better insight into the shifts of selected microorganisms and genes by investigating several candidate microorganisms and associated genes observed by Berry et al. (2012) was aspired.

6.1 When the inflammation arises

The indicator for inflammation is the body weight loss of the mice. Taking a closer look on all the weight curves for the mice in all experiments (Figure 6-1), their weight loss started six to seven days after DSS treatment. This goes well along other observations where the onset of the inflammation was between four to seven days after DSS treatment (Johansson et al., 2010). In this study, this effect was observed both for the different trials (variations in the DSS treatment (Table 6-1)) and the different mouse genotypes. For Trial A, where wt and STAT1^{-/-} knockout mice were used, the weight loss was most severe in the wt mice. This outcome was expected as it was reported before (Bandyopadhyay et al., 2008). The inflammation for the Trial A wt mice was more severe than for the wt mice of the other trials which were investigated for at least ten days (G and I) which might be explained by the longer DSS treatment of seven days in Trial A. Nonetheless, the onset of inflammation for all the trials was at the same time. The reason why the control mice of Trial A gained weight most of the time was because at the beginning of the DSS treatment they were six to eight weeks of age and therefore not full-grown (Berry et al., 2012). The initial age of the mice also explains why the Trial I mice even gained weight in comparison with their initial weight in the recovery phase after the inflammation.

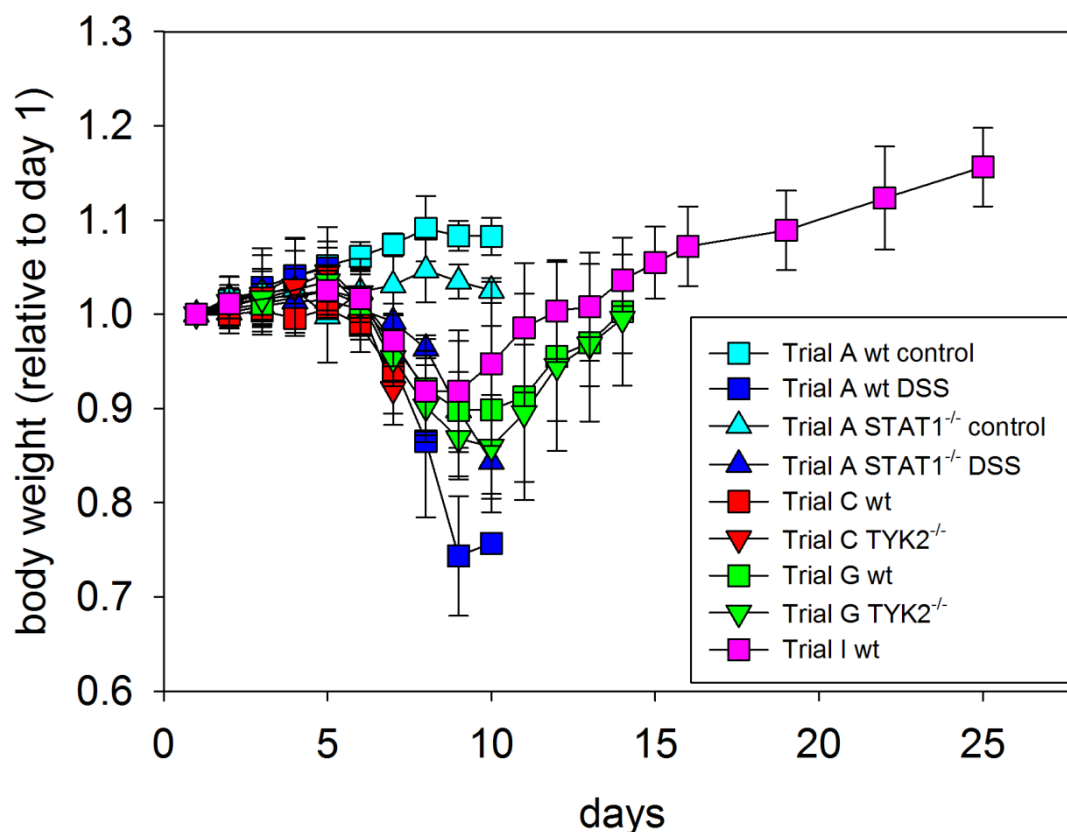


Figure 6-1: Weight curves for DSS induced murine colitis merged for the Trials A, C, G and I. For Trial A and C the DSS treatment lasted for seven consecutive days, for Trial G and I for five days.

Table 6-1: DSS-treatment and DSS free days for the different trials.

Trial	day															
	1	2	3	4	5	6	7	8	9	10	11	12	13	14	16 - 23	25
A																
C																
G																
I																

	DSS treatment	not investigated
	no DSS treatment	sampling

Regarding the amount of total bacteria 16S rRNA as measured by qPCR, there was no significant change between the different models and mouse genotypes for each trial. The same observation was made by Png et al. (2010). However, starting on phylum level, shifts in the community composition were reported (Packey and Sartor, 2009; Peterson et al., 2008; Png et al., 2010; Reiff and Kelly, 2010; Sokol et al., 2008; Walker et al., 2011).

6.2 *Akkermansia* and its increase during inflammation

The abundance of *Akkermansia* 16S rRNA genes in acute murine colitis was significantly increased in the DSS treated compared to the control mice. For the metatranscriptomic analysis of the same samples, Berry et al. (2012) also observed an increase of *Akkermansia* 16S rRNA genes in these mice (not detectable to 2.2 % in both genotypes) which emphasizes the reproducibility. Accordingly, the *Akkermansia* 16S rRNA transcripts were elevated for the DSS treated mice. The increased amount of *Akkermansia* 16S rRNA transcripts was also obtained by Berry et al. (2012) in the metatranscriptomic analysis.

It was reported before that STAT1^{-/-} mice show an attenuated course of inflammation (Bandyopadhyay et al., 2008) which was in this study indicated by the weight curves, too. However, looking at the increase of *Akkermansia* 16S rRNA gene copies for both genotypes of the DSS treated mice in Trial A, no difference was observed. The increase in gene copies was even much higher for the STAT1^{-/-} mice when the values of the control mice were compared to the ones of the DSS treated mice.

Contrary to Trial A, hardly any difference in abundance of *Akkermansia* was observed in Trial C, which could be due to the short length of seven days of this trial. As IBD is indicated by weight loss and examining the weight curves, the weight loss was just at the beginning on day 6 to 7 which was when Trial C ended. Also, it was reported that inflammation in wt mice just starts after about four to seven days when administrating DSS (Johansson et al., 2010). So the effect on the microbiota may also just be on the onset at the last time point in the disease development model.

In the recovery model where a longer time course was analyzed, the *Akkermansia* 16S rRNA genes increased after day 1 with a maximum on day 8 where the inflammation, according to the weight curves, was the most severe. However, the increase of the transcripts started after day 8.

Summarizing, the abundance of *Akkermansia* 16S rRNA genes was the highest the more pronounced the inflammation was. This can also be seen in Figure 6-2 where the single values for each sample of the Trial A, C and I wt mice for the gene copies are depicted against the relative body weight of the corresponding mouse. *Akkermansia* 16S rRNA abundance was negatively correlated to the body weight of the mice, so

Akkermansia is more abundant the less the mice weigh (Pearson Product Moment Correlation: $r_s = -0.472$, $p = 0.00843$, $N = 30$).

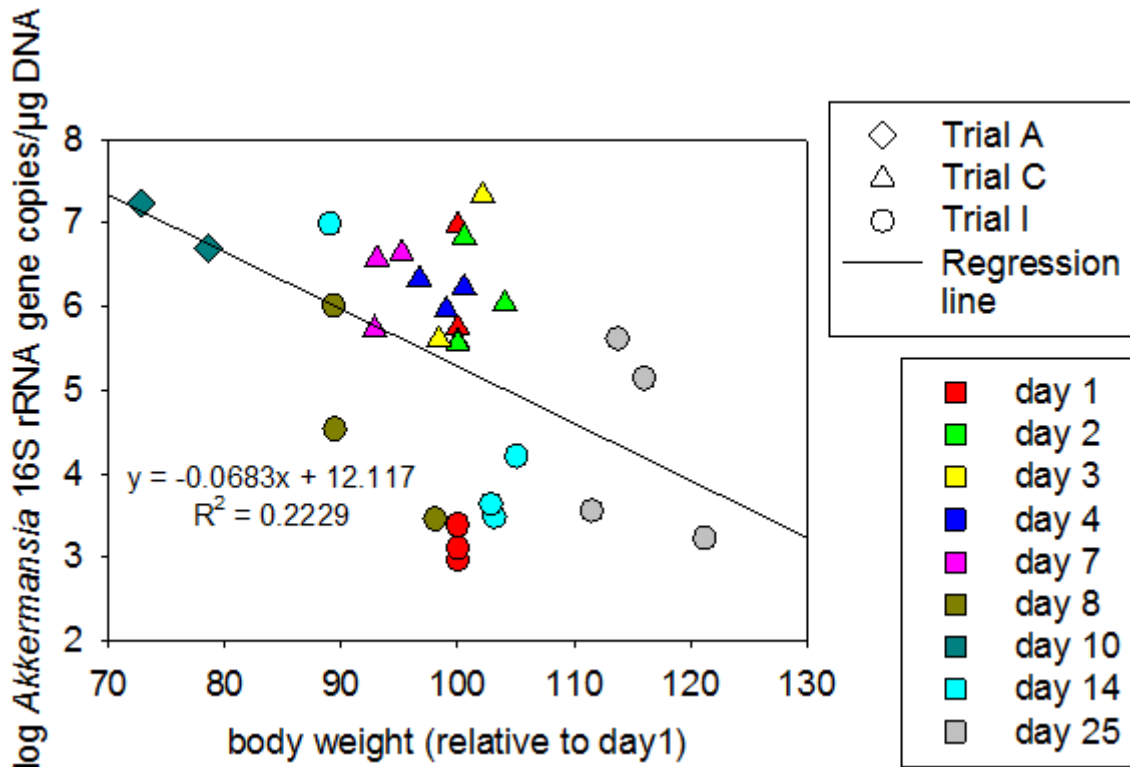


Figure 6-2: The *Akkermansia* 16S rRNA gene copies plotted against the relative body weight of each mouse. Every data point represents one sample. For this plot, the values for the wt mice of Trial A, C and I were used. The regression line was added. Day 5 of Trial I is missing as the body weight was not measured then for these mice.

This observation could be explained by the lifestyle of *A. muciniphila*, the only cultivated species of the genus *Akkermansia*, which is using mucin as sole carbon and nitrogen source (Derrien et al., 2004): in mice suffering from colitis, mucin is detached from the epithelium and therefore more accessible (Johansson et al., 2010). Accordingly, Morgan et al. (2012) proposed that an increase in cysteine metabolism and N-acetylgalactosamine transporters during inflammation indicated a greater abundance of microbes which use mucin as primary energy source, too, as mucin, which is rich in cysteine and glycosylated sugars, is upregulated during inflammation. The same observation of an increase of *Akkermansia* was made for Burmese pythons (Costello et al., 2010) and Syrian hamsters (Sonoyama et al., 2009) which were food deprived as mucin degrading bacteria benefit in states of nutrient deficiencies. Contradictory to the present study, a decrease of *Akkermansia* was noticed in IBD

suffering (Png et al., 2010) and obese people (Zhang et al., 2009). However, the stool samples of the obese group analyzed by Zhang et al. (2009) showed an increase of *Prevotellaceae* (phylum Bacteroidetes) which are carbohydrate and protein fermenters. Due to the different eating habits of obese people it is believed that more carbohydrates occur in their gut which is why carbohydrate fermenters are able to outcompete *Akkermansia*. The assumption of Png et al. (2010) why *Akkermansia* was decreased in IBD was that *Akkermansia* and the other mucosa-associated bacteria are in an equilibrium where *Akkermansia* is more abundant in health and the other bacteria outcompete *Akkermansia* during inflammation due to the increased substrate availability.

The same observation as for the *Akkermansia* 16S rRNA was made for the *rbr*, *bnh* and *epsc* genes and transcripts. Their abundance in Trial A was always higher in the DSS treated mice. Also, in Trial C and I the functional genes mirrored the 16S rRNA genes and transcripts. However, the increase during inflammation was not significant for every functional gene for every trial which may be due to the huge standard deviations.

For *rbr*, there was a significant increase for the different mouse genotypes and for the genes and transcripts, respectively. When calculating the transcripts to gene ratio, which indicates gene expression, of *rbr* for Trial A, this ratio was always higher in the DSS treated mice (wt: 0.40 % \pm 0.01 to 11.13 % \pm 0.01 after DSS treatment, STAT1^{-/-}: 0.32 % \pm 0.01 to 8.78 % \pm 0.01 after DSS treatment). *Rbr*, which has also been detected in the piglet gut (Poroyko et al., 2010), is proposed to function as a protection against oxidative stress in air-sensitive bacteria as it is a hydrogen peroxide reductase (Kurtz, 2006). Thus, it can be used as an indicator transcript for oxidative stress which displays a change to more oxygen in the environment. Also, Morgan et al. (2012) observed an increase in, for example, glutathione metabolism which indicates a response of the microbiome towards oxidative stress caused by gut inflammation. It is known that during inflammation, a response of the immune system is to generate reactive oxygen species (Arseneau et al., 2007) which would fit the pattern. This was also indicated by the increased *rbr* expression in Trial A for the DSS treated mice. Since the *Akkermansia rbr* transcripts were more abundant in the DSS treated mice, Berry et al. (2012) postulated this could be due to a bigger exposure to reactive oxygen and/or nitrogen species during inflammation.

The genes and transcripts of *bnh*, which may be involved in mucin degradation (Turroni et al., 2010) and therefore assumed to be a marker for this process, were also

increased in the DSS treated mice. Calculating the gene expression via the transcripts to gene ratio showed that more *bnh* was expressed for both the Trial A control mice (wt: 17.63 % \pm 0.97 to 0.39 % \pm 0.00, STAT1^{-/-}: 109.36 % \pm 1.44 to 0.39 % \pm 0.00) and for the day 1 and day 5 Trial I mice (day 1: 28.93 % \pm 0.91, day 5: 12.85 % \pm 0.58, days 8 to 25: between 0.34 % \pm 0.01 and 2.31 % \pm 0.08). The expression of *bnh* was more increased for the control mice and the early colitis development (Trial A and I) than in acute inflammation. *Bnh* is predicted to be involved in mucin degradation (Turrone et al., 2010). However, during inflammation, other mucolytic bacteria may increase leading to a decrease of *Akkermansia* possibly due to a less attractive niche for them (Png et al., 2010) which may be a reason for the decrease in *bnh*. Reasons why no increase of *bnh* could be observed in the recovery phase might be that either the higher abundance of other mucolytic bacteria sustains longer than the acute phase of inflammation, alterations towards other substrates occur or due to technical issues because the samples investigated were obtained from luminal content and not from biopsy. Another possibility could be that mucin was not so easy to access when the mucosa was intact so the bacteria would have to be at all times prepared to utilize as much mucin as available whereas when the mucosa was detached and the mucin was easily accessible, the substrate for mucolytic bacteria was permanently available. The expression of *epsc* was only increased in the DSS treated STAT1^{-/-} mice. The *epsc* gene is involved in the capsular polysaccharide biosynthesis (van Passel et al., 2011) for which it was shown for *Bacteroides fragilis* that the capsular polysaccharides are essential for colonization of the intestinal tract (Liu et al., 2008).

6.3 The decrease of flagellin genes and transcripts in murine colitis

The analysis for the abundance of functional categories of mRNA transcripts by Berry et al. (2012) showed that there were less motility and chemotaxis associated transcripts in the DSS treated mice (for both wt and STAT1^{-/-} mice). Since this category mainly consisted of clostridial flagellin transcripts, it was expected that there were fewer flagellin transcripts in the samples of DSS treated mice. Therefore, a focus was on analyzing their changes in abundance during inflammation. Additionally to the flagellin gene, the clostridial clusters IV (*Clostridium leptum* subgroup) and XIVa (*Clostridium coccoides* group) were examined to which the *Lachnospiraceae* and *Ruminococcaceae* belong.

Discussion

The amplicons obtained by the *fla* primers (both for the ones targeting the whole gene (Duck et al., 2007) and the newly designed ones targeting the C-terminus of the flagellin gene) were sequenced and subsequently indeed identified as genes for clostridial flagellins.

The abundance of the flagellin genes and transcripts decreased during inflammation for the majority of the samples in all trials. The same observation, using serological expression cloning, was made by Ye et al. (2008) and Lodes et al. (2004). The flagellin protein detected by the latter ones was assigned to the clostridial cluster XIVa (*Lachnospiraceae*) by Duck et al. (2007).

For the Trial C wt mice, the flagellin gene abundance was just about 10^5 at the beginning and then increased up to almost 10^8 gene copies per μg DNA. For Trial A and I, the abundance was already at the beginning at about 10^8 . This effect may be attributed to individuality (which is also indicated by the huge standard deviation and may have been caused by the caging conditions) or a technical problem (for all the other trials, the ascent and descent of the transcripts mirrored the ones of the genes which could have been caused during DNA extraction or problems when qPCR was performed). Considering this assumption and looking at all the wt mice of the Trials C, G and I together (Figure 6-3), the lowest abundance of flagellin genes and transcripts occurred on day 8 reflecting the inflammation indicating weight curves. The low copy numbers at the first days in the graph with the merged data of the trials C, G and I DNA were due to the low flagellin copy numbers obtained for the Trials C and G (lower than 10^7) as explained above.

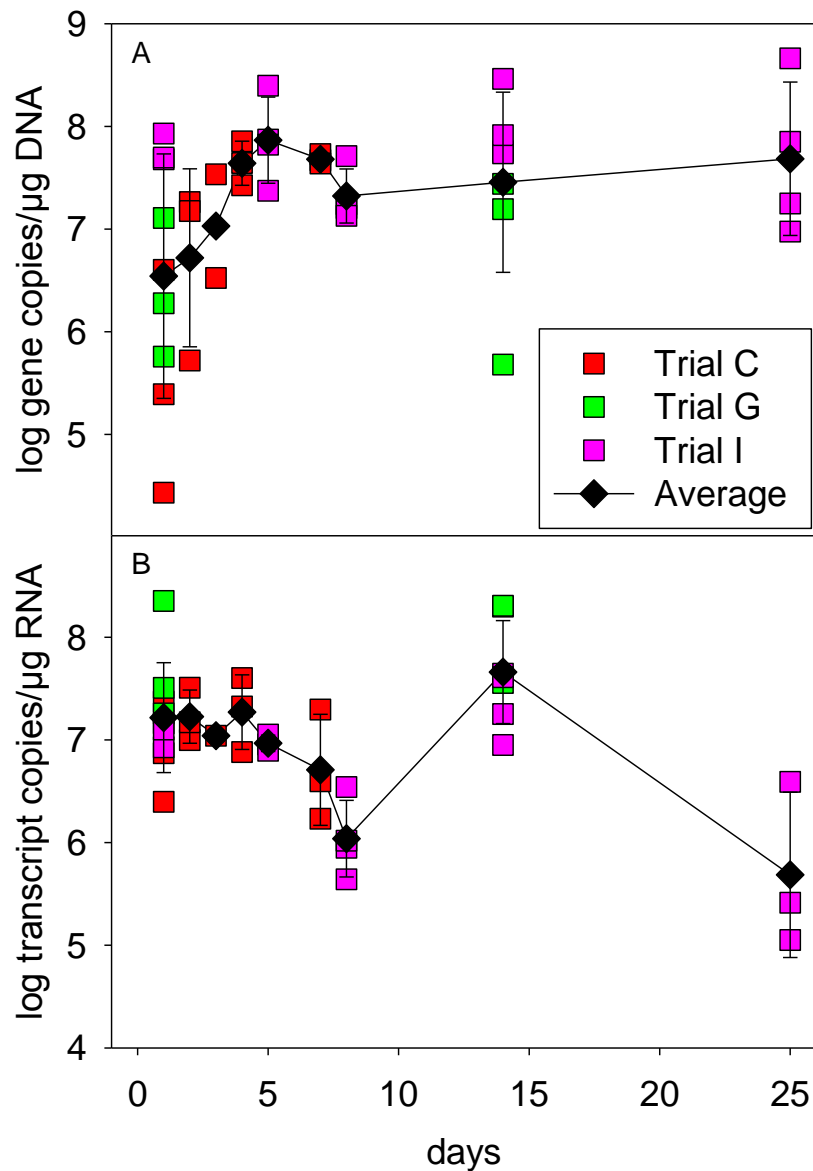


Figure 6-3: Abundance of flagellin gene (A) and transcripts (B) for the wt mice of Trial C, G and I. DSS treatment for Trial C mice lasted seven days and for Trial G and I five days. Each red, green and pink square belongs to individual data points whereas the black diamonds represent their average for each day.

The decrease of flagellin with inflammation could be due to the disruption of the mucus layer (Johansson et al., 2010) and the increased permeability of the epithelium (Himmel et al., 2008) which increases the accessibility of TLR5. If the mucus layer is intact the mucosa does not respond to flagellin proteins whereas if it is disrupted, the severity of the inflammation is increased (Rhee, 2005). Johansson et al. (2010) postulated that an intact mucus layer is important to protect the colon and when it is disrupted, inflammation is triggered by the immune system. One quarter of the immunodominant antigens involved in murine colitis were found to be flagellins from

commensal bacteria (Lodes et al., 2004). Hence, also bacteria which are not pathogens can cause acute inflammation (Vijay-Kumar and Gewirtz, 2009). TLR5 can only be activated by flagellin monomers and not filamentous flagella (Smith et al., 2003). Flagellin monomers are constantly released to the surroundings of the bacteria (Vijay-Kumar and Gewirtz, 2009). This release may be spontaneous or controlled by the host via proteases and/or detergents (Ramos et al., 2004). Also, the bacteria might regulate a removal of flagella in the mucosa where physico-chemical conditions cause a transformation from filamentous flagella to flagellin monomers (Ramos et al., 2004). When the mucus layer is disrupted, the flagellin protein can easier access TLR5 and thus induce the production of genes with antibacterial activity which helps the host keeping the bacteria under control by killing mucosal bacteria which could otherwise drive disease (Vijay-Kumar and Gewirtz, 2009). By stimulating TLR5 on T cells, depending on the flagellin protein concentration, the balance of effector and regulatory T cells could be altered in IBD (Himmel et al., 2008).

6.3.1 Establishment of microscopic techniques to identify flagellated bacteria

A main topic of this study was the observation of changes in abundance of the flagellin which, as a structural protein, contributes a major part in flagella formation (Ramos et al., 2004). These flagella can, by means of different dyes, be visualized using microscopy. On the one hand, general flagella stains (basic fuchsin and NanoOrange®), on the other hand, a specific one (primary antibody against clostridial flagellin) were used. The aim was to combine these techniques with each other or with FISH to be able to assign the flagella to specific bacteria or a family and to get an estimation of how many bacteria are flagellated.

6.3.1.1 The basic fuchsin approach – a general flagella stain

Following the protocol by Mellies (2008), good results were obtained for the basic fuchsin stain although the background was sometimes grainy. The flagella were easy to recognize as they get enlarged (Mellies, 2008) and good to distinguish from the bacteria. Nonetheless, one disadvantage of this method is that broken off flagella are

easily missed. Also, the combination with fluorescent dyes was not possible although conditions needed for FISH, especially, were tested and when applied to the basic fuchsin stain alone mostly did not cause a problem. The exception was the mounting medium, where Vectashield immediately discoloured the basic fuchsin stain and using Citifluor, the slides had to be examined right away. Hence, it is likely that the combination of the conditions needed for fluorescent dyes or the fluorescent dyes themselves caused a crossreaction which inhibited the successful combination of basic fuchsin with the other stains. Unfortunately, the reason for it could not be determined.

6.3.1.2 NanoOrange® - the search for fluorescent flagella

Besides the basic fuchsin stain NanoOrange® was used as a general flagella stain, too. This method is easy to apply and stains every protein, so all the bacteria and proteinaceous structures are visualized. Contrary to the basic fuchsin stain, the flagella do not get enlarged using NanoOrange® which made it more difficult to detect the flagella. However, Grossart et al. (2000) managed to visualize flagella using NanoOrange® at a magnification of $\times 320$ but the maximal magnification available for this study was $\times 100$. Hesse and Kim (2009) even used a scanning electron microscope. Hence, the lack of flagella observation or the difficulties doing that, respectively, could be explained due to these technical limitations.

All extracellular proteinaceous structures get stained, too, which increased the difficulty to reliably detect the flagella. An attempt to circumvent this problem was the combination with other staining techniques. An aggravating factor was that NanoOrange® is visible as well in the TRITC as the FITC channel, so it could only be combined with Cy5 probes. Unfortunately, the combination with immunofluorescence and FISH did not make the identification of the flagella much easier. Additionally, as well as with the basic fuchsin stain, broken off flagella cannot be distinguished as the bacteria and flagella have the same colouring.

Furthermore, using a combination with DAPI which is a DNA stain showed that NanoOrange® is capable of staining more bacteria as some are missed by DAPI.

6.3.1.3 Assignment of flagella by combining IF and FISH

Using immunofluorescence, the flagella were easy to detect. Also, contrary to the basic fuchsin and NanoOrange® stain, flagella which were broken off were visible. Although the primary antibody was already specific for the clostridial flagellin, a more precise assignment was desired. Therefore, immunofluorescence was combined with FISH probes specific on different phylogenetic levels. For the combination of these two techniques very little literature was available. The majority of the authors experienced difficulties for this combination and had to try different approaches or adjustments (Donadoni et al., 2004 (on brain and muscle tissues); Gmür and Lüthi-Schaller, 2007 (on single cells of dental plaque); Chaumeil et al., 2008 (investigating X chromosome inactivation); Nehmé et al., 2011 (on brain tissue sections)). Especially Gmür and Lüthi-Schaller (2007) tried several variations (more than 20) to improve the results by changing some parameters or the order in which the different steps were performed. However, in contrast to their observations, no difficulties occurred in this study by combining these two standard methods, so no changes in the protocols were applied. To investigate which order of applying immunofluorescence or FISH first yields the better outcomes, both orders were tried out with the result that the signals for especially FISH were better when immunofluorescence was performed first. The same observation was made by Gmür and Lüthi-Schaller (2007). However, Nehmé et al. (2011) observed better results when starting with FISH.

6.3.2 Quantification of flagellated *Lachnospiraceae*

The OTU specific probes for *Lachnospiraceae* were used to specifically assign the flagella. A previous study by Berry et al. (2012) for Trial A showed that the *Lachnospiraceae* OTU_11021 was just present in the control mice whereas *Lachnospiraceae* OTU_9468 just occurred in the DSS treated ones. Hence, their assumption was that OTU_11021 was flagellated and OTU_9468 carried no or less flagella as the metatranscriptomic analysis showed a decrease in flagellin transcripts for DSS treated mice. However, combining immunofluorescence with FISH probes specific for these two OTU's showed that both OTU's carried flagella. Hence, flagellated *Lachnospiraceae* were present in every sample, as well in the control as the DSS treated ones. Thus, the former hypothesis could be falsified. Therefore, the

decrease in flagellin genes and transcripts during inflammation was not due to shifts in the *Lachnospiraceae*.

After receiving this result, the question was whether a change in the amount of flagellated bacteria could be observed on protein level for the *Lachnospiraceae* comparing the control with the DSS treated mice as it was obtained for the metatranscriptome (Berry et al., 2012) and qPCR for genes and transcripts. Therefore, the Erec482 probe (Franks et al., 1998), representing the *Lachnospiraceae*, was chosen. Looking at the outcome, a trend within the control and within the DSS treated mice could be observed (Figure 6-4). Whereas the percentage of flagellated *Lachnospiraceae* and the flagellin gene decreased when sample A12 was compared with A14 (both samples originate from DSS treated mice), the obtained values for A17 and A19 (both from control mice) were about the same in both techniques. Independently regarded, the trends were the same with especially sample A12 sticking out from the expected outcome, as well for qPCR as for the IF-FISH quantification. As there were just four samples examined, no correlation could be observed. Therefore, further investigations using more samples would be required.

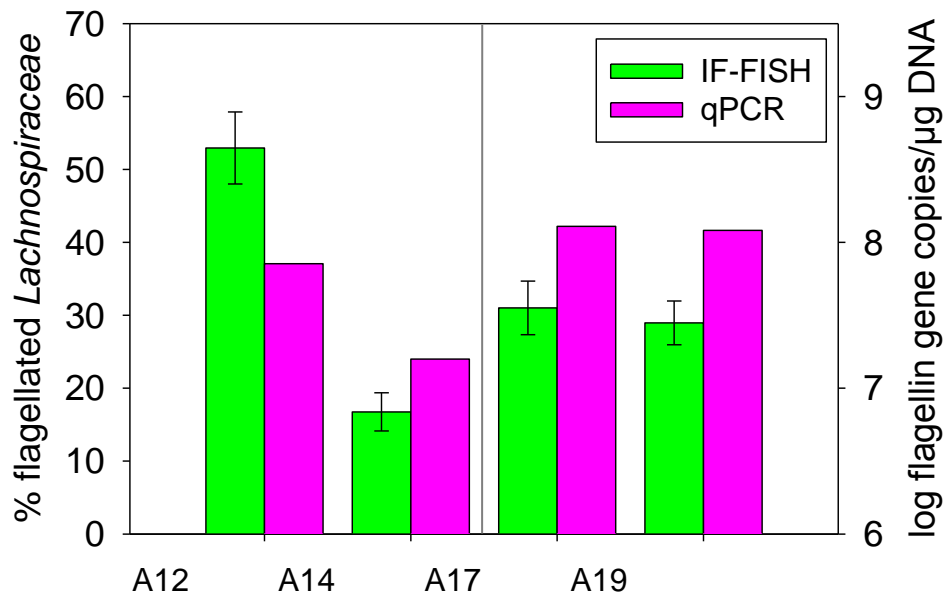


Figure 6-4: Comparison for the flagella/flagellin gene results of IF-FISH and qPCR for randomly selected STAT1^{-/-} mice of Trial A. A12 and A14 represent the DSS treated whereas A17 and A19 embody the control mice.

6.4 The influence of the mouse genotype on gut microbiota differences

In this study, three different mouse genotypes were investigated: the wt, STAT1^{-/-} and TYK2^{-/-} mice. It was desired to analyse whether differences of the gut microbiota composition between these genotypes, especially when comparing the wt to the knockout mice, occurred. However, no alterations could be observed. Although, in Trial A the weight loss of the STAT1^{-/-} mice was attenuated which hints to a smoother or delayed course of disease which was also reported by Bandyopadhyay et al. (2008). Also, no difference comparing the wt and TYK2^{-/-} mice could be observed. The reason for this may be the short duration of Trial C and the few data points available for Trial G. Also, no influence of the mouse genotype was observed on the abundance of *Akkermansia* and flagellin genes and transcripts.

7 Conclusion

The aim of this study was to verify if the *Akkermansia* abundance increases and the flagellin abundance decreases during murine colitis as both of them are associated with IBD. Therefore, an experimental setup with mice suffering from DSS induced colitis was used where samples were taken at several time points during acute inflammation, inflammation development and the recovery. To investigate the shifts, qPCR using specific primers was utilized. Additionally, to verify the qPCR data for the flagellin gene, a combination of IF and FISH was performed.

As expected, *Akkermansia* and the flagellin gene, both, were found to be indicators of gut inflammation with an increased *Akkermansia* and decreased flagellin abundance. However, these changes just occurred in the acute phase and the shifts could not be observed during development so they are not suitable as early markers. Therefore, the use of *Akkermansia* and flagellin as preventive markers in clinical trials might be challenging but they are potential markers for acute IBD. Until now, an increase of *Akkermansia* abundance in humans suffering from IBD has not yet been observed. This study shows first insights into the lifestyle of *Akkermansia* by means of shifts in functional genes. Also, the findings of the study could indicate an increased abundance of *Akkermansia* due to an advantage of using the increased mucin availability or due to the capability to cope with oxidative stress.

A method of combining immunofluorescence, targeting the clostridial flagellin, and FISH was established which is a useful tool to assign, in this case, flagella to bacteria on different phylogenetic levels. In future experiments, shifts in the flagella possessing bacteria should be determined to find out, if these are bacteria triggering the immune system. Quantification of stained bacteria and flagella coincided with the amount of flagella obtained by qPCR for the flagellin gene. To verify this result, more samples should be analyzed. Also, the usage of primary antibodies specific for other antigens for IF in combination with FISH is conceivable.

8 Zusammenfassung

Die Gesundheit des Menschen und insbesondere die des Verdauungsapparats ist abhängig von der Aktivität von Mikroorganismen. Die ständige Anwesenheit einer Vielzahl von Bakterien in unserem Körper erfordert ein sensibles Gleichgewicht zwischen der Aktivität des Immunsystems und der Mikrobiota. Leidet man an einer chronisch-entzündlichen Darmerkrankung wie Morbus Crohn oder Colitis Ulcerosa ist dieses Gleichgewicht gestört. Bis heute sind die Auslöser für diese beiden Krankheiten nicht bekannt. Daher ist die Suche nach verlässlichen diagnostischen Markern Gegenstand reger Forschung. Im Rahmen eines Kooperationsprojektes (InflammoBiota) wurden Indizien gefunden, dass das Bakterium *Akkermansia*, beziehungsweise die Flagelline der Clostridien Indikatoren für Darmentzündungen sein könnten.

Das Ziel dieser Studie war daher, zu überprüfen, ob *Akkermansia* und die Flagelline der Clostridien tatsächlich geeignete Indikatoren für akute Darmentzündungen sind. Dafür wurde ein Mausmodell verwendet, bei dem die Entzündung durch die Verabreichung von Dextran-Natriumsulfat hervorgerufen wird. Veränderungen in der Abundanz von bakteriellen Gruppen und der Expression ausgewählter Gene wurden mittels quantitativer Polymerase-Kettenreaktion (qPCR) anhand von Proben aus dem Darmlumen untersucht, die während akuter Entzündung, ihrer Entstehung und der Genesung genommen worden waren. Zusätzlich zu der 16S rRNA von *Akkermansia* wurden noch drei seiner funktionellen Gene (Rubrerythrin, β -N-Acetylhexosaminidase und kapsulare Exopolysaccharidsynthese) untersucht. Um die Flagellen außerdem zu visualisieren wurden verschiedene Mikroskopieansätze verwendet, darunter Immunofluoreszenz (IF).

Es konnte gezeigt werden, dass die Anzahl an *Akkermansia* 16S rRNA Genen während der akuten Darmentzündung bis zu 20.000 fach anstieg und negativ mit dem Körpergewicht der Mäuse korrelierte. Die Ursache für den Anstieg von *Akkermansia* könnte die Ablösung von Mukus vom Darmepithel sein. Dadurch würde die Nährstoffzugänglichkeit für *Akkermansia* Zellen erhöht, welche Mukus als alleinige Kohlenstoff-, Stickstoff- und Energiequelle nutzen. Außerdem deutete der Anstieg von Transkripten des Rubrerythrins, welches Schutz vor oxidativem Stress bietet, auf eine durch Sauerstoff ausgelöste Stressreaktion von *Akkermansia* bei akuter Darmentzündung hin.

Zusammenfassung

Die Abundanz der Clostridienflagelline war während der akuten Darmentzündung reduziert. Da die Durchlässigkeit des Darmepithels während der Entzündung erhöht ist, könnte dies zu einer erhöhten Aktivierung des Immunsystems durch das starke Flagellinantigen geführt haben. Eine Methode zur Kombination von IF und Fluoreszenz *in situ* Hybridisierung (FISH) wurde etabliert, wodurch die Flagellen spezifischen Bakterien zugeordnet werden konnten. Die Ergebnisse von IF-FISH und qPCR waren konsistent. Zur Bestätigung der Kompatibilität dieser Methoden sollten jedoch noch weitere Studien mit mehreren Proben durchgeführt werden.

Insgesamt konnte bestätigt werden, dass *Akkermansia* und die Flagelline der Clostridien als Indikatoren für akute Darmentzündungen bei Mäusen dienen können. Zukünftige Studien werden zeigen, ob diese Resultate auf Darmentzündungen des Menschen übertragbar sind.

9 References

- Aaronson, D.S., and Horvath, C.M. (2002). A road map for those who don't know JAK-STAT. *Science* 296, 1653–1655.
- Amann, R.L., Binder, B.J., Olson, R.J., Chisholm, S.W., Devereux, R., and Stahl, D.A. (1990). Combination of 16S rRNA-targeted oligonucleotide probes with flow cytometry for analyzing mixed microbial populations. *Appl. Environ. Microbiol.* 56, 1919–1925.
- Arseneau, K.O., Tamagawa, H., Pizarro, T.T., and Cominelli, F. (2007). Innate and adaptive immune responses related to IBD pathogenesis. *Curr Gastroenterol Rep* 9, 508–512.
- Backhed, F. (2005). Host-Bacterial Mutualism in the Human Intestine. *Science* 307, 1915–1920.
- Bäckhed, F., Ley, R., Sonnenburg, J., and Gordon, J. (2006). The human intestinal microbiota and its relationship to energy balance. *Scandinavian Journal of Food & Nutrition* 50, 121–123.
- Bandyopadhyay, S.K., de la Motte, C.A., Kessler, S.P., Hascall, V.C., Hill, D.R., and Strong, S.A. (2008). Hyaluronan-Mediated Leukocyte Adhesion and Dextran Sulfate Sodium-Induced Colitis Are Attenuated in the Absence of Signal Transducer and Activator of Transcription 1. *The American Journal of Pathology* 173, 1361–1368.
- Baumgart, D.C., and Carding, S.R. (2007). Inflammatory bowel disease: cause and immunobiology. *The Lancet* 369, 1627–1640.
- Belzer, C., and de Vos, W.M. (2012). Microbes inside—from diversity to function: the case of Akkermansia. *The ISME Journal* 6, 1449–1458.
- Berry, D., Schwab, C., Milinovich, G., Reichert, J., Ben Mahfoudh, K., Decker, T., Engel, M., Hai, B., Hainzl, E., Heider, S., et al. (2012). Phylotype-level 16S rRNA analysis reveals new bacterial indicators of health state in acute murine colitis. *The ISME Journal*.
- Brötz-Oesterhelt, H., and Brunner, N. (2008). How many modes of action should an antibiotic have? *Current Opinion in Pharmacology* 8, 564–573.

References

- Bulgheresi, S., Schabussova, I., Chen, T., Mullin, N.P., Maizels, R.M., and Ott, J.A. (2006). A New C-Type Lectin Similar to the Human Immunoreceptor DC-SIGN Mediates Symbiont Acquisition by a Marine Nematode. *Applied and Environmental Microbiology* 72, 2950–2956.
- Carbonnel, F., Jantchou, P., Monnet, E., and Cosnes, J. (2009). Environmental risk factors in Crohn's disease and ulcerative colitis: an update. *Gastroenterol. Clin. Biol.* 33 *Suppl* 3, S145–157.
- Chaumeil, J., Augui, S., Chow, J.C., and Heard, E. (2008). Combined immunofluorescence, RNA fluorescent in situ hybridization, and DNA fluorescent in situ hybridization to study chromatin changes, transcriptional activity, nuclear organization, and X-chromosome inactivation. *Methods Mol. Biol.* 463, 297–308.
- Clark, W.A. (1976). A simplified Leifson flagella stain. *J. Clin. Microbiol.* 3, 632–634.
- Collado, M.C., Derrien, M., Isolauri, E., de Vos, W.M., and Salminen, S. (2007). Intestinal Integrity and *Akkermansia muciniphila*, a Mucin-Degrading Member of the Intestinal Microbiota Present in Infants, Adults, and the Elderly. *Applied and Environmental Microbiology* 73, 7767–7770.
- Costello, E.K., Gordon, J.I., Secor, S.M., and Knight, R. (2010). Postprandial remodeling of the gut microbiota in Burmese pythons. *ISME J* 4, 1375–1385.
- Daims, H., Brühl, A., Amann, R., Schleifer, K.H., and Wagner, M. (1999). The domain-specific probe EUB338 is insufficient for the detection of all Bacteria: development and evaluation of a more comprehensive probe set. *Syst. Appl. Microbiol.* 22, 434–444.
- Daims, H., Stoecker, K., Wagner, M. (2005). Fluorescence in situ hybridisation for the detection of prokaryotes. *Advanced Methods in Molecular Microbial Ecology*. Bios-Garland: Abingdon, UK, pp 213–238.
- Daims, H., Lückner, S., and Wagner, M. (2006). daime, a novel image analysis program for microbial ecology and biofilm research. *Environmental Microbiology* 8, 200–213.
- Danese, S., Sans, M., and Fiocchi, C. (2004). Inflammatory bowel disease: the role of environmental factors. *Autoimmun Rev* 3, 394–400.

References

- Derrien, M., Vaughan, E.E., Plugge, C.M., and de Vos, W.M. (2004). *Akkermansia muciniphila* gen. nov., sp. nov., a human intestinal mucin-degrading bacterium. *Int. J. Syst. Evol. Microbiol.* **54**, 1469–1476.
- DiBaise, J.K., Zhang, H., Crowell, M.D., Krajmalnik-Brown, R., Decker, G.A., and Rittmann, B.E. (2008). Gut microbiota and its possible relationship with obesity. *Mayo Clin. Proc.* **83**, 460–469.
- Donadoni, C., Corti, S., Locatelli, F., Papadimitriou, D., Guglieri, M., Strazzer, S., Bossolasco, P., Salani, S., and Comi, G.P. (2004). Improvement of combined FISH and immunofluorescence to trace the fate of somatic stem cells after transplantation. *J. Histochem. Cytochem.* **52**, 1333–1339.
- Duck, L.W., Walter, M.R., Novak, J., Kelly, D., Tomasi, M., Cong, Y., and Elson, C.O. (2007). Isolation of flagellated bacteria implicated in Crohn's disease. *Inflammatory Bowel Diseases* **13**, 1191–1201.
- Eckburg, P.B., Bik, E.M., Bernstein, C.N., Purdom, E., Dethlefsen, L., Sargent, M., Gill, S.R., Nelson, K.E., and Relman, D.A. (2005). Diversity of the human intestinal microbial flora. *Science* **308**, 1635–1638.
- Frank, D.N., St Amand, A.L., Feldman, R.A., Boedeker, E.C., Harpaz, N., and Pace, N.R. (2007). Molecular-phylogenetic characterization of microbial community imbalances in human inflammatory bowel diseases. *Proc. Natl. Acad. Sci. U.S.A.* **104**, 13780–13785.
- Franks, A.H., Harmsen, H.J., Raangs, G.C., Jansen, G.J., Schut, F., and Welling, G.W. (1998). Variations of bacterial populations in human feces measured by fluorescent in situ hybridization with group-specific 16S rRNA-targeted oligonucleotide probes. *Appl. Environ. Microbiol.* **64**, 3336–3345.
- Garantziotis, S., Hollingsworth, J.W., Zaas, A.K., and Schwartz, D.A. (2008). The effect of toll-like receptors and toll-like receptor genetics in human disease. *Annu. Rev. Med.* **59**, 343–359.
- Gewirtz, A.T., Vijay-Kumar, M., Brant, S.R., Duerr, R.H., Nicolae, D.L., and Cho, J.H. (2006). Dominant-negative TLR5 polymorphism reduces adaptive immune response to flagellin and negatively associates with Crohn's disease. *Am. J. Physiol. Gastrointest. Liver Physiol.* **290**, G1157–1163.

References

- Gill, S.R., Pop, M., Deboy, R.T., Eckburg, P.B., Turnbaugh, P.J., Samuel, B.S., Gordon, J.I., Relman, D.A., Fraser-Liggett, C.M., and Nelson, K.E. (2006). Metagenomic analysis of the human distal gut microbiome. *Science* 312, 1355–1359.
- Gmür, R., and Lüthi-Schaller, H. (2007). A combined immunofluorescence and fluorescent in situ hybridization assay for single cell analyses of dental plaque microorganisms. *J. Microbiol. Methods* 69, 402–405.
- Grossart, H.P., Steward, G.F., Martinez, J., and Azam, F. (2000). A simple, rapid method for demonstrating bacterial flagella. *Appl. Environ. Microbiol.* 66, 3632–3636.
- Hayashi, F., Smith, K.D., Ozinsky, A., Hawn, T.R., Yi, E.C., Goodlett, D.R., Eng, J.K., Akira, S., Underhill, D.M., and Aderem, A. (2001). The innate immune response to bacterial flagellin is mediated by Toll-like receptor 5. *Nature* 410, 1099–1103.
- Hesse, W.R., and Kim, M.J. (2009). Visualization of flagellar interactions on bacterial carpets. *J Microsc* 233, 302–308.
- Hill, M.J. (1997). Intestinal flora and endogenous vitamin synthesis. *Eur. J. Cancer Prev.* 6 Suppl 1, S43–45.
- Himmel, M.E., Hardenberg, G., Piccirillo, C.A., Steiner, T.S., and Levings, M.K. (2008). The role of T-regulatory cells and Toll-like receptors in the pathogenesis of human inflammatory bowel disease. *Immunology* 125, 145–153.
- Johansson, M.E.V., Gustafsson, J.K., Sjöberg, K.E., Petersson, J., Holm, L., Sjövall, H., and Hansson, G.C. (2010). Bacteria penetrate the inner mucus layer before inflammation in the dextran sulfate colitis model. *PLoS ONE* 5, e12238.
- Johansson, M.E.V., Ambort, D., Pelaseyed, T., Schütte, A., Gustafsson, J.K., Ermund, A., Subramani, D.B., Holmén-Larsson, J.M., Thomsson, K.A., Bergström, J.H., et al. (2011). Composition and functional role of the mucus layers in the intestine. *Cell. Mol. Life Sci.* 68, 3635–3641.
- Kurtz, D.M., Jr (2006). Avoiding high-valent iron intermediates: superoxide reductase and rubrerythrin. *J. Inorg. Biochem.* 100, 679–693.
- Lee, D.H., Zo, Y.G., and Kim, S.J. (1996). Nonradioactive method to study genetic profiles of natural bacterial communities by PCR-single-strand-conformation polymorphism. *Appl. Environ. Microbiol.* 62, 3112–3120.

References

- Lehmann, Y., Meile, L., and Teuber, M. (1996). Rubrerythrin from *Clostridium perfringens*: cloning of the gene, purification of the protein, and characterization of its superoxide dismutase function. *J. Bacteriol.* *178*, 7152–7158.
- Leifson, E. (1951). Staining, shape and arrangement of bacterial flagella. *J. Bacteriol.* *62*, 377–389.
- Ley, R.E., Peterson, D.A., and Gordon, J.I. (2006). Ecological and evolutionary forces shaping microbial diversity in the human intestine. *Cell* *124*, 837–848.
- Liu, C.H., Lee, S.M., VanLare, J.M., Kasper, D.L., and Mazmanian, S.K. (2008). From the Cover: Regulation of surface architecture by symbiotic bacteria mediates host colonization. *Proceedings of the National Academy of Sciences* *105*, 3951–3956.
- Lodes, M.J., Cong, Y., Elson, C.O., Mohamath, R., Landers, C.J., Targan, S.R., Fort, M., and Hershberg, R.M. (2004). Bacterial flagellin is a dominant antigen in Crohn disease. *J. Clin. Invest.* *113*, 1296–1306.
- Luckey, T.D. (1972). Introduction to intestinal microecology. *Am. J. Clin. Nutr.* *25*, 1292–1294.
- Macnab, R.M. (1999). The bacterial flagellum: reversible rotary propellor and type III export apparatus. *J. Bacteriol.* *181*, 7149–7153.
- Matsuki, T., Watanabe, K., Fujimoto, J., Miyamoto, Y., Takada, T., Matsumoto, K., Oyaizu, H., and Tanaka, R. (2002). Development of 16S rRNA-gene-targeted group-specific primers for the detection and identification of predominant bacteria in human feces. *Appl. Environ. Microbiol.* *68*, 5445–5451.
- Matsuki, T., Watanabe, K., Fujimoto, J., Takada, T., and Tanaka, R. (2004). Use of 16S rRNA gene-targeted group-specific primers for real-time PCR analysis of predominant bacteria in human feces. *Appl. Environ. Microbiol.* *70*, 7220–7228.
- Meraz, M.A., White, J.M., Sheehan, K.C., Bach, E.A., Rodig, S.J., Dighe, A.S., Kaplan, D.H., Riley, J.K., Greenlund, A.C., Campbell, D., et al. (1996). Targeted disruption of the Stat1 gene in mice reveals unexpected physiologic specificity in the JAK-STAT signaling pathway. *Cell* *84*, 431–442.
- Misch, E.A., and Hawn, T.R. (2008). Toll-like receptor polymorphisms and susceptibility to human disease. *Clin. Sci.* *114*, 347–360.

References

- Morgan, X.C., Tickle, T.L., Sokol, H., Gevers, D., Devaney, K.L., Ward, D.V., Reyes, J.A., Shah, S.A., LeLeiko, N., Snapper, S.B., et al. (2012). Dysfunction of the intestinal microbiome in inflammatory bowel disease and treatment. *Genome Biology* 13, R79.
- Mullis, K., Faloona, F., Scharf, S., Saiki, R., Horn, G., and Erlich, H. (1986). Specific enzymatic amplification of DNA in vitro: the polymerase chain reaction. *Cold Spring Harb. Symp. Quant. Biol.* 51 Pt 1, 263–273.
- Nehmé, B., Henry, M., and Mougnot, D. (2011). Combined fluorescent in situ hybridization and immunofluorescence: limiting factors and a substitution strategy for slide-mounted tissue sections. *J. Neurosci. Methods* 196, 281–288.
- Niedergang, F., Didierlaurent, A., Kraehenbuhl, J.-P., and Sirard, J.-C. (2004). Dendritic cells: the host Achilles's heel for mucosal pathogens? *Trends in Microbiology* 12, 79–88.
- Packey, C.D., and Sartor, R.B. (2009). Commensal bacteria, traditional and opportunistic pathogens, dysbiosis and bacterial killing in inflammatory bowel diseases. *Current Opinion in Infectious Diseases* 22, 292–301.
- Van Passel, M.W.J., Kant, R., Zoetendal, E.G., Plugge, C.M., Derrien, M., Malfatti, S.A., Chain, P.S.G., Woyke, T., Palva, A., de Vos, W.M., et al. (2011). The genome of *Akkermansia muciniphila*, a dedicated intestinal mucin degrader, and its use in exploring intestinal metagenomes. *PLoS ONE* 6, e16876.
- Peterson, D.A., Frank, D.N., Pace, N.R., and Gordon, J.I. (2008). Metagenomic approaches for defining the pathogenesis of inflammatory bowel diseases. *Cell Host Microbe* 3, 417–427.
- Png, C.W., Lindén, S.K., Gilshenan, K.S., Zoetendal, E.G., McSweeney, C.S., Sly, L.I., McGuckin, M.A., and Florin, T.H.J. (2010). Mucolytic bacteria with increased prevalence in IBD mucosa augment in vitro utilization of mucin by other bacteria. *Am. J. Gastroenterol.* 105, 2420–2428.
- Poroyko, V., White, J.R., Wang, M., Donovan, S., Alverdy, J., Liu, D.C., and Morowitz, M.J. (2010). Gut microbial gene expression in mother-fed and formula-fed piglets. *PLoS ONE* 5, e12459.

References

- Ramos, H.C., Rumbo, M., and Sirard, J.-C. (2004). Bacterial flagellins: mediators of pathogenicity and host immune responses in mucosa. *Trends Microbiol.* 12, 509–517.
- Reiff, C., and Kelly, D. (2010). Inflammatory bowel disease, gut bacteria and probiotic therapy. *Int. J. Med. Microbiol.* 300, 25–33.
- Rhee, S.H. (2005). Pathophysiological role of Toll-like receptor 5 engagement by bacterial flagellin in colonic inflammation. *Proceedings of the National Academy of Sciences* 102, 13610–13615.
- Rinttilä, T., Kassinen, A., Malinen, E., Krogus, L., and Palva, A. (2004). Development of an extensive set of 16S rDNA-targeted primers for quantification of pathogenic and indigenous bacteria in faecal samples by real-time PCR. *J. Appl. Microbiol.* 97, 1166–1177.
- Savage, D.C. (1977). Microbial ecology of the gastrointestinal tract. *Annu. Rev. Microbiol.* 31, 107–133.
- Sheil, B., Shanahan, F., and O'Mahony, L. (2007). Probiotic effects on inflammatory bowel disease. *J. Nutr.* 137, 819S–24S.
- Smith, K.D., Andersen-Nissen, E., Hayashi, F., Strobe, K., Bergman, M.A., Barrett, S.L.R., Cookson, B.T., and Aderem, A. (2003). Toll-like receptor 5 recognizes a conserved site on flagellin required for protofilament formation and bacterial motility. *Nature Immunology* 4, 1247–1253.
- Sokol, H., Lay, C., Seksik, P., and Tannock, G.W. (2008). Analysis of bacterial bowel communities of IBD patients: What has it revealed? *Inflammatory Bowel Diseases* 14, 858–867.
- Sonoyama, K., Fujiwara, R., Takemura, N., Ogasawara, T., Watanabe, J., Ito, H., and Morita, T. (2009). Response of Gut Microbiota to Fasting and Hibernation in Syrian Hamsters. *Applied and Environmental Microbiology* 75, 6451–6456.
- Stoecker, K., Dorninger, C., Daims, H., and Wagner, M. (2010). Double labeling of oligonucleotide probes for fluorescence in situ hybridization (DOPE-FISH) improves signal intensity and increases rRNA accessibility. *Appl. Environ. Microbiol.* 76, 922–926.

References

- Strober, W., Fuss, I., and Mannon, P. (2007). The fundamental basis of inflammatory bowel disease. *J. Clin. Invest.* *117*, 514–521.
- Turroni, F., Bottacini, F., Foroni, E., Mulder, I., Kim, J.-H., Zomer, A., Sánchez, B., Bidossi, A., Ferrarini, A., Giubellini, V., et al. (2010). Genome analysis of *Bifidobacterium bifidum* PRL2010 reveals metabolic pathways for host-derived glycan foraging. *Proc. Natl. Acad. Sci. U.S.A.* *107*, 19514–19519.
- Ubeda, C., and Pamer, E.G. (2012). Antibiotics, microbiota, and immune defense. *Trends in Immunology* *33*, 459–466.
- Vijay-Kumar, M., and Gewirtz, A.T. (2009). Role of flagellin in Crohn's disease: emblematic of the progress and enigmas in understanding inflammatory bowel disease. *Inflamm. Bowel Dis.* *15*, 789–795.
- Walker, A.W., Sanderson, J.D., Churcher, C., Parkes, G.C., Hudspith, B.N., Rayment, N., Brostoff, J., Parkhill, J., Dougan, G., and Petrovska, L. (2011). High-throughput clone library analysis of the mucosa-associated microbiota reveals dysbiosis and differences between inflamed and non-inflamed regions of the intestine in inflammatory bowel disease. *BMC Microbiol.* *11*, 7.
- Wang, X., Smith, C., and Yin, H. (2013). Targeting Toll-like receptors with small molecule agents. *Chemical Society Reviews*.
- Wong, S.H., and Ng, S.C. (2013). What Can We Learn From Inflammatory Bowel Disease in Developing Countries? *Current Gastroenterology Reports* *15*.
- Xu, J., and Gordon, J.I. (2003). Honor thy symbionts. *Proc. Natl. Acad. Sci. U.S.A.* *100*, 10452–10459.
- Zhang, H., DiBaise, J.K., Zuccolo, A., Kudrna, D., Braidotti, M., Yu, Y., Parameswaran, P., Crowell, M.D., Wing, R., Rittmann, B.E., et al. (2009). Human gut microbiota in obesity and after gastric bypass. *Proc. Natl. Acad. Sci. U.S.A.* *106*, 2365–2370.
- Zoetendal, E.G., Akkermans, A.D., and De Vos, W.M. (1998). Temperature gradient gel electrophoresis analysis of 16S rRNA from human fecal samples reveals stable and host-specific communities of active bacteria. *Appl. Environ. Microbiol.* *64*, 3854–3859.

Websites

http://blast.ncbi.nlm.nih.gov/Blast.cgi?PROGRAM=blastx&BLAST_PROGRAMS=blastx&PAGE_TYPE=BlastSearch&SHOW_DEFAULTS=on&BLAST_SPEC=&LINK_LOC=blasttab&LAST_PAGE=blastx (22.05.2013)

<http://gutmicrobiota.univie.ac.at/inflammobiota> (22.05.2013)

<http://tools.neb.com/NEBcutter2/index.php> (22.05.2013)

Mellies, J. (2008). Bacterial flagella stain protocol:

<http://www.microbelibrary.org/component/resource/laboratory-test/3153-bacterial-flagella-stain-protocol> (22.05.2013)

10 Appendix

List of Abbreviations

%	percent
&	and
°C	degree celsius
Ø	diameter
µg	microgram(s)
µl	microlitre(s)
AA	amino acid
<i>A. muciniphila</i>	<i>Akkermansia muciniphila</i>
BF	basic fuchsin stain
blast	basic local alignment search tool
blastx	compares nucleotide sequence against a protein sequence data base (translated in all six reading frames)
<i>bnh</i>	β-N-acetylhexosaminidase
bp	base pair(s)
ca.	approximately
CD	Crohn's Disease
cDNA	complementary DNA
cont.	control
Cy3	5,5'-di-sulfo-1,1'-di-(X-carbopentynyl)-3,3,3',3'-tetra-methylindol-Cy3.18-derivative N-hydroxysuccimidester
Cy5	5,5'-di-sulfo-1,1'-di-(X-carbopentynyl)-3,3,3',3'-tetra-methylindol-Cy5.18-derivative N-hydroxysuccimidester
DAPI	4',6'-Diamidino-2-phenylindole dihydrochloride
DEPC	diethylpyrocarbonate
DNA	deoxyribonucleic acid
DNase	deoxyribonuclease
dNTP	deoxynucleotide Triphosphate
DSS	dextran sodium sulfate
DTT	dithiothreitol
<i>E. coli</i>	<i>Escherichia coli</i>

Appendix

<i>E. rectale</i>	<i>Eubacterium rectale</i>
EDTA	ethylenediaminetetraacetic acid
<i>epsc</i>	capsular exopolysaccharide
et al.	et alii (lat., “and others”)
EtBr	ethidium bromide
EtOH	ethanol
FA	formamide
FISH	fluorescence <i>in situ</i> hybridization
FITC	fluorescein-5-isothiocyanate
<i>fla</i>	flagellin
Fluos	5,(6)-carboxyfluorescein-N-hydroxysuccimidester
For	forward
g	gram(s)
GEN-AU	Genomforschung in Österreich
GI	gastrointestinal
h	hour(s)
IBD	inflammatory bowel disease
IF	immunofluorescence
JAK	Janus kinase
kb	kilo base
LB	Luria Bertani
M	molar
MAMP	microbe-associated molecular pattern
max. ident.	maximal identity
Milli-Q water	ultrapure water
min	minute(s)
ml	millilitre
mM	millimolar
mRNA	messenger RNA
N	normal
NaAZ	sodium azide
NcoI	restriction endonuclease from <i>Gordonia rubriperticnta</i>
n.d.	not determined
nm	nanometer
NO	NanoOrange®
NotI	restriction endonuclease from <i>Nocardia otitidiscaviarum</i>

Appendix

nt	nucleotide
OTU	operational taxonomic unit
PBS	phosphate buffered saline
PCR	polymerase chain reaction
pH	potentia hydrogenii (decimal logarithm of the reciprocal of the hydrogen ion activity in a solution)
pmol	picomol
PstI	restriction endonuclease from <i>Providencia stuartii</i>
qPCR	quantitative PCR
<i>rbr</i>	rubrerythrin
rDNA	ribosomal DNA
Rev	reverse
RNA	ribonucleic acid
rpm	rotations per minute
rRNA	ribosomal RNA
SDS	sodium dodecyl sulfate
sec	second(s)
SOB	super optimal broth
SOC	SOB with catabolite repression
spp.	species
STAT	signal transducer and activator of transcription
STAT1 ^{-/-}	STAT1 knockout
TAE	tris-acetate-EDTA
Taq polymerase	<i>Thermus aquaticus</i> DNA polymerase
TLR	toll-like receptor
Tris	tris(hydroxymethyl)aminomethane
TRITC	tetramethyl rhodamine isothiocyanate
TYK	tyrosine kinase
TYK2 ^{-/-}	TYK2 knockout
u	units
UC	Ulcerative Colitis
wt	wild-type
x	times
X-Gal	5-bromo-4-chloro-indolyl- β -D-galactopyranoside

List of Tables

Table 3-1: Compositions of hybridization and washing buffers at different FA concentrations.	17
Table 4-1: Trial A – labelling of the mice.	24
Table 4-2: Trial C – labelling of the mice.	25
Table 4-3: Trial G – labelling of the mice.	25
Table 4-4: Trial I – labelling of the mice.	26
Table 4-5: Efficiency and R^2 of the primers used for qPCR.	32
Table 5-1: 16S rRNA primers tested with qualitative PCR using Trial A DNA as template.	45
Table 5-2: Testing protein gene targeting primers with qualitative PCR using Trial A DNA as template.	46
Table 5-3: Best hits for the blastx search for the sequences derived for the clones containing sequences of the samples A6 and A8 using the <i>fla</i> primers.	49
Table 5-4: Results for the blastx search for the sequences using the <i>fla</i> Rev and CR1For primers.	50
Table 5-5: Combination of stains – which could be used together and which not.	75
Table 6-1: DSS-treatment and DSS free days for the different trials.	78

Table of Figures

- Figure 2-1:** Relative abundance of different bacterial phyla along the intestinal tract, comparing healthy and IBD suffering humans (Peterson et al., 2008). **5**
- Figure 2-2:** The human TLR signalling pathway in an overview (Misch and Hawn, 2008). TLR ligation induces a signalling cascade which leads by translocation of transcription factors to an acute inflammatory response in the nucleus. **7**
- Figure 2-3:** The body weight (relative to day 1) for each mouse of the acute murine colitis model (Berry et al., 2012). The red bar indicates DSS treatment, lasting from day 1 to day 7. The sampling took place on day 10. **9**
- Figure 2-4:** Taxonomic composition of rRNA and mRNA reads in acute murine colitis from metatranscriptomic libraries which were assigned to 'order' levels (Berry et al., 2012). The differences in wt compared to STAT1^{-/-} mice and of a control versus a DSS treated group was observed. **11**
- Figure 2-5:** Electron microscopic pictures of *Akkermansia muciniphila* (Derrien et al., 2004). A: Transmission electron microscopic picture. B: Scanning electron microscopic picture, showing extensive capsule fibres of the cells. The bar on each picture indicates 0.5 µm. **11**
- Figure 2-6:** Metabolism of mucin degradation of *Bifidobacterium bifidum* and the predicted target sites of involved enzymes (modified from Turrone et al., 2010). Ser: serine; Thr: threonine; GlcNAc: N-acetylglucosamine; GalNAc: N-acetylgalactosamine. **12**
- Figure 2-7:** Abundance of functional gene categories in acute murine colitis (Berry et al., 2012). **13**
- Figure 5-1:** Weight curve during DSS induced acute murine colitis for Trial A. DSS treatment started on day 1 and lasted until day 7. The samples for the metatranscriptome analysis were taken on day 10. Three of the five DSS treated wt mice succumbed before day 10. **41**
- Figure 5-2:** Weight curve during DSS induced murine colitis development for Trial C. DSS treatment started on day 1 and lasted until day 7. Samples for the metatranscriptome analysis were taken on the days 1, 2, 3, 4 and 7. **42**
- Figure 5-3:** Weight curve for DSS induced murine colitis recovery for Trial G. DSS treatment started on day 1 and lasted until day 5. Samples for the metatranscriptome analysis were taken on the days 1 and 14. **43**
- Figure 5-4:** Weight curve during the DSS induced murine colitis recovery for Trial I. DSS treatment started on day 1 and lasted until day 5. Samples for the metatranscriptome analysis were taken on the days 1, 5, 8, 14 and 25. **43**
- Figure 5-5:** Agarose gel electrophoresis picture for the gradient PCR of the *fla* primers using sample A8. The temperatures for the lanes are as follows: 1: 44 °C, 2: 44.3 °C, 3: 45.2 °C, 4: 46.4 °C, 5: 47.8 °C, 6: 49.2 °C, 7: 50.8 °C, 8: 52.2 °C. **44**
- Figure 5-6:** Schematic overview of the flagellin gene. The highly conserved N- and C-termini are targeted by the *fla* primers (1 & 2) with a sequence length of about 1,500 bp (Duck et

al., 2007). In order to target a shorter sequence, new primers were designed. Covering the C-terminus, *fla* Rev was used with CR1For (3, product length: 185 bp) or CR1Rev (4, product length: 123 bp), combining *fla* For with Nr1Rev (5, product length: 93 bp) targeted the N-terminus.

47

Figure 5-7: Agarose gel electrophoresis for the colony PCR for the clones containing sequences obtained by a PCR with the *fla* primers. The red squares indicate the products used for sequencing. A: sample A6; B: sample A8.

48

Figure 5-8: Agarose gel electrophoresis picture for the PCR products obtained with the TB primers targeting the 16S rRNA to validate the cDNA synthesis using Trial A (STAT1^{-/-}) samples as an example. The expected length is 200 bp. 1: A11, 2: A12, 3: A13, 4: A14, 5: A15, 6: A16, 7: A17, 8: A18, 9: A19, 10: A20, 11: neg. contr.

51

Figure 5-9: Agarose gel electrophoresis picture for the restriction digest (AM, *bnh*, *rbr*) in comparison to the uncut plasmid. The obtained length was as expected. The samples are as follows: 1: AM, 2: *bnh*, 3: *rbr*, ^a NotI, ^b PstI, ^c uncut plasmid.

51

Figure 5-10: Trial A wt and STAT1^{-/-} – quantification for total bacteria 16S rRNA, *Akkermansia* 16S rRNA, the rubrerythrin, β -N-acetylhexosaminidase and capsular exopolysaccharide protein genes. The DSS treatment lasted for seven consecutive days and sampling took place on day 10. The different letters indicate a significant difference of gene or transcript abundance between treatments ($p \leq 0.05$). A: using DNA as template; B: using cDNA as template.

53

Figure 5-11: Trial C – time series for the quantification of total bacteria 16S rRNA, *Akkermansia* 16S rRNA, the rubrerythrin, β -N-acetylhexosaminidase and capsular exopolysaccharide protein genes. The DSS treatment lasted for seven consecutive days. Samples were taken on the days 1, 2, 3, 4 and 7. The different letters indicate a significant difference of gene or transcript abundance between treatments for *Akkermansia* ($p \leq 0.05$). A: wt, using DNA as template; B: TYK2^{-/-}, using DNA as template; C: wt, using cDNA as template; D: TYK2^{-/-}, using cDNA as template.

55

Figure 5-12: Trial I wt – time series for the quantification of total bacteria 16S rRNA, *Akkermansia* 16S rRNA, the rubrerythrin, β -N-acetylhexosaminidase and capsular exopolysaccharide protein genes. DSS treatment lasted for five consecutive days. Samples were taken on the days 1, 5, 8, 14 and 25. For day 8, only one cDNA sample was available, therefore it was omitted. The different letters indicate a significant difference of gene or transcript abundance between treatments for *Akkermansia* ($p \leq 0.05$). A: using DNA as template; B: using cDNA as template.

56

Figure 5-13: Trial A wt and STAT1^{-/-} – quantification for total bacteria 16S rRNA, clostridial cluster IV and XIVa 16S rRNA and the flagellin protein gene. DSS treatment lasted for seven consecutive days and the sampling took place on day 10. The different letters indicate a significant difference of gene or transcript abundance between treatments ($p \leq 0.05$). A: using DNA as template; B: using cDNA as template.

58

Figure 5-14: Trial C – time series for the quantification of total bacteria 16S rRNA, clostridial cluster IV and XIVa 16S rRNA and the flagellin protein gene. The DSS treatment lasted for seven consecutive days. Samples were taken on the days 1, 2, 3, 4 and 7. The different letters indicate a significant difference of gene or transcript abundance between treatments for the flagellin ($p \leq 0.05$). A: wt, using DNA as template; B: TYK2^{-/-}, using DNA as template; C: wt, using cDNA as template; D: TYK2^{-/-}, using cDNA as template. **59**

Figure 5-15: Trial G wt and TYK2^{-/-} - quantification for the days 1 and 14 of total bacteria 16S rRNA, clostridial cluster IV and XIVa 16S rRNA and the flagellin protein gene. The DSS treatment lasted for five consecutive days. Samples were taken on the days 1 and 14. The different letters indicate a significant difference of gene or transcript abundance between treatments ($p \leq 0.05$). A: using DNA as template; B: using cDNA as template. **61**

Figure 5-16: Trial I wt – time series for the quantification of total bacteria 16S rRNA, clostridial cluster IV and XIVa 16S rRNA and the flagellin protein gene. The DSS treatment lasted for five consecutive days. Samples were taken on the days 1, 5, 8, 14 and 25. The different letters indicate a significant difference of gene or transcript abundance between treatments for the flagellin ($p \leq 0.05$). A: using DNA as template; B: using cDNA as template. **62**

Figure 5-17: The basic fuchsin stain using sample A9 (A – D). A & B show the same bacterium at different focal planes, so the bacteria and flagella have a different colouring. The white bar on each image indicates 10 μm . **64**

Figure 5-18: Basic fuchsin stain for sample A12. The slide was treated with poly-L-lysine before applying the sample. At the poles of the bacterium, cracks in the poly-L-lysine layer occurred which could be mistaken for flagella, especially when they were less pronounced. A & B display the same detail at different focal planes. The white bar on each image indicates 10 μm . **65**

Figure 5-19: NanoOrange® stain using sample A6. All three pictures show the same bacterium. A: FITC channel; B: TRITC channel; C: light microscope. The white bar on each image indicates 10 μm . **66**

Figure 5-20: NanoOrange® stain for sample A6. The structures arising from the bacterium (A, indicated by the arrows) could be flagella. A: FITC channel; B: light microscope. The white bar on each image indicates 10 μm . **66**

Figure 5-21: A flagellated bacterium of sample A6. The flagella was visualized by immunofluorescence (Cy3). A: TRITC channel, B: light microscope. The white bar on each image indicates 10 μm . **67**

Figure 5-22: A combination of immunofluorescence, basic fuchsin stain and DAPI. Each column shows the same bacterium with the different stains. A, E, I and B, F, J represent sample A9; C, G, K and D, H, L show sample A12. The pictures in the upper row display immunofluorescence, the middle row illustrates the basic fuchsin stain and the lower row the DAPI stain. The arrows in the pictures B and F indicate flagella. For the basic fuchsin

stain, they are just visible for the bacterium in image F where the signal for immunofluorescence was very faint. The white bar on each image indicates 10 μm . **68**

Figure 5-23: A combination of the basic fuchsin stain (A) and FISH (B & C, using two probes for *Lachnospiraceae* OTU_11021 in Fluos and Cy3). The flagellum visible using the basic fuchsin stain is indicated with an arrow. Unfortunately, a “halo” surrounded the bacterium which made the identification of flagella more difficult, especially if they would be broken off because then they could hardly be distinguished from the bacteria. A: light microscope, B: FITC channel, C: TRITC channel. The white bar on each image indicates 10 μm . **69**

Figure 5-24: A combination of the NanoOrange® stain (A, FITC channel) and DAPI (B) using sample A6. The bacteria indicated with the arrows were visible with the NanoOrange® stain but not with DAPI. The white bar on each image indicates 10 μm . **70**

Figure 5-25: A combination of NanoOrange® and FISH for sample A6. A & C show the merged pictures for the stains (NanoOrange® for the FITC and TRITC channel; EUBmix in Cy5 for FISH). B & D illustrate the range indicator picture for the same bacteria. The arrows indicate the flagella which were hardly visible on the image for the fluorescent dyes. On the range indicator pictures, the flagella were better detectable. The white bar on each image indicates 10 μm . **71**

Figure 5-26: Immunofluorescence in combination with the light microscope and DAPI. Each row shows the same bacteria, both from sample A9. The left column (A & D) represents immunofluorescence, the middle row (B & E) shows light microscope pictures and the right row (C & F) illustrates the DAPI stain. The white bar on each image indicates 10 μm . **72**

Figure 5-27: A combination of immunofluorescence (Cy5) and FISH (*Lachnospiraceae* OTU_9468 in Cy3 and Fluos, resulting in yellow when specific). A & B: sample A12; C & D: sample A13. The white bar on each image indicates 5 μm . **73**

Figure 5-28: A combination of immunofluorescence (Cy5) and FISH (*Lachnospiraceae* OTU_11021 in Cy3 and Fluos, resulting in yellow when specific). A, B, C, E & F: sample A6; D: sample A9. In picture C, presumably broken off flagella are visible. The white bar on each image indicates 10 μm . **74**

Figure 5-29: A selection of pictures combining immunofluorescence (Cy3) and FISH (Erec482 in Cy5 and EUBmix in Fluos) representing sample A17. The white bar on each image indicates 10 μm . **74**

Figure 5-30: Percent of flagellated *Lachnospiraceae* for the samples A12 and A14 (DSS treated mice) and A17 and A19 (control mice). A One-Way ANOVA was performed to compare the percentage of flagellation ($p < 0.05$). **76**

Figure 6-1: Weight curves for DSS induced murine colitis merged for the Trials A, C, G and I. For Trial A and C the DSS treatment lasted for seven consecutive days, for Trial G and I for five days. **78**

Figure 6-2: The *Akkermansia* 16S rRNA gene copies plotted against the relative body weight of each mouse. Every data point represents one sample. For this plot, the values for the wt

mice of Trial A, C and I were used. The regression line was added. Day 5 of Trial I is missing as the body weight was not measured then for these mice. **80**

Figure 6-3: Abundance of flagellin gene (A) and transcripts (B) for the wt mice of Trial C, G and I. DSS treatment for Trial C mice lasted seven days and for Trial G and I five days. Each red, green and pink square belongs to individual data points whereas the black diamonds represent their average for each day. **84**

Figure 6-4: Comparison for the flagella/flagellin gene results of IF-FISH and qPCR for randomly selected STAT1^{-/-} mice of Trial A. A12 and A14 represent the DSS treated whereas A17 and A19 embody the control mice. **88**

Curriculum vitae

Persönliche Daten

Vorname:	Ina Maria
Nachname:	Rennisch
Nationalität:	Österreich
Muttersprache:	Deutsch

Ausbildung

seit März 2011	Diplomarbeit am Department für Ökogenetik Titel der Diplomarbeit: „Investigations on Murine Colitis-Associated Bacteria: a quantitative PCR and microscopy approach“
seit Jänner 2008	Diplomstudium Ökologie Diplomstudium Anthropologie
seit Oktober 2005	Diplomstudium Biologie, Universität Wien
Oktober 2003 – 2005	Diplomstudium Humanmedizin, Medizinische Universität Wien
1995 – Juni 2003	Bundesgymnasium Kurzweide, Eisenstadt, Österreich
1991 – 1995	Volksschule Eisenstadt, Österreich

Sprachkenntnisse

Englisch in Wort und Schrift
Französisch: Grundkenntnisse

Wissenschaftliche Tätigkeiten

September 2011 – Februar 2012	Studienassistentin am Department für Ökogenetik
-------------------------------	---